JCAR ATRACE

The effects of nature-based solutions on high and low flows in the Vecht using hydrological model Wflow sbm

Master Thesis

William Cazemier

Enschede

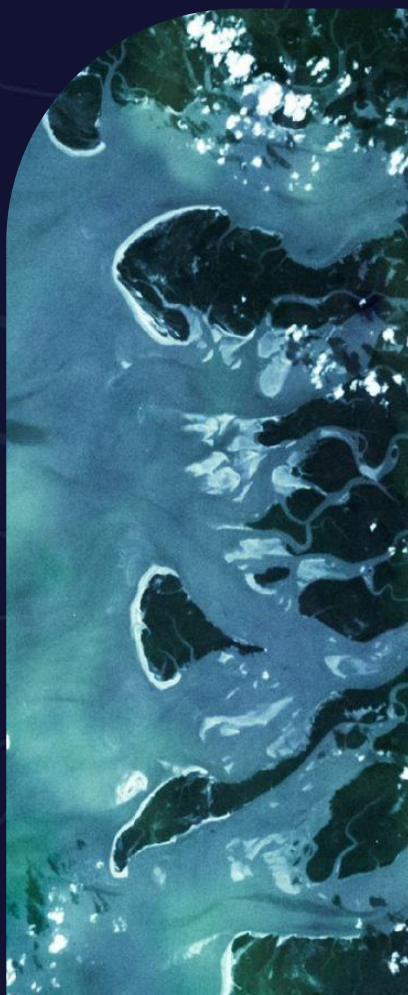

UNIVERSITY OF TWENTE.

Deltares

Civil Engineering — Master Thesis

The effects of nature-based solutions on high and low flows in the Vecht using hydrological model Wflow sbm

Master Thesis

to obtain the degree of Master of Science at the University of Twente

to be presented on 19^{th} of December 2024

Author: William Cazemier (s2395878)

Supervised by:

Dr. Ir. M.J. Booij
Department of Civil Engineering, University of Twente

Ir. A. Klein
Deltares

Dr. Ir. J. Kwadijk
Deltares

Deltares

UNIVERSITY OF TWENTE.

Preface

With this thesis, I conclude my Master's degree in Civil Engineering and Management at the University of Twente, reflecting on several enriching years in Enschede. This research involved simulating nature-based solutions in the Vecht basin using the hydrological model Wflow sbm. I hope studies like this can inspire practical actions in river basins to reduce the risks and impacts of floods and droughts, contributing to sustainable water management strategies.

During this thesis, I have learned a great deal about hydrology and the modelling of river basins. My programming skills have significantly improved, especially when working with hydrological models and data analysis. Additionally, I have gained a deeper understanding of hydrological processes and their interactions within river basins, as well as the practical application of nature-based solutions to address water management challenges.

I was fortunate enough to have very experienced people around me who deserve some special mentioning. I am grateful to Martijn Booij for his supervision, who encouraged me to think critically about why and how we should do things. He helped me to improve my academic writing skills and provided valuable insights into my methodology and results. I also wish to thank Angela Klein for her daily supervision at Deltares; her expertise in Wflow sbm, modelling nature-based solutions, and evaluating extreme river flows was incredibly valuable. My gratitude extends to Jaap Kwadijk for helping to put my work into the broader perspective of its real-world implications and, of course, the enthusiasm that he always brings into meetings. Furthermore, I would like to acknowledge Sebastian, Laurene, Joost, and Ferdinand at Deltares and Jeroen from waterboard Vechtstromen for their assistance with data processing and modelling whenever I encountered challenges. I started at Deltares together with Ivan and Sander, who also did their thesis about similar subjects, and I would also like to thank them for their support and fun moments, like driving around in the Vecht basin looking for discharge stations.

Finally, I also want to thank my family and friends for their never-ending support and for providing much-needed distractions from the intensity of thesis work during the past months. Since Deltares is not around the corner from Enschede, I had to stay around Delft for many days. I was fortunate to stay at the home of family friends during this period, and I want to extend special thanks to them for their generous hospitality, which made this experience much more manageable.

I hope you enjoy reading my thesis!

William Cazemier

Enschede, December 2024

Summary

Climate change is projected to change weather patterns over the entire world, increasing the frequency and intensity of extreme heavy rainfall and prolonged dry periods. These lead to extreme high and low river flows and cause floods and droughts. Such extreme weather events have also occurred in north-west Europe in recent history. For instance, in July 2021, the Geul catchment in the south of the Netherlands was subject to extremely high river discharges due to intense rainfall, causing floods. This led to enormous societal and economic costs. Germany and Belgium also experienced severe floods, causing more than 200 deaths. On the other hand, 2018 was an extremely dry year in the Netherlands. Such events emphasise the need for measures to mitigate the impacts of extreme events. Nature-based solutions have emerged as sustainable and promising measures to reduce extreme high and low flows. However, accurate modelling of the effects of such nature-based solutions remains a significant challenge.

This study evaluates the effectiveness of nature-based solutions on high and low flows in the Vecht river basin using the hydrological model Wflow sbm (v0.8.01). The Vecht is a transboundary basin of 4,190 km^2 in Germany and the Netherlands. Firstly, the Wflow sbm model is calibrated and validated using historical weather and discharge data. Then, nature-based solutions are selected and parametrised based on their applicability in the Vecht basin and hydrological model. Lastly, their effects on extremely high and low discharges are evaluated through different indicators.

Overall, the Wflow sbm model shows satisfactory performance in simulating discharge under historical periods. The performance is defined by a multi-objective function focusing on high flows, low flows and the water balance. Through calibration and validation, the model simulates the German part of the Vecht more accurately than the Dutch part. The model shows good performance on high flows and poor to satisfactory performance on low flows. The water balance of the Vecht simulation is satisfactory, except for four sub-catchments where the Relative Volume Error is more than 15 %.

A total of 12 different nature-based solutions are selected and parametrised. These are divided into four categories: land use change, changing roughness, enhancing infiltration and water storage.

The evaluation of nature-based solutions concerns a quick assessment where all 12 NBS are simulated for the Dinkel sub-catchment only. Afforestation and wetlands appear to have the most effects on high and low flows and are further evaluated in the detailed assessment using different spatial layouts and scales for the entire Vecht basin. In this detailed assessment, wetlands and afforestation lead to a similar decrease in peak flows, between 5 and 30 % under summer conditions, depending on the scale and precipitation event. Both nature-based solutions decreased the average discharge. Afforestation slightly increases the low flows, as indicated by the average 7-day minimum discharge, while wetlands significantly decrease the low flows. The influence of spatial scale is the primary driver of the effectiveness of NBS. Large scales are necessary to effectively mitigate high and low flows, as the minimum spatial scale in this study is 25 % of the entire catchment area (not considering urban area), resulting in less than 10 % of peak flow reduction and less than 5 % in low flow increase, in case of afforestation.

To improve the accuracy of simulating nature-based solutions, it is recommended to couple Wflow sbm with a groundwater model as Wflow sbm lacks deeper groundwater dynamics. This study focuses on river discharges, while groundwater levels are also very relevant indicators for droughts and could be included in future studies. Additionally, future research could also focus on evaluating the NBS using climate change scenarios to see whether they can mitigate the changing weather patterns due to climate change.

keywords: Nature-based solutions, Wflow sbm, hydrological modelling, floods, droughts, high flows, low flows, hydrology

Table of contents

List of symbols

Symbol	Description	Unit
Parameters in sensitivity analysis		
$KsatHorFrac$	Horizontal saturated hydraulic conductivity	-
$KsatVer$	Vertical saturated hydraulic conductivity	mm/day
$f - parameter$	Decay parameter of *KsatVer* over depth	mm^{-1}
$InfiltCapPath$	Infiltration capacity of paved area	mm/day
$InfiltCapSoil$	Infiltration capacity of non-paved area	mm/day
$rootdistpar$	Defines the sharpness of transition between fully wet and fully dry roots	-
Multi-objective function		
n	Total number of timesteps	-
Q_{sim}	Simulated discharge at time step i	m^3/s
Q_{obs}	Observed discharge at time step i	m^3/s
NS_w	Weighted Nash-Sutcliffe Efficiency	m^3/s
NS_{inv}	The Nash-Sutcliffe Efficiency based on the inversed flow	-
RVE	Relative Volume Error	%
$y_{combined}$	Multi-objective function for both low and high flows	-
Low & high flow indices		
Q_{max}	Maximum daily discharge	m^3/s
$MAM7$	Minimum average 7-day discharge	m^3/s
Q_{mean}	Average discharge	m^3/s
V_{flood}	Flood volume	m^3

1

Introduction

1.1 Problem context

Climate change is projected to affect weather patterns over the earth, increasing the frequency of extreme weather events (Bessembinder et al., 2023). These extreme weather events include extreme heavy rainfall and prolonged dry periods, leading to extreme high and low river flows in basins. Such events have also taken place in recent history in northwest Europe. In July 2021, an extreme rainfall event occurred in the Netherlands, Belgium and Germany (Asselman et al., 2022). In the Netherlands, the province of Limburg was hit the most, resulting in large floods and damage to houses and companies. In Belgium and Germany, the floods cause more than 200 deaths. On the other hand, the Netherlands has encountered droughts in recent years, of which 2018 and 2022 are examples and have negative impacts on agriculture and water availability (Bessembinder et al., 2023). These two examples led to extreme high and low discharges in Dutch rivers and raised concern in the Netherlands about its preparedness for such events (Hendriks & Mens, 2024). The Ministry of Infrastructure and Water found that the Netherlands needs to do more work to cope with both flooding and droughts (Ministerie van Infrastructuur en Waterstaat, 2022) (Ministerie van Infrastructuur en Waterstaat, 2019). This raises the question: what can we do in our river basins to minimise the occurrence of floods and droughts and reduce their impacts?

Floods have traditionally been controlled using hard-engineered infrastructure, such as dams and dikes, commonly referred to as grey infrastructure solutions. As stated by Ferreira et al. (2022), grey infrastructure, like controlled dams and floodgates, is typically designed for specific conditions and scenarios and cannot adjust when these conditions change due to climate change, resulting in limited flexibility and adaptability. Grey infrastructure can also have negative consequences for society and the environment. In response, nature-based solutions have gained popularity all across the world. This is defined by the IUCN (International Union for Conservation of Nature) as "actions to protect, sustainably manage, and restore natural or modified ecosystems, that address societal challenges effectively and adaptively, simultaneously providing human well-being and biodiversity benefits" (Cohen-Shacham et al., 2016). In the context of extreme weather, this means using natural or modified ecosystems to minimise the occurrence of extreme high and low river flows, which result from intense precipitation or prolonged droughts (Sarigil et al., 2024). Examples of nature-based solutions are river re-meandering, wetland restoration and managed aquifer recharge (Cohen-Shacham et al., 2016).
Simulation of nature-based solutions can help to estimate their potential effects on extremely high and low flows, with hydraulic and hydrological models being promising tools for this purpose.

The extreme rainfall event of 2021 led to the creation of the JCAR-ATRACE program, which this thesis is part of. It focuses on research on transboundary river basins in the Netherlands, Belgium, Germany and Luxembourg.

1.2 State-of-the-art

The state-of-the-art outlines the state-of-the-art concepts of nature-based solutions and hydrological models. These numerical models simulate the relationship between rainfall and runoff by distinguishing hydrological processes within a river basin. Since nature-based solutions influence this relationship, such models are essential for evaluating the potential impacts of nature-based solutions.

1.2.1 Nature-based solutions

Nature-based solutions (NBS), in the context of hydrology, are measures that include nature. As this is a broad term, there is a need for more specific applications. In the literature, nature-based solutions are often considered in urban areas, e.g. green roofs or wadi's. These mainly help to reduce flooding within urban areas but do not necessarily affect the discharge in the river of an entire basin. Examples of nature-based solutions for regional river basins can be found in Table 1. NBS influence the hydrological processes in a river basin, such as transpiration, interception, evaporation, infiltration, surface runoff and water retention (Ferreira et al., 2022). Measures in Table 1 focus on storing, slowing, or redirecting water to make sure that water is kept in the landscape and delay runoff.

Table 1: Examples of nature-based solutions that can be implemented in a regional river basin (Raška et al., 2022) (Debele et al., 2023) (McVittie et al., 2018)

NBS group	**Frequently reported types of NBS**
Floodplain retention and polders	Floodplain restoration, restoring fluid connectivity, retention reservoirs, polders, wetlands
River restoration	Re-meandering, riverbanks restoration, supporting riparian vegetation, preserving natural buffer zones along rivers
Nature-based river dams	Log dams, wood check dams, leaky dams, sediment traps
Channel alterations and diverging flows	Flood moulds in forests and agricultural land, channel restoration, supporting natural levees, bio drainage, bioswales, live pole drains, live crib walls
Improving soil conditions	Increasing soil organic matter, supporting deep infiltration, reducing soil erosion by vegetation cover
Land use/land cover changes	(Re-) forestation, agroforestry, grassing, vegetation filter strips, supporting woodland buffer zones and riparian forests, delimiting agricultural floodable land, multifunctional agriculture

1.2.2 Hydrological models

Hydrological models are a simplified digital representation of the real-world system to simulate the complex interactions between different processes of the hydrological system (Sorooshian & Moradkhani, 2009). The choice for a hydrological model depends on the characteristics and application of the model as well as the area of interest and required simulation period (Singh, 2018).

There are numerous hydrological models that can be classified based on their characteristics: incorporation of randomness, spatial representation, and process description (Singh, 2018).
As for incorporating randomness, models are either stochastic, meaning randomness is included, or

deterministic, meaning randomness is excluded (Devia et al., 2015).
Spatial representation varies among lumped, semi-distributed, and distributed models. Lumped models treat the entire basin as a single area, using average parameters and input data to represent the whole basin, thus spatial variability is neglected (Sorooshian & Moradkhani, 2009). Semi-distributed models divide the basin into smaller sub-basins, using averages for each sub-basin, while distributed models employ a grid system to represent the basin spatially, determining hydrological processes and fluxes for each grid cell (Singh, 2018).
The process description of a model varies from empirical, conceptual, or physically based. Empirical models are based on statistical relationships between input and output from historical data and do not explicitly consider the underlying physical processes (Devia et al., 2015). Conceptual models aim to represent the hydrological system using simplified conceptualisations of the physical processes. These models divide the basin into conceptual components such as reservoirs, channels, and storage units, each characterised by parameters representing physical processes (Singh, 2018). Physically-based models represent the hydrological system using physics principles to describe the processes in a river basin. A physically based model does require a vast amount of data regarding the physical characteristics of a basin, e.g., soil moisture content, initial water depths, topography, river dimensions, etc. (Singh, 2018).

Table 1 presents NBS groups that influence hydrological processes like transpiration, interception, evaporation, infiltration, surface runoff and water retention. These processes are spatially variable and must be accurately represented in the hydrological model. Therefore, a spatially distributed, physically based model is most suitable. Additionally, sufficient documentation and software requirements (e.g. use of Windows) are also relevant aspects to consider when selecting a hydrological model. Wflow sbm contains these characteristics and is easily available through Deltares. Thus, the choice is made to use this model, which is further explained in Chapter 2.2.1.

1.3 Research gap

Nature-based solutions have emerged as promising approaches to minimise the occurrence of extreme high and low flows in river basins. However, despite growing interest in NBS, several research gaps remain in modelling these solutions. As stated by Ruangpan et al. (2020), there is significantly more literature on modelling small-scale NBS than large-scale NBS, possibly due to the complexity of implementing NBS at larger regional scales in models. Therefore, there is a need for further research on the effectiveness of large-scale nature-based solutions (Ruangpan et al., 2020) (Jeuken et al., 2023). Additionally, most literature focuses on modelling NBS to minimise the risk of floods, while modelling of low flows is becoming more relevant in the future (Ruangpan et al., 2020). There is a need for more research into the effectiveness of nature-based solutions with regard to low flows. Jeuken et al. (2023) highlights the difficulty of simulating NBS using hydrological models due to the low plot scale of NBS. He also describes the relevance of using hydrological models in the assessment of nature-based solutions and the need for more knowledge on how to implement nature-based solutions in hydrological models. Klein and van der Vat (2024) identified several research gaps in a scoping study about the Vecht basin. One research gap describes the need for a better understanding of the potential sponge functioning in the area and possible measures that reduce the occurrence of floods and droughts.

To summarise, there is a need for more research on the quantitative effectiveness of nature-based solutions at large scales through hydrological models for the assessment of both flood and drought risks. These nature-based solutions can enhance the sponge functioning of a river basin.

1.4 Research aim

This study aims to **quantify the effects of nature-based solutions on high and low flows** [1] **in the river Vecht basin under extreme hydroclimatic conditions** [2]**, using the distributed hydrological model 'Wflow sbm'.**

[1] The analysis focuses on the river's low and high discharge regimes to evaluate the effectiveness of nature-based solutions under extreme events.

[2] To evaluate the effectiveness of nature-based solutions on extremely high and low flows, extreme precipitation series are used.

1.5 Research questions

To achieve the research aim, three research questions have been formulated. The first two questions focus on setting up a distributed, physically based hydrological model for the river Vecht basin and representing nature-based solutions in the model. The third question studies the effect that these nature-based solutions have on high and low flows.

1. **What is the performance of the distributed Wflow sbm model in simulating historical discharge series in the river Vecht basin?**

First, the hydrological model needs to be set up for the river basin. Sensitive parameters are identified through a sensitivity analysis, followed by a calibration and validation procedure using a multi-objective function.

2. **Which nature-based solutions can help to reduce high flows and increase low flows in river Vecht basin and how can these be implemented in Wflow sbm?**

These nature-based solutions are selected based on their effectiveness in influencing hydrological processes relevant to reducing high flows and increasing low flows in the river basin. Then, a parametrisation is made to implement them into Wflow sbm.

3. **What are the quantitative effects of nature-based solutions on high and low flows in the river Vecht?**

In the evaluation and quantification of the effects of nature-based solutions on high and low flows, their type, location and scale are considered. These factors are relevant for understanding how different interventions influence the hydrological responses within the River Vecht basin. The influence of NBS is assessed under different meteorological conditions.

1.6 Research scope

This study focuses on implementing nature-based solutions in the Wflow sbm model and their effect on high and low flows. The economic, social and political aspects of implementing nature-based solutions in a river basin are not considered.
This study is part of a series of master theses that study the relevance of using hydrological models to evaluate nature-based solutions to mitigate extreme river discharges. In this thesis, only Wflow sbm is used, and a comparison between different hydrological models is not provided.
While climate change is a significant factor affecting the hydrological behaviour of a river basin, this study does not include extensive climate change scenarios when creating meteorological data. Instead, the hydrological modelling relies on historical meteorological data and other scenarios used by Deltares in the Netherlands.

2

Study area, models and data

2.1 Study area

The JCAR ATRACE project, of which this study is part, focuses on cooperative research on the transboundary river basins in the Netherlands, Belgium, Germany and Luxembourg. The study area of this thesis, the river Vecht basin, is one of these transboundary river basins. This river basin is shown in Figure 1. The outflow point of this basin is considered downstream of Dalfsen to exclude the influence of the backwater effect of the Zwarte Water on the discharge of the Vecht.

2.1.1 Geography

The Vecht basin, shown in Figure 1, originates close to Darfeld in Nordrhein Westfalen. It enters the Netherlands east of Hardenberg and flows into the Zwarte Water close to the city of Zwolle (Spruyt & Fujisaki, 2021). The Vecht basin, as defined in Figure 1, covers an area of 4,190 km^2, of which 2,035 km^2 is located in the Netherlands and has some noteworthy tributaries such as the Steinfurter Aa, the Dinkel, and the Regge (Spruyt & Fujisaki, 2021). Critical cities along the river's course include Nordhorn, Gronau, Neuenhaus, and Emlichheim in Germany and Hardenberg and Ommen in the Netherlands. Many canals in the Vecht basin influence the water system and are further discussed in Chapter 2.1.3.

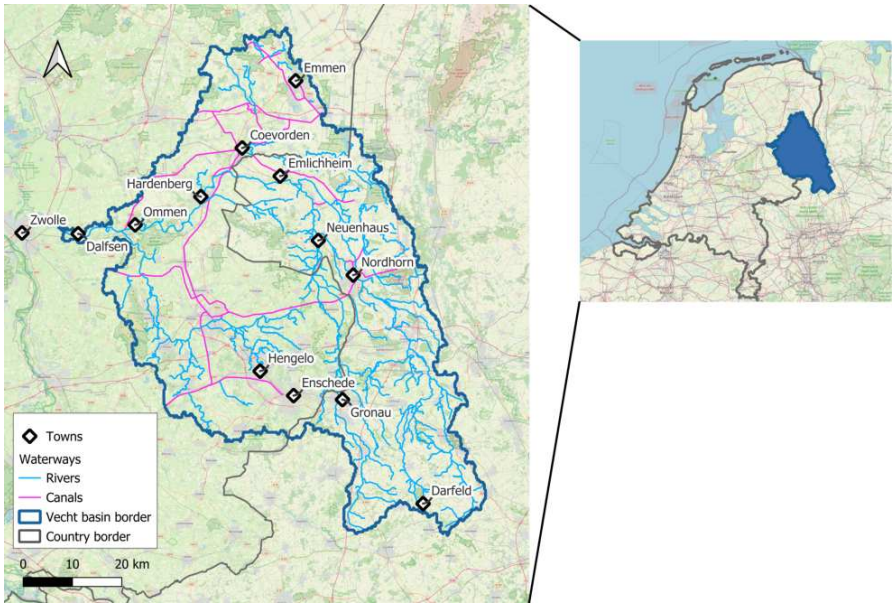

Figure 1: Study area of the Vecht basin

The elevation and soil types of the Vecht basin are shown in Figure 2. The elevation differences within a river basin are crucial in hydrology studies, as they significantly influence hydrological processes. Large elevation variations can lead to rapid runoff, impacting flood dynamics and water distribution. In the Vecht basin, the elevation differences are relatively small, particularly within the Netherlands. Upstream in Germany, the elevation reaches up to 170 meters. Overall, the basin is characterized by flat terrain, with a few hilly regions mainly located in Germany. The soil types in the Vecht basin primarily concern 'sandy loam' and 'loamy sand', with some areas with 'loam', especially in the very upstream part of the basin. These sandy-like soils are generally characterized by a high permeability and high infiltration capacity (Klein & van der Vat, 2024).

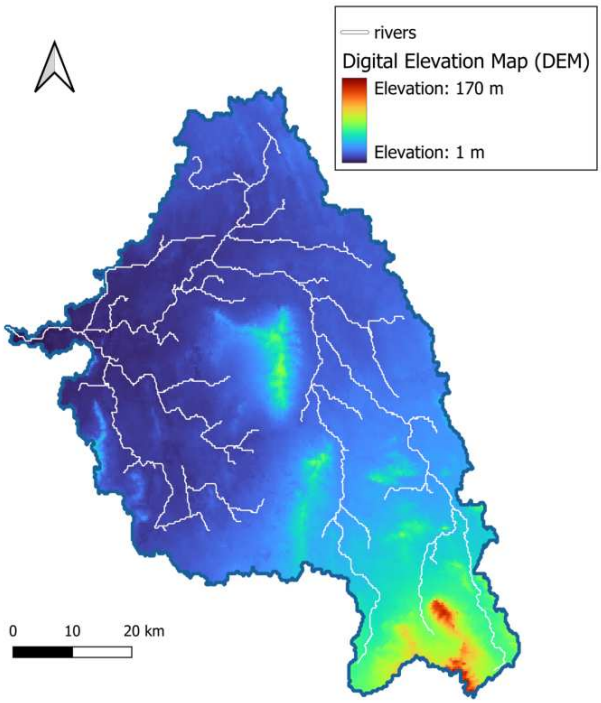

(a) Digital Elevation Map (DEM) (Yamazaki et al., 2019)

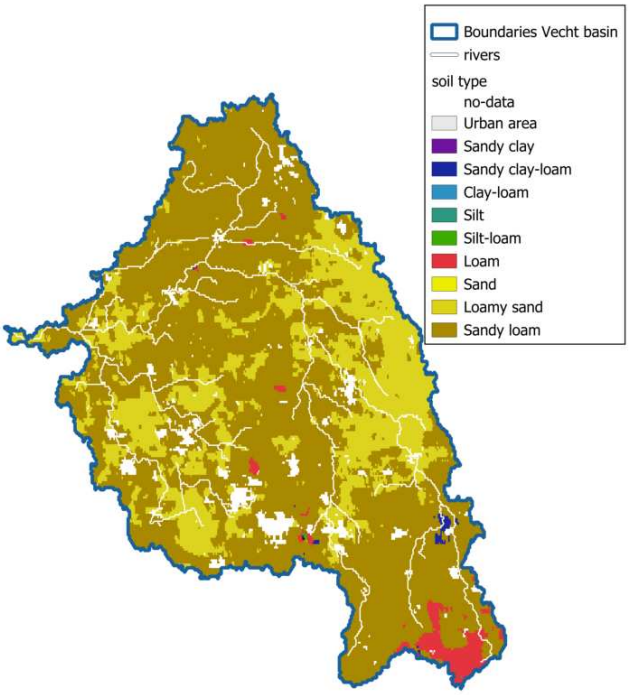

(b) Soil type map based on Soilgrids_2020 data (Poggio et al., 2021); no-data areas are interpolated by HydroMT-wflow (Eilander et al., 2023)

Figure 2: Elevation and soil types in the Vecht basin; river course derived from HydroMT-wflow (Eilander et al., 2023)

The land use map of the Vecht basin, illustrated in Figure 3, provides a detailed overview of the various land cover types within the region. Derived from the CORINE land cover data, this map categorizes the landscape into distinct categories such as agricultural land, forests, urban settlements, and grasslands (Büttner & Kosztra, 2011). Land use in a river basin is relevant since it influences hydrological processes. Different types of land uses, such as agricultural fields, forests, and urban areas, each interact with rainfall in different ways, affecting how water is absorbed, stored, and transported across the landscape.

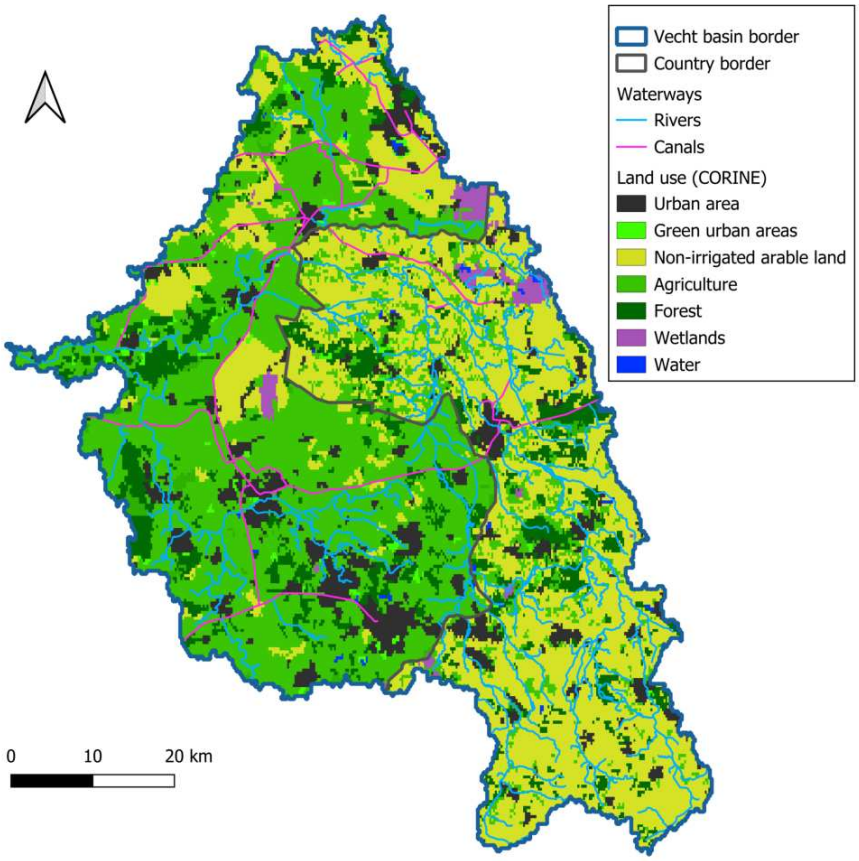

Figure 3: Land use in the Vecht basin (CORINE land cover)

All land uses in the Vecht basin are grouped into categories, with the most prominent groups summarized in Table 2. Agriculture is the predominant land use, covering 48 % of the basin. This includes fields used for growing crops and other agricultural activities. Meadows, which make up 22 % of the land use, are primarily used for grazing livestock and maintaining hayfields. Forests cover 17 % of the basin. Urban areas, which constitute 10 % of the land use, include residential, commercial, and industrial zones within cities and towns.

Table 2: Land use groups in the river Vecht basin

Land Use	**Percentage**
Agriculture	48 %
Meadows	22 %
Forest	17 %
Urban	10 %

2.1.2 Sub-catchments

Figure 4 shows the sub-catchments of the Vecht basin that are used in this thesis. These sub-catchments are based on the discharge stations, as shown in Figure 8. The areas of all sub-catchments can be seen in Table 3. The total area of the basin is 4,190 km^2. The largest single sub-catchment corresponds to the discharge station Archem TOT. All sub-catchments are referred to with their outflow discharge

station. Together, the sub-catchments of Lage Gesamt and Gronau form the Dinkel catchment, which also significantly contributes to the discharge at the outflow point of the entire basin.

Table 3: sub-catchments with their corresponding areas in km^2; areas are derived from the model constructed by HydroMT-wflow

sub-catchment	**Area (km^2)**	**sub-catchment**	**Area (km^2)**
Wettringen	161	Emlichheim	191
Bilk	187	De Haandrik	15
Gronau	199	Ane Gramsbergen	575
Ohne	47	Ommen	396
Neuenhaus	312	Ommerkanaal	149
Lage Gesamt	426	Archem TOT	1200
Osterwald	230	Dalfsen	104

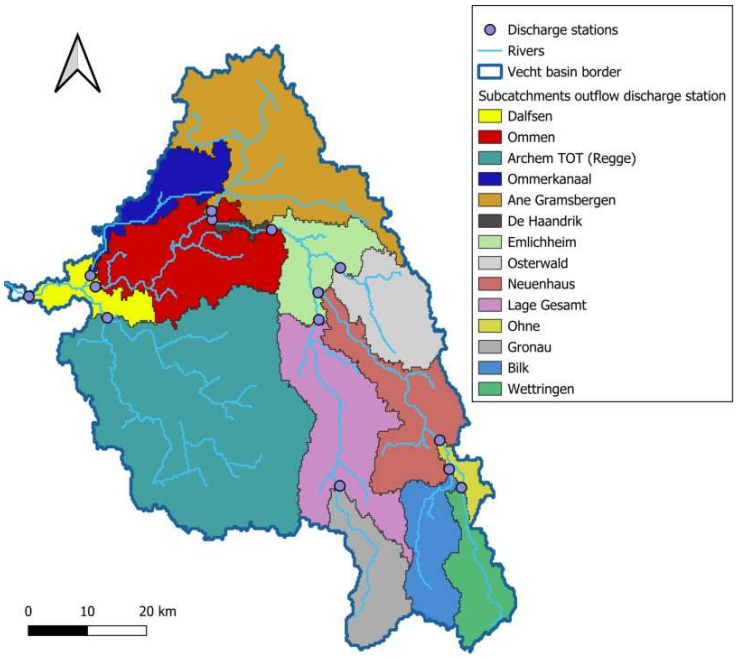

Figure 4: Sub-catchments; derived using HydroMT-wflow based on the outlet discharge station of sub-catchments

2.1.3 Hydrology in the river Vecht basin

The Vecht River is a rain-fed river system, meaning all 'natural' water flowing through it originates from rainfall within its basin. Most water originates from precipitation, but water is added to the system from canals during summer. Figure 5 shows the average monthly sums of observed discharge at Dalfsen in mm, daily precipitation in mm and the potential evaporation in mm, derived using the Makking method through Wflow sbm. The yearly accumulations of these three are shown on the right of the figure. The average discharge at Dalfsen is approximately 30 m^3/s, with low flows during the summer season ranging from 3 to 5 m^3/s and high flows reaching between 200 and 250 m^3/s. The largest discharge measured at Dalfsen was 380 m^3/s, which occurred in 1998.

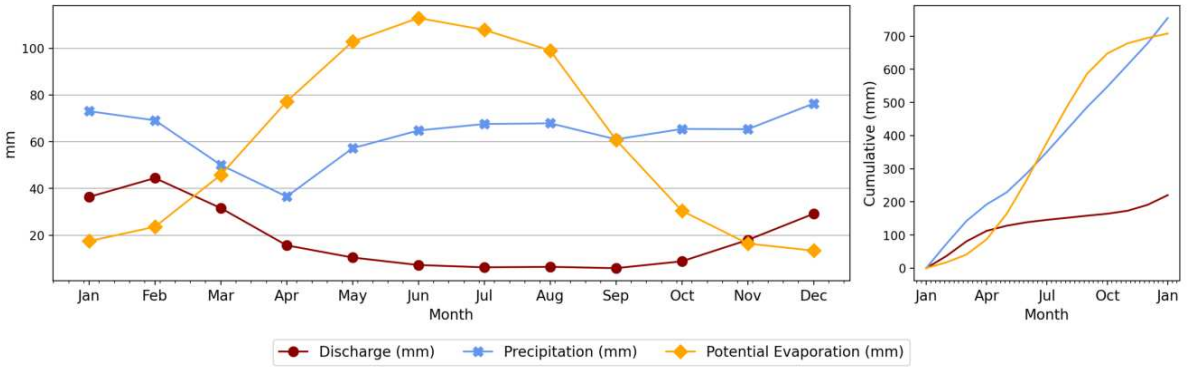

Figure 5: Total monthly observed discharge (at Dalfsen) in mm, total monthly precipitation (averaged over all precipitation stations in Figure 8) and total monthly potential evaporation using Makkink's equation; Based on average values from 2013 - 2022

Extensive drainage interventions in the Vecht basin have changed its hydrological behaviour. The natural peat in the area has been excavated since the Middle Ages, and the area was drained to make it suitable for agricultural use. Large areas of the natural floodplain have become disconnected from the river system, reducing storage capacity (Waterschap Vechtstromen, 2021). Many ditches were constructed for agricultural purposes while the river was straightened to improve its transport function, and canals were constructed, especially in the Dutch part. Due to all these interventions, the whole river basin drains rainwater faster. These interventions happened in both Germany and the Netherlands but were more intense in the Dutch part of the Vecht basin. As a result, during dry periods, the base flow of the river is low, leading to a shortage of water for both natural ecosystems and agricultural purposes. To increase the base flow in case of little precipitation, water is let into the Vecht river through canals. On the other hand, during wet periods with a lot of rain, water is discharged quickly, leading to an intense discharge peak.

The Vecht has several larger lateral flows that significantly contribute to the Vecht discharge at Dalfsen. These are shown in Figure 6, which describes the contributions of lateral flows under regular conditions. About two-thirds of the water at Dalfsen comes from the Dinkel, Afwateringskanaal, Regge and Ommerkanaal. The remaining one-third comes from small streams. The Dinkel enters the Vecht in Germany, while the other lateral flows enter the Vecht in the Netherlands.

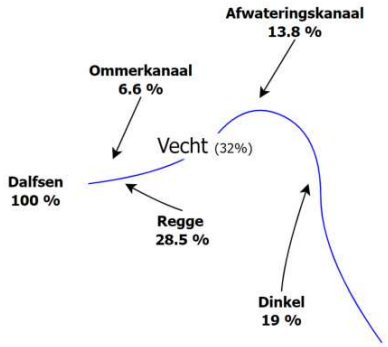

Figure 6: Contributions of lateral flows in the Vecht basin under regular conditions compared to outflow point at Dalfsen

2.1.4 Water-related infrastructure

The river Vecht has undergone much human intervention, especially in the Dutch part of the river basin. Several weirs and numerous canals in the Vecht basin also influence the water system. The canals can be seen in Figure 1. There are weirs in the German part near Schüttorf, Brandlecht, Nordhorn, Neuenhaus and Tinholt (Klein & van der Vat, 2024, p. 60). In the Dutch part, the river Vecht contains weirs at De Haandrik, Hardenberg, Mariënberg, Junne, Vilsteren and Vechterweerd (Spruyt & Fujisaki, 2021). Most of these weirs have a passage for transport or fish. Without these weirs, the water level in the Vecht is low, making transport by ship difficult.

Besides weirs, the water system is also influenced by pumping stations. During dry periods, the primary external water source for the Dutch section of the Vecht is the Twentekanaal, which supplies water to the Vecht at De Haandrik. De Haandrik is a crossing between the Vecht river and the canal between Almelo and Coevorden, close to the border between Germany and the Netherlands. A large pumping station with a capacity of 22 m^3/s is located at the sluice complex in Eefde, where it draws water from the IJssel into the Twentekanaal, which is then eventually connected to De Haandrik. The crossing of the canal with the Vecht river is shown in Figure A.1b.

2.2 Model (Wflow sbm)

2.2.1 Model description

The model used in this thesis is the open-source Wflow sbm (Simple Bucket Model) (v0.8.01). The Wflow sbm model can be constructed through HydroMT-Wflow (Eilander et al., 2023). Wflow sbm is a (partly) physically based and conceptual, fully distributed hydrological model. Wflow simulates hydrological processes on a rectangular grid. The model schematization is shown in Figure 7, with all hydrological processes present in Wflow sbm.

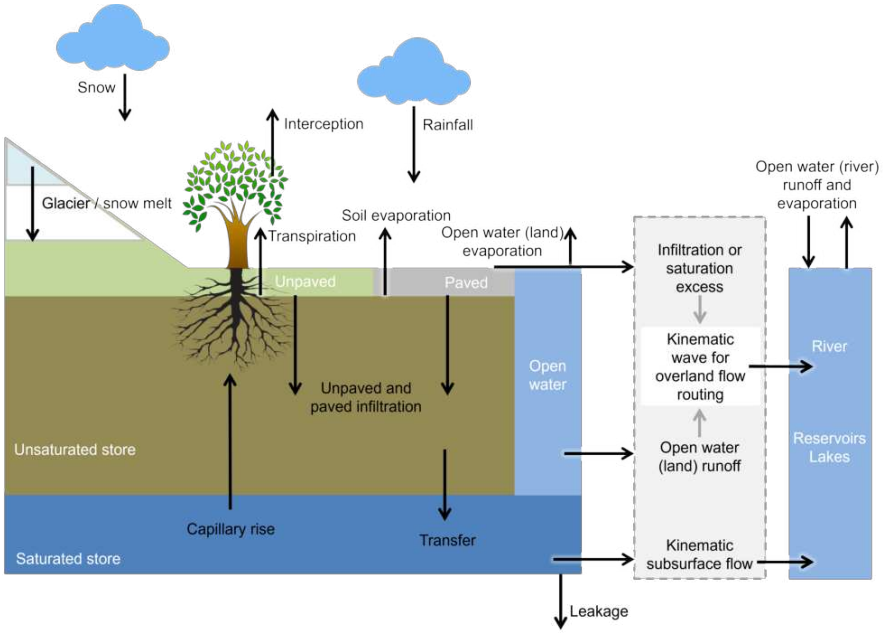

Figure 7: Concept of the Wflow sbm model

Wflow sbm distinguishes vertical and lateral processes. The vertical processes involve the interactions between the saturated zone, the unsaturated zone, the surface and vegetation within each grid cell. The lateral processes govern how river, overland, and subsurface flows are routed throughout the model domain. It is important to note that Wflow sbm uses a maximum soil column of 2 m depth, which means that (deep) groundwater is not modelled by Wflow sbm.

2.2.2 Vertical processes (SBM)

The vertical processes in Wflow sbm are largely based on the Topog_SBM concept (Simple Bucket Model) described by Vertessy and Elsenbeer (1999). The soil is considered a bucket, having an unsaturated and saturated zone that both have their own storage. The differences between Wflow sbm and Topog_SBM are the addition of evapotranspiration and interception losses, the root water uptake, capillary rise and the introduction of division of soil layers to allow for water transfer within the unsaturated zone (Van Verseveld et al., 2022).

Forcing
The Wflow sbm model is driven by meteorological forcing data, namely precipitation, temperature, and potential evapotranspiration in mm/day.

Interception
In the case of a daily timestep, Wflow sbm uses the Gash model to compute interception (Gash, 1979). The model assumes that rainfall events can be divided into distinct phases, focusing on the interception, evaporation, and wetting of the canopy. Initially, rainfall is intercepted by the vegetation canopy until complete saturation is reached. Once the canopy is saturated, excess rainfall passes through to the ground as throughfall. Evaporation from the canopy occurs both during and after the rainfall event, reducing the amount of intercepted water that ultimately reaches the ground. It is assumed that the evaporation from the saturated canopy occurs at a constant rate as long as the canopy remains wet. Maps containing land use data are used to derive parameters regarding interception.

Infiltration
Water first infiltrates based on the infiltration capacity. Water transfer within the soil depends on the soil's properties, such as the vertical hydraulic conductivity and the capacity of the unsaturated zone. Daily infiltration is limited by the specific water retention characteristics and saturation thresholds of the soil, determining water entry into soil versus runoff pathways, directly impacting flow rates in response to rainfall (Van Verseveld et al., 2022). Once water becomes surface runoff, it cannot re-infiltrate in the soil. However, in a recently added option, this can be enabled. Further explanation is given below. A map containing soil characteristics is used to derive the soil parameters.

Evapotranspiration
In Wflow sbm, evaporation occurs through transpiration, bare soil and open water evaporation. Transpiration occurs through root water uptake from the unsaturated and saturated zones in Wflow sbm, of which the latter one accounts for the most transpiration. This root water uptake concept has been proposed by Feddes (1982). Each type of land use has a certain root depth over which transpiration can occur. Vegetation with deeper roots is more likely to reach the water table, allowing higher transpiration rates, as roots can extract water directly from the saturated zone. Soil evaporation depends on soil moisture and crop fraction, which is between 0 and 1, while open-water evaporation is equal to the potential evaporation. Maps containing land use data are used to derive parameters related to evapotranspiration. Next to land use maps, LAI maps are used to derive parameters regarding the amount of leaf area per grid cell.

Capillary rise
As mentioned before, the soil consists of a saturated and unsaturated zone with their own storages. Water can move both downward and upward, referred to as capillary rise and transfer, in the soil column based on Brooks and Corey (1964). The capillary rise is related to changing soil moisture, which is relevant for processes like transpiration since transpiration mainly occurs when the water table exceeds the root depth.

2.2.3 Lateral processes

The Wflow sbm model enables the user to use two different flow routing approaches, namely the kinematic wave approach and local inertial approach, for both overland and channel flow. Both approaches are simplifications of the Saint-Venant momentum conservation equations, described by Chow et al. (1988) and both use the D8 network to spatially route water flow between pixels. The D8 network is a routing method that directs water from each grid cell to one of its eight neighbouring cells based on the steepest descent. The choice between these approaches involves a trade-off between computational time and simulation accuracy, where the kinematic wave approach is less accurate but requires less computational power.

The kinematic wave approach assumes that the topography controls water flow mostly and is described by Chow et al. (1988). It only considers the gravitational and friction terms of the Saint-Venant momentum equations (Chow et al., 1988). This means that, in a uniform channel or river, the peak velocity of the flood wave remains constant, and the flood wave propagates without distortion (Hartgring, 2023).

Like in the kinematic wave approach, the local inertial approach is an approximation of the Saint-Venant momentum conservation equation. It only neglects the convective acceleration term in the Saint-Venant equations according to Bates et al. (2010). By using this method, the backwater effect and flood wave attenuation are considered. The backwater effect means the influence of downstream conditions on upstream flow, and the flood wave attenuation means the reduction of flood peak magnitude as it moves downstream.

Overland & subsurface flow
In this thesis, the Wflow sbm model employs a kinematic wave approach for overland and subsurface flow to determine the runoff from cells. The kinematic wave approach is used because the local inertial approach increases computational time too much. While the kinematic wave approach is slightly less accurate for the overland flow, the reduction in computational time outweighs the loss of accuracy.

Channel flow
In this thesis, the local inertial approach is used for channel flow. This increases the computational time and accuracy of the model when simulating peak flows.

1D floodplain
Hydrological models do not model floodplains by default. However, Wflow sbm offers the possibility to incorporate an approximation of the floodplains through a 1D or 2D floodplain option. In this thesis, the 1D floodplain option is used.
In the 1D Floodplain option, a subgrid approach is used. The volume of water in a channel grid cell is firstly determined and, using a look-up table derived with the HAND methodology (Height Above

Nearest Drainage), its distribution among surrounding subgrid cells is estimated based on the original DEM resolution, which is finer than the model resolution. The water depth in the channel grid cell is corrected and used in the momentum equation. This water depth correction leads to extra friction and reduced water depth caused by smaller channels within each grid cell. Applying this correction decreases flow velocity, leading to a damping effect in the flow simulation. This approach is very similar to the subgrid approach described by Neal et al. (2012).

***re-infiltration* option**
Recently, the option '*re-infiltration*' has been added to the Wflow sbm model. This option allows for surface water to be re-infiltrated into the soil between time steps, which was originally not possible in the Wflow sbm model. The new *'re-infiltration'* option is still under development. The error in a test case was 6 mm per year when there was 1600 mm of rain, almost twice as much as the Vecht basin. In this new option, it is possible to set a threshold in mm (h_{thresh}), which blocks surface water from travelling to adjacent cells when this threshold is not exceeded. Surface water can then infiltrate in cells with a h_{thresh}, as long as the depth of the surface water is lower than the h_{thesh}.

2.3 Data

2.3.1 Measurement stations

To execute the calibration and validation of the model, discharge data is gathered. Precipitation data is gathered for a comparison of raster precipitation data with station measurement data to find the most accurate raster precipitation data. This is further described in section 2.3.2. The precipitation and discharge data of the measurement stations are gathered according to Figure 8.

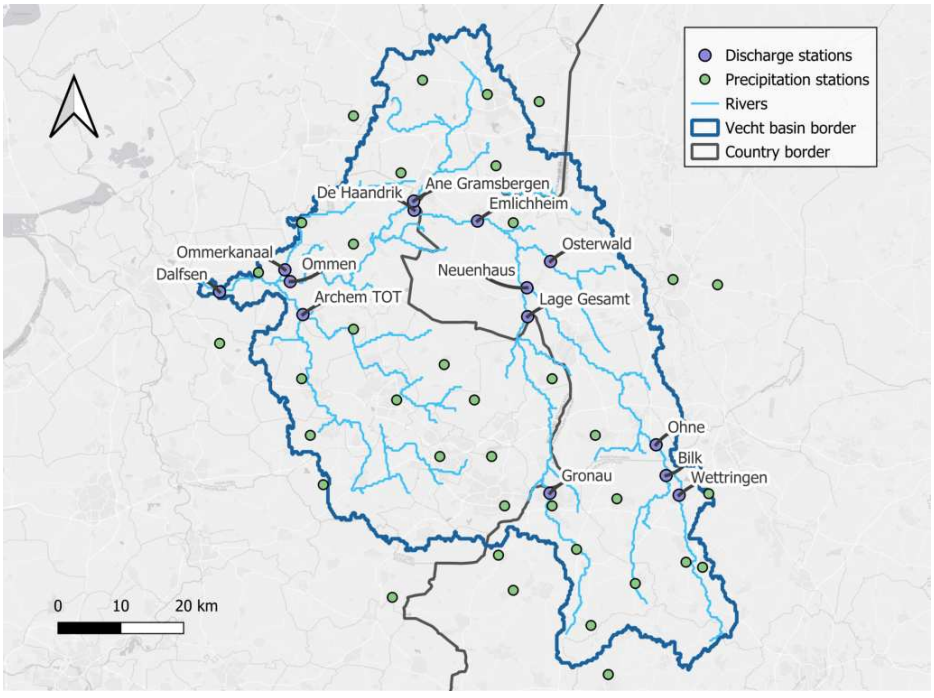

Figure 8: Overview of all available discharge and precipitation stations

2.3.2 Precipitation data

Wflow sbm requires the precipitation to be in a raster data type. Several data sources could be used and are shown in Table 4. The spatial and temporal scales of each data source and the period and area they cover are provided. A comparison is conducted to select the most suitable data source. The raster precipitation data should contain accurate data compared with data from precipitation stations (Figure 8). In addition to accuracy, precipitation data should have a sufficiently long time series and high resolution and cover the entire Vecht basin.

Table 4: Overview of data sources for precipitation data

Source	Name	Spatial Scale	Temporal Scale	From	Until	Extent
KNMI	rad_nl21_rac_mfbs_01h	2.4km	Hourly	1998-01-01	2024-05-01	Only NL
	rad_nl25_rac_mfbs_01h	1km	Hourly	2008-01-01	2024-05-01	Only NL
IRC	International Radar Composite (IRC)	1km	5min	2018-12-07	2024-05-01	NL, BE & GE
Copernicus	E-OBS	7km	Daily	1950-01-01	2024-6-31	Europe
	ERA5	17 km	Daily	1940-01-01	2024-06-31	Europe
DWD	RADOLAN	1km	Hourly	2006-01-01	2023-12-31	Entire Vecht

The precipitation data from the KNMI only covers the Dutch part of the basin, making it not a suitable source. The IRC precipitation data only contains data from 2018-12-07, which is too short as there are interesting dry and wet periods before 2018 that will be considered. E-OBS, ERA5 and RADOLAN are promising data sources and are further assessed. This assessment can be seen in Appendix E. In the end, E-OBS is considered the most accurate precipitation source.

2.3.3 Discharge data

Discharge data from different organizations is gathered. Rijkswaterstaat, Waterschap Drentse Overijsselse Delta, Waterschap Vechtstromen, Niedersächsischer Landesbetrieb für Wasserwirtschaft, Küsten- und Naturschutz (NLWKN), Landesamt für Nature, Umwelt und Verbraucherschutz Nordrhein-Westfalen (LANUV NRW), Deltares and FEWS-Vecht, which is the operational system used for water management in the Vecht. The result of all gathered data is shown in Figure 9. The stations are ordered from upstream to downstream, and green indicates the availability of discharge data. Some stations are not considered in this thesis since they are located close to a weir, leading to inaccurate data. Table C.1 in Appendix C shows all found data from the discharge stations and describes from what source it was gathered. The excluded stations in Figure 9 are shown in Appendix C.

For conducting sensitivity analysis, calibration, and validation, periods that align with the study's objectives are selected, thus periods with extreme high and low flows. Periods are selected based on their representation of extreme flows and the availability of comprehensive data across measurement stations.

For high flows, the top five years with the highest observed daily average discharges are identified for each

station. From these, the three years with the most consistently high discharges across multiple stations are chosen. This ensures that the selected years represent periods of extremely high flows with robust data coverage.

A similar approach is applied to identify low-flow periods. For each year, discharge volumes are calculated for the summer months (March through October) across all stations. Years with over 25 % missing data are excluded, and the three years with the lowest discharge volumes across stations are selected.

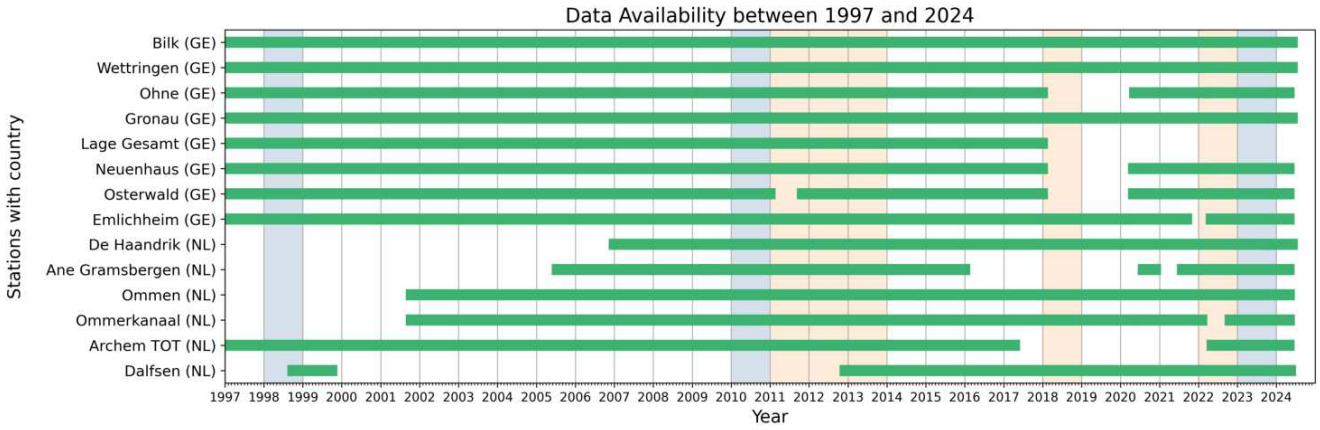

Figure 9: Data availability of discharge stations; green bars show the years with available data, blue years represent years of extremely high flows while red highlights years with extremely low flows. Station names can be found in Figure 8

2.3.4 Static maps

The parameters to simulate the hydrological processes in Wflow sbm are derived from data maps. The necessary maps in order to use Wflow sbm are listed in Table 5. The forcing data contains precipitation, potential evaporation and temperature. Since the spatial resolution of the potential evapotranspiration and temperature does not need to be as high as the precipitation, ERA5 is used. The static maps contain information to derive parameters used in Wflow sbm. The parameters are directly derived from the static maps by a look-up table or pedo-transfer functions. Pedotransfer functions (PTFs) are indirect methods for predicting soil hydraulic properties based on available soil data (Nasta et al., 2021). A study by Imhoff et al. (2020) formed the basis for the use of pedo-transfer functions in Wflow sbm. Tables B.4 and B.5 show the parameters derived from the land use look-up table and soil map using a PTF. Some model parameters are not derived from the static maps and have a default value.
To set up the Wflow sbm model, the datasets described in Table 5 are used.

Table 5: Used datasets to set-up the Wflow_sbm model for the Vecht basin

Category	**Maps**	**Dataset**	**Resolution**
Forcings	Precipitation	E-OBS	∼7 km
	Potential evapotranspiration	ERA5	∼17 km
	Temperature	ERA5	∼17 km
Static maps	Land cover (land use)	CORINE 2018	100 m
	River hydrography	MERIT Hydro	90 m
	Soil map	Soilgrids Version 2	250 m
	DEM map	MERIT Hydro	90 m
	LAI map	MODIS	500 m

For all parameters that are used in Wflow sbm and are derived from these maps, see Tables B.1, B.2 and B.3 in Appendix B.

3

Methods

An outline of the methods applied to evaluate the effects of nature-based solutions on high and low flows in the Vecht basin using Wflow is shown in Figure 10.

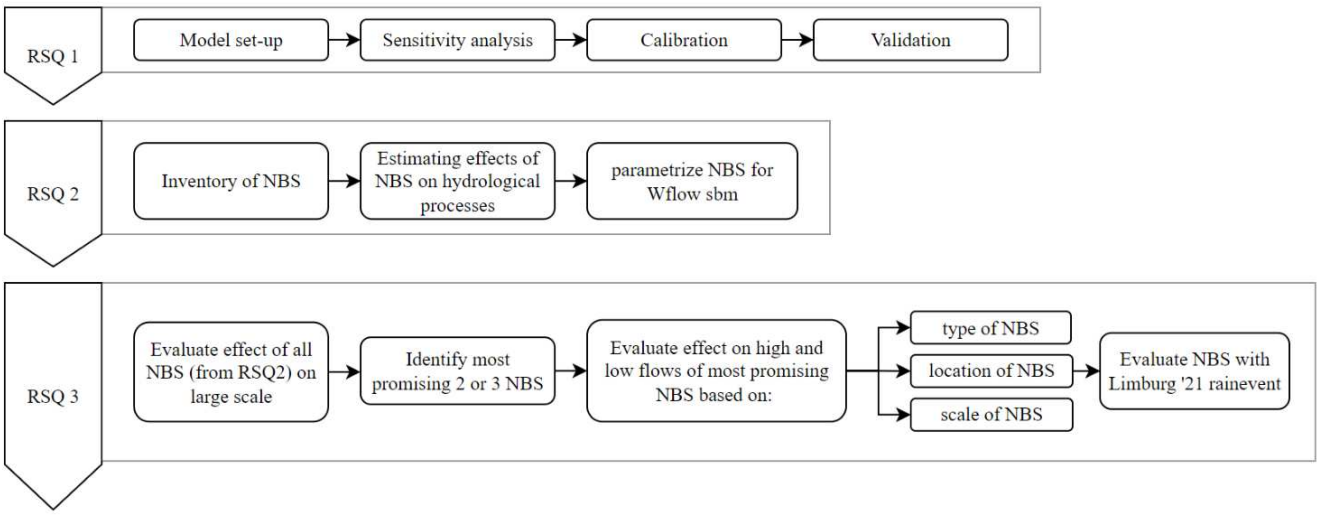

Figure 10: Methdology of study; *NBS* means nature-based solutions

In order to evaluate nature-based solutions, a Wflow sbm hydrological model is set up, calibrated and validated (research question 1). Next, an inventory of possible nature-based solutions is made with their application in the Wflow sbm model in research question 2. Lastly, the described nature-based solutions are evaluated using the Wflow sbm model covered in research question 3.

3.1 RQ1: Evaluation of Wflow sbm model under historic discharge series

The goal of the Wflow sbm model is to simulate the discharge in the river Vecht basin as close to reality as possible, with a specific focus on high and low flows since the nature-based solutions should affect these. Several steps are necessary before the model is ready to use, which are further described in the following sections.

3.1.1 Model set up

The Wflow sbm model can be set up when the input data is gathered. The model's resolution depends on the input data and runtime. The higher the resolution, the longer the runtime, which means there is a trade-off. Moreover, the resolution is also limited by the resolution of the input maps, meaning that the model resolution cannot be higher than the input maps.

Most parameters are derived from the input maps using pedo-transfer functions and look-up tables. Table B.4 shows the soil parameters derived from soil maps, and only *KsatHorFrac* is not derived using a pedo-transfer function. Table B.5 shows the parameters derived from land use maps. The most crucial default values are addressed in the sensitivity analysis and calibration; see sections 3.1.3 and 3.1.4.

The Wflow sbm model will be set up based on a 200 m x 200 m resolution. The highest resolution possible in Wflow sbm is 100 m x 100 m, but due to the computational time of such a resolution, the choice is made to use 200 m x 200 m. Simulating with a grid size of 100 m x 100 m would lead to four times longer computational times. This is expected to be sufficient for NBS simulation since these
The Wflow sbm model will have a timestep of 1 day. The study is interested in simulating the effects of nature-based solutions on high and low flows. An hourly timestep would be more appropriate for high flows, but for low flows, a daily timestep is sufficient. An hourly timestep would increase the runtime significantly.

3.1.2 Multi-objective function

To execute the sensitivity analysis and calibration, a performance metric is required. As stated by Booij and Krol (2010), when a model has multiple purposes, the sensitivity analysis and calibration should be considered in a multi-objective framework. In this study, Wflow sbm should be able to simulate a correct water balance and accurately simulate low and high flows. Thus, the multi-objective function should focus on this. These three aspects are further described below.

Low flows
The performance of the model during low flow periods is determined using the Nash-Sutcliffe of inverse flows; see equation 1. Since the inverse of the discharge is used, the absolute low flows have the largest influence on the value of NS_{inv}. This equation was initially used by Le Moine (2008) and also suggested by Pushpalatha et al. (2012) when the focus is on low flows. A value of one means that there is a perfect simulation.

$$NS_{inv} = 1 - \frac{\sum_{i=1}^{n} \left(q_{sim}^{i} - q_{obs}^{i}\right)^2}{\sum_{i=1}^{n} \left(q_{obs}^{i} - \overline{q}_{obs}\right)^2} \quad \text{with} \quad q^i = \frac{1}{Q^i} \tag{1}$$

Where,
Q^i = Discharge [m^3/s]
q_{sim} = Inverse of simulated discharge at day i [m^3/s]
q_{obs} = Inverse of observed discharge at day i [m^3/s]
$\overline{q_{obs}}$ = Mean of inverse of observed discharge [m^3/s]
n = Total number of timesteps
i = Time step

High flows
Where the NS_{inv} focuses on low flows, the NS_w focuses on high flows. The metric is designed to account

for the variability in the observed discharge, with the observed discharge being used as weights. This way, the high flows increasingly influence the value of NS_w, focusing on the higher part of the hydrograph. The value of NS_w ranges from negative infinity to 1. A value of 1 indicates a perfect match between the model simulations and the observed data, meaning the model's predictions are exactly on target. It was first used by Hundecha and Bárdossy (2004).

$$NS_w = 1 - \frac{\sum_{i=1}^{n} w_i \left(Q_{sim}^i - Q_{obs}^i\right)^2}{\sum_{i=1}^{n} w_i \left(Q_{obs}^i - \overline{Q}_{obs}\right)^2} \quad \text{with} \quad w_i = Q_{obs}^i \tag{2}$$

Where,
Q_{sim}^i = Simulated discharge at day i
Q_{obs}^i = Observed discharge at day i
$\overline{Q_{obs}}$ = Mean observed discharge over n days

Water balance
One way to examine whether the hydrological response is modelled accurately is to look at whether the model simulates the water balance correctly, which is reflected by the Relative Volume Error (RVE). Booij and Krol (2010) also indicate the effectiveness of the RVE to assess the accuracy of the simulations with regard to the water balance. An RVE of 0 indicates that the model perfectly predicts the total discharge volume, meaning the simulated and observed volumes are identical. A positive RVE value means an overestimation made by the model, while a negative RVE means an underestimation.

$$RVE = \frac{\sum_{i=1}^{n} \left(Q_{sim}^i - Q_{obs}^i\right)}{\sum_{i=1}^{n} (Q_{obs}^i)} \tag{3}$$

Multi-objective function
The previously described metrics can be combined into one multi-objective function. This is already done by ten Berge (2024) in a similar way to a study from Akhtar et al. (2009). The multi-objective function is described by equation 4 where a value of 1 means a perfect simulation since the optimal solution for NS_{inv} and NS_w is 1 and RVE is 0.

$$y_{combined} = \frac{NS_w + NS_{inv}}{2(1 + |RVE|)} \tag{4}$$

3.1.3 Sensitivity analysis

In the sensitivity analysis, the influence of several parameters on the multi-objective function is examined, as outlined in Table 6. The goal of the sensitivity analysis is to identify parameters that have the greatest impact on the model output (Herman et al., 2013). The sensitivity analysis can help to understand the model's behaviour and estimate the effect of parameter uncertainty on the output, $y_{combined}$. Parameters with minimal influence on model output contribute less to overall uncertainty, which helps to focus on parameters that contribute the most to model uncertainty and are relevant for calibration.

The Morris method was chosen for the sensitivity analysis in this study due to its computational efficiency (Herman et al., 2013). By varying one parameter at a time across a range of values and observing their influence on model outputs, the sensitivity of the model output based on its parameters can be identified.

As highlighted by Herman et al. (2013), the Morris method reduces the computational time of global sensitivity analysis for distributed hydrological models due to its relative simplicity.

The period used in the sensitivity analysis and calibration covers 2010 and 2011. In 2010, extreme high flows were measured in the Vecht river, while in 2011, extreme low flows were measured, as also depicted in Figure 9. The presence of high and low flows in 2010 and 2011 makes this period suitable for sensitivity analysis and calibration.

The selection of the parameters is based on the literature. Table 6 shows the parameters used in the sensitivity analysis, where all relevant parameters with a default value are included. Next to that, two parameters regarding vertical subsurface flow are included.

In Wflow sbm, the *KSatHorFrac* parameter is often used in sensitivity analysis and calibration due to its nature and influence. This parameter is related to the horizontal hydraulic conductivity. It is defined as the ratio between the horizontal and vertical hydraulic conductivity, $\frac{k_h}{K_v}$. Imhoff et al. (2020, p.11) identifies several parameters with significant influence and notes whether these parameters have a pedo-transfer function (PTF). The *KSatHorFrac* parameter is highlighted for its substantial impact and lack of an associated PTF, which is why it is frequently used in calibration efforts. Since it is difficult to measure the *KSatHorFrac*, no PTF is available. The default value of *KSatHorFrac* is set to 100. The value range of *KSatHorFrac* is set from 0.1 to 10,000 (Imhoff et al., 2020).

Besides the *KSatHorFrac*, there are several other interesting parameters for the sensitivity analysis. In Wflow sbm, the infiltrating water into the soil is split into two parts: the part that falls on pervious areas and the part that falls on non-pervious areas. Both have a different parameter for the maximum infiltration rates, namely *InfiltCapPath* (for non-pervious areas) and *InfiltCapSoil* (for pervious areas). These two parameters partly determine the amount of water that infiltrates into the soil or flows over the soil if it cannot infiltrate anymore, making them interesting for sensitivity analysis. The default value of *InfiltCapPath* is 5 $mm\ day^{-1}$ and of *InfiltCapSoil* is 600 $mm\ day^{-1}$.

As mentioned before, *KSatHorFrac* is related to the vertical hydraulic conductivity, defined by *KSatVer* in the Wflow sbm model. The vertical hydraulic conductivity is not uniform over the soil column but declines with depth. This decline is determined by a scaling parameter called *f-parameter*. Both the *KSatVer* and *f-parameter* are interesting parameters for the sensitivity analysis since their influence on water flow in the soil is large (Klein, 2022).

The parameter *RootDistPar* is a parameter that controls how roots of vegetation and trees are connected to the water table and is uniform over the whole basin, while there is no available pedo-transfer function for this parameter. This makes it interesting to assess the influence of this parameter in the sensitivity analysis. The default value for the *RootDistPar* is -500.

Table 6: Parameters in sensitivity analysis

Parameter	Description and effect	Unit	Default	Range
KSatHorFrac	KsatHorFrac is the ratio between horizontal and vertical saturated hydraulic conductivity, thereby determining the lateral connectivity between grid cells. A higher KsatHorFrac increases base flow while reducing peak discharges.	-	100	20 - 250
InfiltCapPath	Infiltration capacity of non-pervious (paved) areas. Increasing the infiltration capacity leads to less overland flow, a slower response time and lower peak discharge.	mm day^{-1}	5	5 - 60
InfiltCapSoil	Infiltration capacity of pervious (non-paved) areas. Increasing the infiltration capacity leads to less overland flow a slower response time and lower peak discharge.	mm day^{-1}	600	50 - 600
KSatVer	KsatVer is the vertical saturated hydraulic conductivity. Increasing KsatVer will lower the base flow and flatten the peaks.	mm h^{-1}	PTF	25% - 175% (scaled)
f parameter	The f-parameter determines the decay of KsatVer with depth. It controls the base flow recession and parts of the storm flow curve.	mm^{-1}	PTF	25% - 175% (scaled)
rootdistpar	The parameter rootdistpar defines the sharpness of the transition between fully wet and fully dry roots. It controls how roots are linked to the water table.	-	-500	-0.01 - -800

3.1.4 Calibration

During the calibration, parameter values are optimised to ensure the best possible performance of the model. The primary goal of calibration is to maximise the model's accuracy by minimising the differences between the simulated and observed discharge, depending on the objective function. Systematically adjusting parameters identified through sensitivity analysis increases the model performance based on the multi-objective function (Chapter 3.1.2). The calibration period covers 2010 and 2011, the same as in the sensitivity analysis.

The choice of calibration parameters is dependent on the results of the sensitivity analysis. Parameters with low influence on $y_{combined}$ are less suitable to use in the calibration, as it is difficult to increase the model performance with these parameters.

Next to that, the physical background of parameters also needs to be taken into account (Imhoff et al., 2020). Physically based parameters, like $KSatVer$, are supported by empirical data and theoretical principles, leaving little flexibility for adjustment without violating fundamental physical laws. The model should realistically simulate various hydrological processes by closely following physical laws, which is not possible if physically based parameters are changed significantly during calibration. In contrast, using parameters with less direct physical interpretations during calibration can provide greater flexibility for

compensating for unknown or poorly understood processes. These more abstract parameters can be used in calibration to enhance the model performance by mitigating errors in the model or data without conflicting with known physical laws present in the model.

Since there are multiple sub-catchments in the Vecht basin, shown in Figure 4, the model is calibrated on a sub-catchment level. This is also done for the current Wflow models of the Rhine and Meuse. Parameters are adjusted from upstream to downstream sub-catchments, as shown in Table 7. The area of the De Haandrik sub-catchment is very small and, therefore, considered the same as Emlichheim since these are located very closely.

Table 7: Order of calibration

Round	Sub-catchments
1	Bilk, Wettringen, Gronau, Osterwald, Ane Gramsbergen, Ommerkanaal, Archem TOT
2	Ohne, Neuenhaus, Lage Gesamt
3	Emlichheim
4	Ommen
5	Dalfsen

The Wflow sbm model will be calibrated manually. It is out of the scope of this study to use an extensive calibration algorithm due to the spatial resolution and runtime of the model. The model consists of NetCDF files that are adjusted by hand, making it difficult to use a calibration algorithm. The runtime of a Wflow sbm model for the described calibration period is also long for extensive calibration algorithms where thousands of simulations are necessary.

3.1.5 Validation

Validation is the final phase of the first research question. It serves as a final check to evaluate whether the calibrated model reliably simulates reality. While model parameters are adjusted during calibration to minimise the difference between simulated and observed discharge data, validation checks the model performance using the same multi-objective function based on an independent period that was not involved in the calibration process. The periods that are selected in the validation are based on Figure 9.

1998 - high flow
In October 1998, there were extremely high flows in the river Vecht observed due to intense precipitation (Klein & van der Vat, 2024). The data availability is sufficient, and especially in Germany, most discharge stations have discharge series during this period (Figure 9). The period used in the validation is from Jan. 1^{st} 1998 until March 28^{th} 1999.

2012, 2013 & 2014 - low flow
After the extreme high discharge event of 2010, several dry years came. It is interesting to model these years using Wflow sbm to evaluate how the model performs over multiple dry years. The evaluated period in the validation is from Jan. 1^{st} 2012 until September 28^{th} 2014. During this period, the data availability was high, making it suitable for validation.

2018 - low flow
The large precipitation deficit during 2018 led to extremely low discharges in the Vecht (Klein & van der

Vat, 2024). There is limited discharge data available for this period, making it hard to evaluate the model's performance in all sub-catchments. The period that is simulated is from Jan. 1^{st} 2018 until December 31^{th} 2018.

2023 - high flow
During Christmas 2023, the precipitation events across the Vecht basin were exceptionally intense, resulting in one of the highest recorded discharges in the region. This period presents the opportunity to test the model's response to extreme precipitation events. The period evaluated in the validation is from October 1^{st} 2023 until March 28^{th} 2024.

3.2 RQ2: Identification and parametrisation of nature-based solutions in the Wflow sbm model

In order to find nature-based solutions that can be implemented in the Wflow sbm model of the Vecht, a flowchart is used, which can be seen in Figure 11.

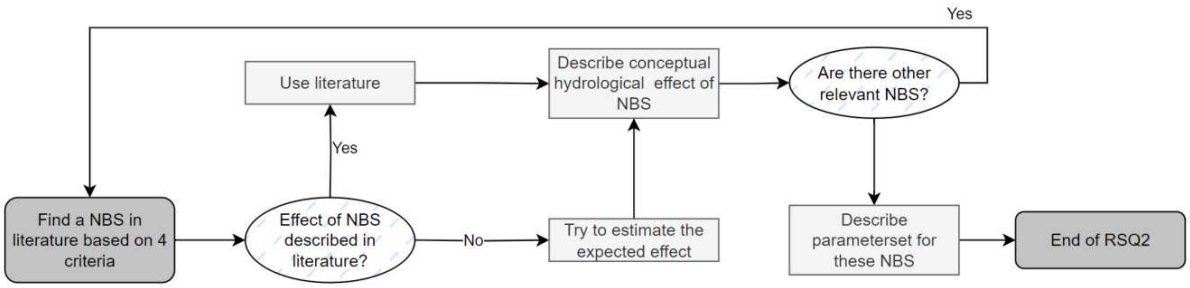

Figure 11: Flowchart of research question 2

Firstly, possible nature-based solutions are explored within the literature. In the literature, many different kinds of nature-based solutions can be found, but a lot of them are irrelevant to this study due to implementation in Wflow sbm or applicability in the Vecht basin. Therefore, some boundaries are formulated from which criteria are derived to select the NBS that are relevant to this study.

Boundaries
This study aims to evaluate the effects of nature-based solutions (NBS) on high and low flows in the Vecht River basin, meaning the nature-based solutions should be selected based on their ability to reduce peak flows and increase low flows. To guide this evaluation, Leegwater (2024) identifies the types of nature-based solutions that are relevant for the Vecht basin. The study emphasises that NbS interventions need to be implemented at a sufficiently large spatial scale to significantly impact the basin's hydrology. Therefore, the spatial scale of these solutions must be considered carefully.
Urban NBS, while being effective in managing stormwater and mitigating local urban flooding, are generally too limited in spatial scale to significantly affect basin-wide processes (Ferreira et al., 2022, p. 18). For instance, though beneficial in urban settings, green roofs, permeable pavements, or rain gardens are not expected to affect peaks or baseflows at basin scale (Ferreira et al., 2022, p. 18). Therefore, urban nature-based solutions are excluded from this study.

Given that a hydrological model is used to assess the performance of NBS, nature-based solutions should be selected that can be simulated using hydrological models. As outlined in Chapter 3.1.1, the Wflow

sbm model utilised in this study operates with a spatial resolution of 200 m x 200 m, meaning very local interventions are difficult to implement in the hydrological model. For instance, interventions such as river re-meandering, which require accurate and detailed flow simulations, are not well-suited for models like Wflow sbm. While Wflow sbm uses roughness coefficients for land and channels to simulate water flow, the model lacks accuracy, which is present in a hydrodynamic model, e.g. SOBEK, and the timestep of 1 day also makes this difficult. Moreover, the spatial resolution of the Wflow sbm model is too low to implement such local nature-based solutions. The nature-based solutions considered in this study will focus on broader land use/land cover practices and retention areas that can influence key hydrological processes such as infiltration and evaporation. Land and channel roughness may also be modified, but these modifications must occur on a large scale due to the use of Wflow sbm. Based on these boundaries, criteria for selecting nature-based solutions can be described.

Criteria

Based on the goals and boundaries, the following criteria are used to examine the literature in finding suitable nature-based solutions:

- Ability to implement NBS on a basin scale
- Applicability in the Wflow sbm model
- Have a positive effect on flood peak reduction and increasing low flows

The different hydrological processes that NBS can affect in the Wflow sbm model are highlighted in Table 8. This table helps in determining ways to implement NBS in the Wflow sbm model, while estimating their effects beforehand is also useful for further analysis of the nature-based solutions.

Table 8: Hydrological processes that NBS can affect in the Wflow sbm model

Hydrological process	**Description**
Interception	Interception refers to the portion of rainfall that falls on vegetation, which then evaporates before reaching the ground. Its portion is considered significant (Klaassen et al., 1998).
Soil & open water evaporation	The process in which water changes from liquid to gaseous state and is returned into the atmosphere. This can be from the soil and open waters (World Meteorological Organization, 2008).
Transpiration	Water is taken up by the roots of plants and transported through the plant. Transpiration is the evaporation from the leaves of the plant into the atmosphere (World Meteorological Organization, 2008).
Infiltration	Process in which water enters and moves down the soil profile at infiltration rate, which defines the speed of this process (Huffman et al., 2013).
River & land runoff	Portion of the precipitation that flows over land or through rivers. The rate of runoff depends mainly on the slope and roughness (Huffman et al., 2013).
Water retention	Areas in which water can be stored, e.g., lakes, tanks, ponds.

The parameterisation of nature-based solutions is dependent on the choice of nature-based solutions, which is yet unknown. The expected effects on the processes described in Table 8 can help to find parameters through which the nature-based solutions can be represented.

3.3 RQ3: Evaluation of nature-based solutions on high and low flows

The Wflow sbm model has been set up, calibrated, and validated, and an inventory of possible nature-based solutions has been made. These nature-based solutions can be implemented in the Wflow sbm model. In order to evaluate the nature-based solutions in a systematic way, the flowchart shown in Figure 12 is followed.

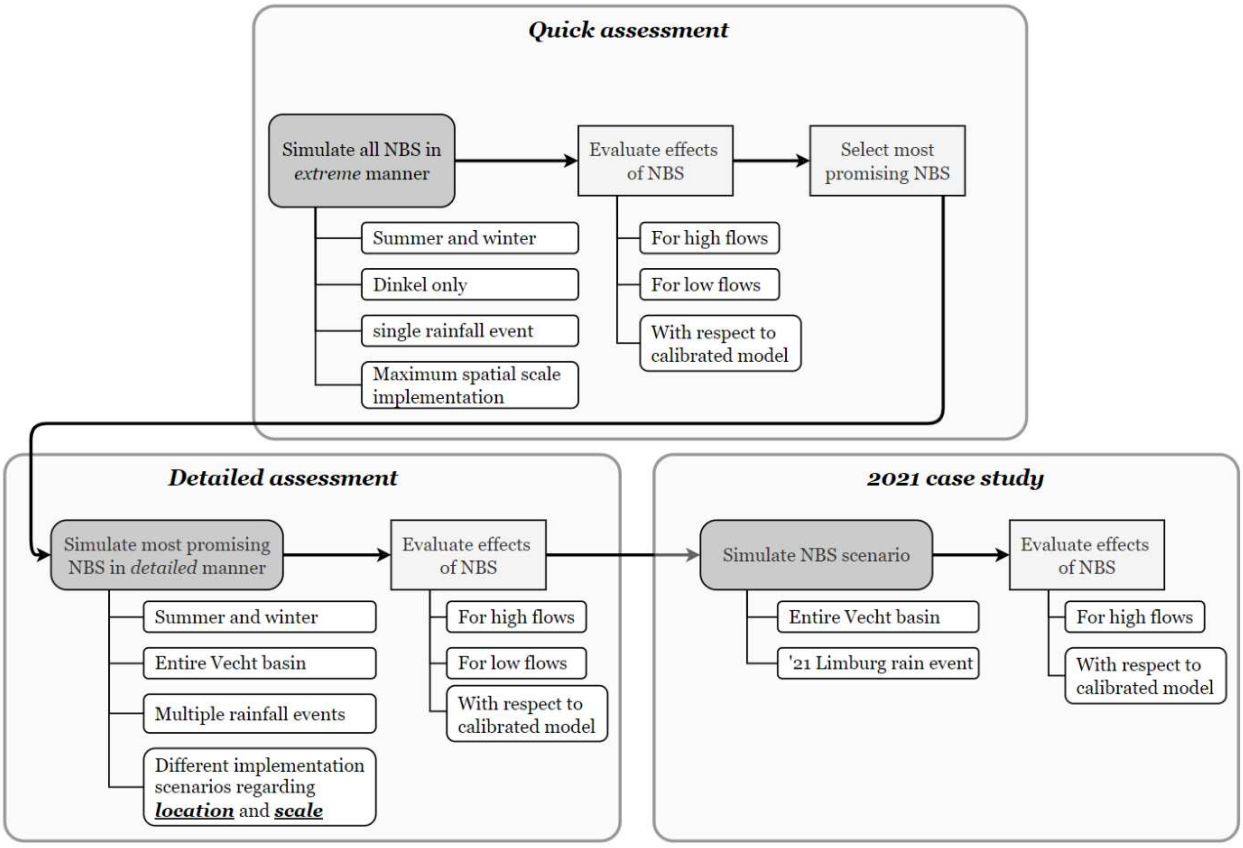

Figure 12: Flowchart of research question 3

The quick assessment aims to find which nature-based solutions have the most impact. The most promising NBS regarding their effects are then further evaluated in the detailed assessment. Lastly, some nature-based solutions scenarios will be tested under the extreme rainfall event in Limburg in 2021 when this is placed in the Vecht basin.

To evaluate the performance of nature-based solutions, relevant flow indicators for the overall water balance and low and high flows are used.

3.3.1 Flow indicators

Daily peak discharge

The daily peak discharge refers to the highest flow rate recorded during the simulation period in a river

during a single day, measured in m^3/s. By analysing daily peak discharge, one can evaluate how nature-based solutions (NBS) influence the high flow peaks and how much water may be stored in the system before ending up in the river (Ruangpan et al., 2020).

Flood volume
Flood volume is the total volume of water that flows through a river during a flood event when the discharge is above a threshold. This threshold is set to 100 m^3/s. Assessing flood volume provides insights into the severity and duration of flooding, which are essential for designing effective NBS to manage flood risks (Ruangpan et al., 2020). Using flood volume as an indicator provides insight into the water storage capacity of an area when implementing an NBS during heavy rain events.

Minimum 7-day average discharge (MAM7)
The Minimum 7-day Average Discharge (MAM7) represents the lowest average flow value over any seven-day period within the simulation period (Smakhtin, 2001). It is a standard low-flow statistic to assess drought conditions and water availability during dry periods. MAM7 can help to identify the effect of nature-based solutions on low flows in the Vecht river.

Average discharge
The average discharge is the mean flow rate over a specified period, providing an overall measure of the river flow regime. Changes in average discharge can indicate modifications to the catchment's hydrology, mainly the ratio between evaporation and discharge, due to the implementation of NBS (Ferreira et al., 2022).

3.3.2 Quick assessment

During the quick assessment, nature-based solutions are only simulated in the Dinkel, which is the upstream area of the discharge station Lage Gesamt shown in Figure I.1. The Dinkel has more or less a constant slope, and no large tributaries flow into the Dinkel. This makes the Dinkel suitable for a quick assessment of nature-based solutions, as the effects observed can be attributed directly to the interventions rather than to the timing of flows from certain areas within the Dinkel.

The nature-based solutions are implemented in the Dinkel on an extreme spatial scale. All areas, except for urban and open water areas, are changed according to the nature-based solution.

The Wflow sbm model will be set up according to Figure 13. 2016 and 2017 were average years, and 2018 was a dry year, allowing for the simulation of low flows. The model has initial conditions derived using the calibrated model based on a period from 2012 to 2015. Given the significant differences introduced by the implementation of nature-based solutions, an additional year (2016) of warm-up is included.

Then, two years of simulation are considered, 2017 and 2018. In 2017, a spatially uniform, one-day rain event was placed in the Dinkel sub-basin. By applying a uniform rain event to the Dinkel sub-basin, we can isolate and evaluate the basin's hydrological response under nature-based solutions. The rain event is based on the 2010 summer floods in Germany, where the maximum average daily rain in the Dinkel was equal to 82 mm according to the E-OBS dataset. This uniform, one-day rain event is placed on the Dinkel in two scenarios, namely in the summer (1st of July) and in the winter (1st of March), since the initial conditions have a significant influence on the hydrological response when a rainfall event occurs (Penning et al., 2024).

After 2017, the dry year of 2018 is simulated to evaluate the effect of nature-based solutions on low flows.

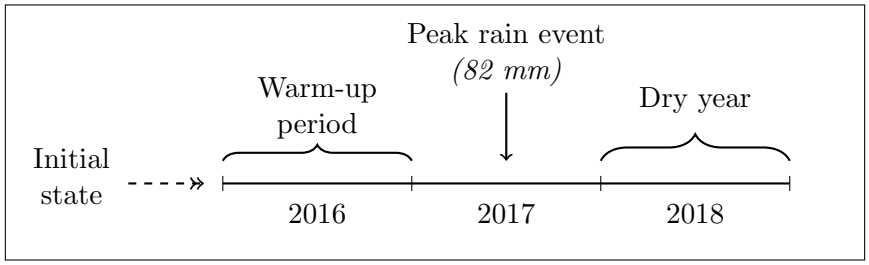

Figure 13: Concept of rainfall series in quick assessment

The effects of nature-based solutions on high and low flows in the quick assessment are evaluated using the daily peak discharge, MAM7 and the mean discharge. The daily peak discharge concerns the discharge wave induced by the rain event of 82 mm, while MAM7 and the mean discharge are determined based on the entire period. The flood volume is not included because the peak discharge is considered sufficient for the quick assessment. The hydrological behaviour of the basin can be identified using these three indices since both the extreme high and low flows are addressed, as well as the change in water balance through the average discharge.

3.3.3 Detailed assessment

In the detailed assessment, the most promising nature-based solutions from the quick assessment are further evaluated. As described in the third research question, the influence of the NBS location and spatial scale on high and low flows is investigated. This will be done in the detailed assessment. The selected nature-based solutions will be assessed in different locations and scales. They will be implemented scattered over the Vecht basin and more clustered, similar to a study by Marhaento et al. (2019). Next to that, the influence of varying rain events is evaluated to identify to what extent nature-based solutions have an effect, which also has been done in a study by Penning et al. (2024).

The Wflow sbm model is set up according to the figure below. The model has initial conditions based on the period of 2012 - 2015. The rainfall series of the detailed assessment consists of 6 years. Similarly, as in the quick assessment, one year of warm-up is added to the start of the simulation, given the significant changes to the basin when nature-based solutions are implemented.

In the second year (2017), spatially uniform, two-day rain events are placed on the entire Vecht basin. Three scenarios with different rain volumes under both summer and winter conditions are used, as in the quick assessment, and can be seen in Table 9. The 150 and 200 mm scenarios are based on 'stress tests' that Deltares performed for different catchments in the Netherlands. The 80 mm scenario is based on the rainfall event in an average catchment size (1656 km^2) of a Waterboard (1/50 exceedance probability), as described by Beersma et al. (2019, p. 134). These are not considered realistic rainfall events but help to evaluate the effectiveness of nature-based solutions for different rainfall intensities.

Table 9: Artifical rain events placed on the Vecht basin in 2017; the rainfall events are being referred to as their two-daily sum

Rainfall intensity	Total volume	Duration	Spatial layout	Source
100 mm/day	200 mm	2 days	Uniform	(Bruijn & Maas, 2023)
75 mm/day	150 mm	2 days	Uniform	(Bruijn & Maas, 2023)
40 mm/day	80 mm	2 days	Uniform	(Beersma et al., 2019, p.134)

The meteorological data from 2018 is repeated four times to simulate low flow conditions over multiple consecutive dry years. This approach allows for the assessment of nature-based solutions on multi-year low-flow periods and their cumulative impact on the hydrological response of the basin.

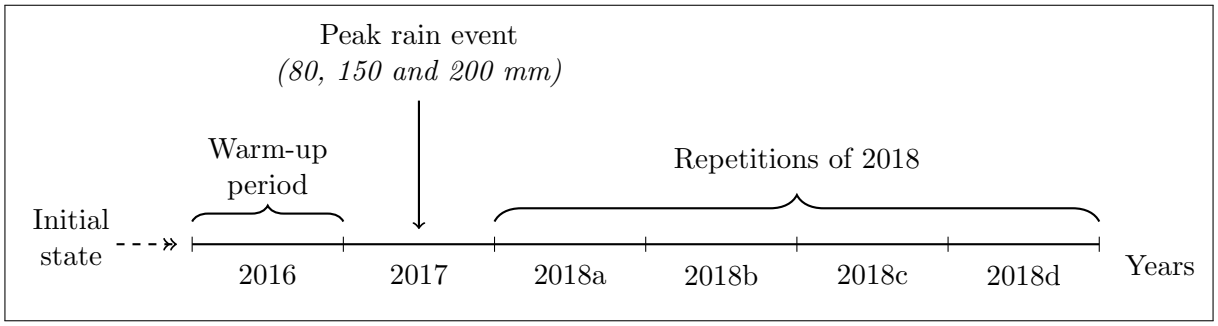

Figure 14: Concept of rainfall series in detailed assessment; years 1 - 2 are historical series of 2016 and 2017 with the peak rain event implemented in 2017; 2018a, b, c and d are repetitions of the dry year 2018; rain events are referred to as their two-daily sum and are placed under summer and winter conditions

In the detailed assessment, all four described flow indicators are used to evaluate the effects of the nature-based solutions on high and low flows in a detailed manner. The daily peak discharge and flood volume are based on the discharge wave induced by the 2-daily rain events, while the MAM7 and mean discharge are based on the entire period of six years.

3.3.4 Evaluation of Limburg '21 rain event

Several NBS scenarios from the detailed assessment are evaluated using the rainfall data from the flooding in Limburg in 2021. As stated by Bruijn and Slager (2022), the rain event that caused the floods in Limburg and parts of Belgium and Germany could also occur elsewhere in the Netherlands. Due to climate change, the frequency and intensity of such rain events are expected to increase, even though these kinds of events are still rare (Tradowsky et al., 2023). Where the detailed assessment helps to assess the influence of location and spatial scale of nature-based solutions, the evaluation of the Limburg '21 rain event helps estimate the effect under a realistic rain scenario. Some warning levels were obtained through waterboard Vechtstromen and NLWKN and will be used to put the simulated discharges in perspective.

The RADFLOOD21 precipitation dataset is used, which has been applied in other Wflow sbm studies (Hartgring, 2023). RADFLOOD21 is a radar product obtained through careful processing of weather radar measurements and merging with validated rain gauge data (Journée et al., 2023). It contains precipitation data for six days, from the 12th of July until the 17th of July 2021. The original temporal resolution is 5 minutes with a precipitation unit of 0.1 mm. The following alterations have been made so it can be used in the Vecht Wflow sbm model.

- Change of coordinates
- Determination of daily precipitation sum
- Converting the unit from 0.1 mm to mm

To account for spatial variability of rain, the 2021 rain event was placed over three locations in the Vecht basin, focusing on the peak rainfall event on the 14th of July, as shown in Figure 15. The peak rain event was placed over the Regge sub-catchment, the main Vecht at Emlichheim, and the Dinkel sub-catchment, as can be seen in Figures 15a, 15b and 15c.

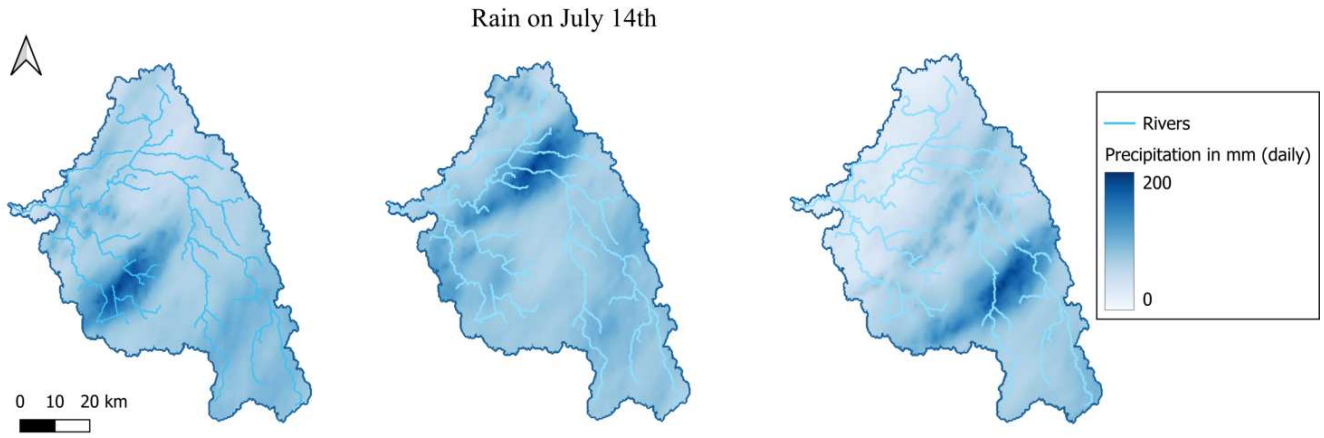

(a) Above Regge **(b)** Above Emlichheim **(c)** Above Dinkel

Figure 15: Locations of '21 Limburg peak rain event

The model simulation period is summarised below. The same initial state and warm-up period are used as in the detailed assessment. At the beginning of July, the six days containing precipitation data from '21 Limburg are placed in the three locations described above.

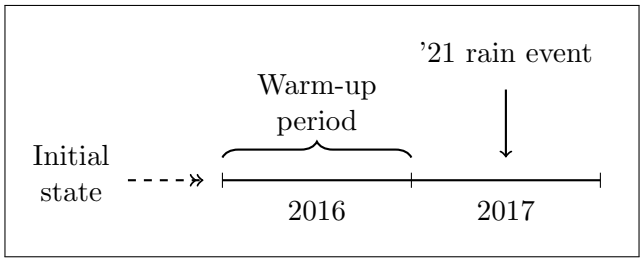

Figure 16: Concept of rainfall series in '21 evaluation

The effects of the nature-based solutions will be evaluated using hydrographs.

4

Results

4.1 RQ1: Evaluation of Wflow sbm model under historic discharge series

As all input data is gathered, see Table 5, the Wflow sbm model can be set up. Parameters that cannot be derived from the input data have a default value, see Table B.6. The initialisation of the model includes setting the spatial and temporal resolution. The model has a spatial resolution of 200 m x 200 m and uses a daily time step. Simulating one year of the Vecht model on the Deltares network computer with an Intel(R) Xeon(R) Platinum 8358 CPU and 32 GB RAM memory takes about 5-6 minutes. Next, the sensitivity analysis will be conducted.

4.1.1 Sensitivity Analysis

The influence of the parameters described in section 3.1.3 is evaluated in the sensitivity analysis. A heatmap and the cumulative discharge at Emlichheim present the results. The heatmap shows the different parameter values on the x-axis and the discharge stations on the y-axis, and the number and colours describe the performance of the model run based on the multi-objective function. Overall, Wflow sbm performs better on the multi-objective function in the German part of the basin, likely due to the lower human interventions in this part of the Vecht, which cannot be simulated through Wflow sbm. Emlichheim is used as a reference in the results because it is the last discharge station in the German part of the Vecht.

The parameters *KsatVer*, *f-parameter*, and *KsatHorFrac* were found to have a significant influence on the discharge; their effects are presented below. In contrast, *InfiltCapPath*, *InfiltCapSoil*, and *rootdistpar* did not significantly affect the discharge and are discussed in Appendix G.

KSatVer

KSatVer has a significant impact, as shown in Figure 17. If the value of *KSatVer* is 1.5, it means that the entire map of *KSatVer* is multiplied by this factor. The heatmap shows that there is not a single multiplication factor (or scale factor) of *KSatVer* that leads to the best results, but it differs per discharge station.

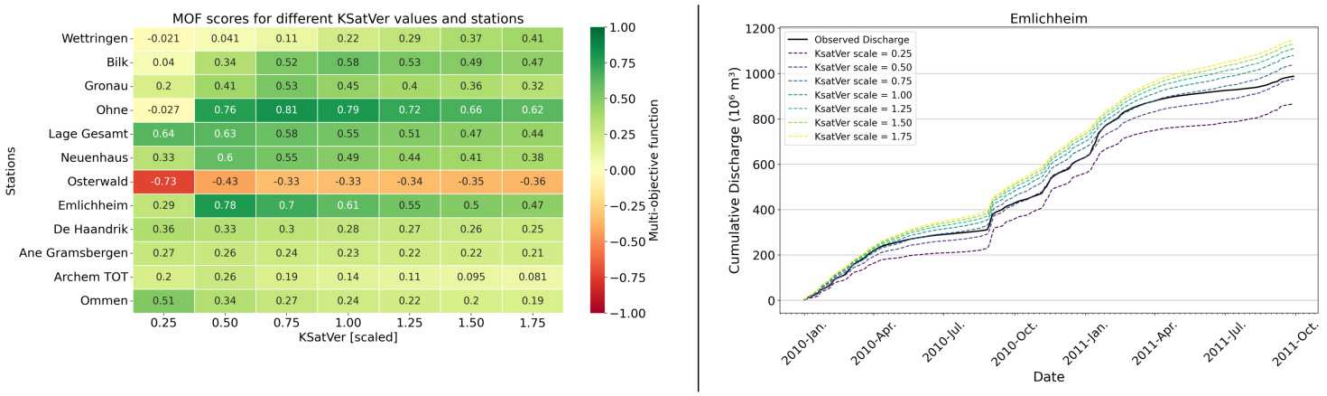

Figure 17: Results sensitivity analysis KSatVer; scores on multi-objective function (MOF) for different stations in heatmap on the left; the right figure shows cumulative discharge at Emlichheim

f-parameter

f-parameter has, like *KSatVer*, significant influence on the model results since they both influence the same process, namely the vertical hydraulic conductivity over the soil depth. Again, the optimal multiplication factor differs per discharge station.

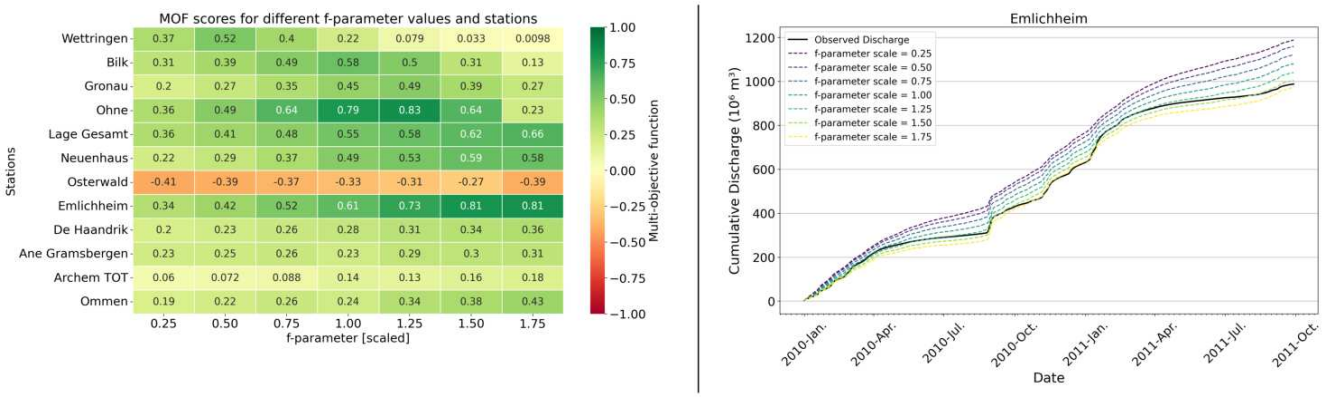

Figure 18: Results sensitivity analysis f-parameter; scores on multi-objective function (MOF) for different stations in heatmap on the left; the right figure shows cumulative discharge at Emlichheim

KSatHorFrac

Changing the value of *KSatHorFrac* has large effects on the results. The optimal value of *KSatHorFrac* is different per station, although most stations find their optimal value around 40 to 100. *KSatHorFrac* determines the horizontal saturated conductivity based on the vertical hydraulic conductivity. When *KSatHorFrac* increases, water can flow quicker in the lateral direction through the soil, meaning more water ends up as discharge in the river. Moreover, water has less time to evaporate from the soil, which is also an important reason for the higher discharge volume; see cumulative discharge at Emlichheim.

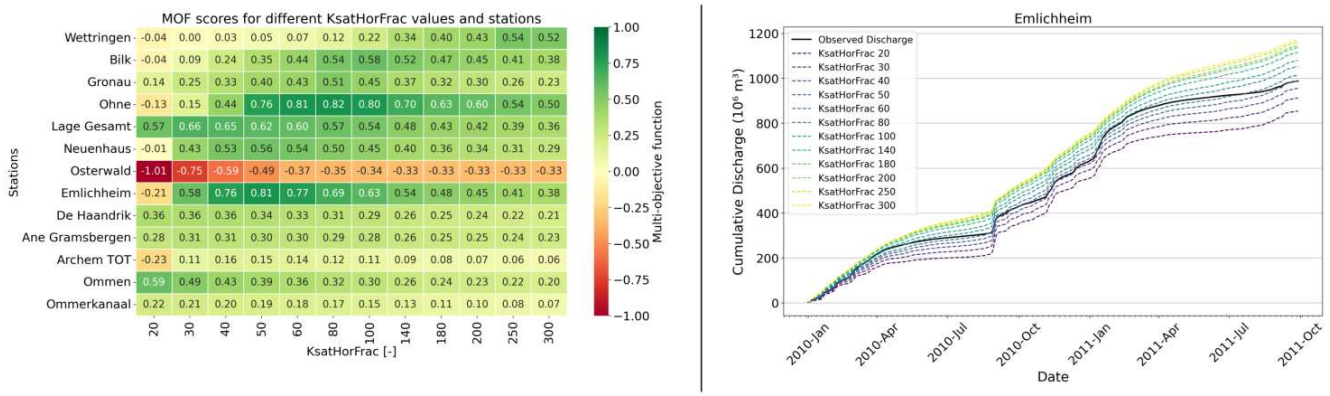

Figure 19: Results sensitivity analysis KsatHorFrac; scores on multi-objective function (MOF) for different stations in heatmap on the left; the right figure shows cumulative discharge at Emlichheim

4.1.2 Calibration

The sensitivity analysis identified three parameters as having the most significant impact on the model: *KSatVer*, *f-parameter*, and *KSatHorFrac*. Since these parameters are related to the same process within the Wflow SBM model, their similar levels of influence are both consistent and expected. Among them, *KSatVer* is the most physically meaningful parameter, as it is directly derived from soil properties using a pedo-transfer function. This strong connection to real-world processes makes *KSatVer* less suitable for calibration. In contrast, the *f-parameter* and *KSatHorFrac* lack pedo-transfer functions and are difficult to measure. Therefore, these two parameters are suitable for calibration.

The calibration is done on sub-catchment level, beginning with the upstream sub-catchments and then followed by the downstream sub-catchments. The sensitivity analysis indicated variation in the optimal parameter value between sub-catchments for both *KsatHorFrac* and *f-parameter*, see figures 19 and 18. This supports the idea of calibrating per sub-catchment. First, *KSatHorFrac* is calibrated since this parameter has slightly more influence.

For upstream catchments, the optimal value of KSatHorFrac is fixed to the sub-catchments corresponding to Figure 19. This is done according to the different calibration rounds presented in Table 7. This results in the spatial distribution of KsatHorFrac shown in Figure 20a.

For the *f-parameter*, the procedure is the same. The difference is that this parameter is scaled since it has spatial variance among cells. The optimal value for the *f-parameter* for most sub-catchments is around 1, meaning no change, except for the sub-catchments with stations Archem TOT, Osterwald and Ohne. This results in the spatial distribution of multiplication factors for *f-parameter* according to Figure 20b.

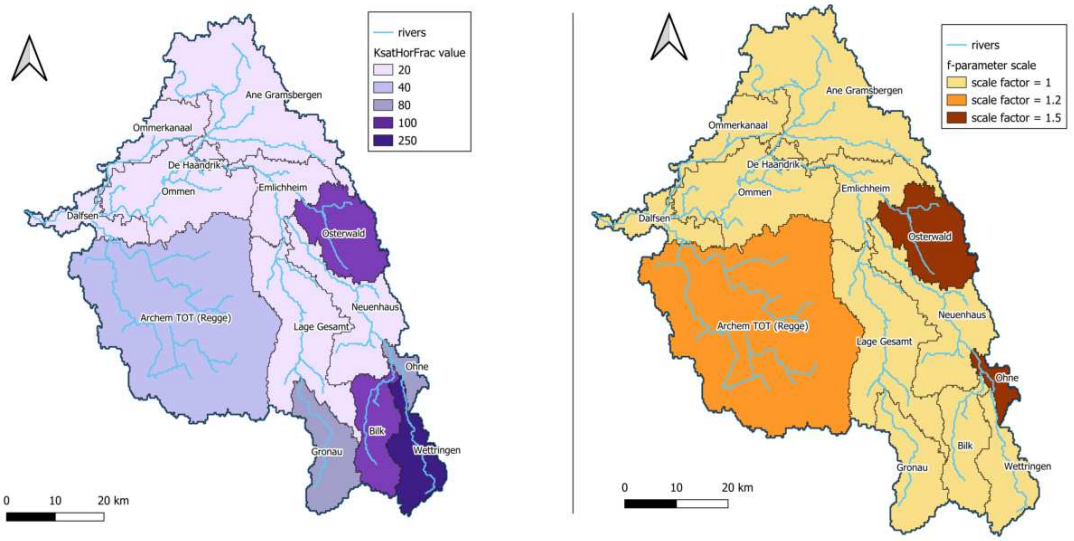

(a) *KsatHorFrac* values after calibration **(b)** Scale factors of *f-parameter* after calibration

Figure 20: Comparison of areas with uniform and sub-catchment-specific parameter values for *KSatHorFrac* and *f-parameter*

The performance of the calibrated model during the calibration period is shown in Table 10. All components of the multi-objective function are shown. The performance on the multi-objective function ranges between 0.5 and 0.76 for German stations, except for Osterwald, while the performance for Dutch stations ranges from 0.15 to 0.49. The German part of the Vecht river is simulated more accurately compared to the Dutch part. Overall, the performance is considered satisfactory.

Despite being located close to each other without additional flow contributions between them, there is a significant performance difference between Emlichheim and De Haandrik. Especially in the low-flow regime, the observed discharges at Emlichheim and De Haandrik are not similar. This is evident in Table 10, where the performance on NSE_{inv} at De Haandrik is much lower compared to Emlichheim. This may be due to a weir at De Haandrik, which disrupts the natural flow and affects discharge measurements.

Osterwald is the only station showing a negative value on the multi-objective function score due to an overestimation of the discharge throughout the calibration period. Osterwald is a small sub-catchment with a baseflow lower than 5 m^3/s, thus a small difference in m^3/s between the simulated and observed discharge can lead to a poor multi-objective function value.

Table 10: Performance of the calibrated model; NSE_{inv} is the inverse of Nash-Sutcliffe Efficiency, NSE_w is the weighted Nash-Sutcliffe Efficiency, RVE is the Relative Volume Error, OF is multi-objective function (see section 3.1.2)

Station		**NSE_{inv}**	**NSE_w**	**RVE**	**OF**
Wettringen	GE	0.33	0.79	-0.03	0.54
Bilk	GE	0.26	0.94	0.03	0.58
Gronau	GE	0.34	0.86	0.17	0.51
Ohne	GE	0.55	0.95	0.02	0.73
Neuenhaus	GE	0.48	0.72	-0.01	0.60
Lage Gesamt	GE	0.64	0.87	-0.14	0.66
Osterwald	GE	0.21	-1.15	0.72	-0.27
Emlichheim	GE	0.70	0.89	-0.04	0.76
De Haandrik	NL	-0.09	0.85	0.00	0.38
Ane Gramsbergen	NL	-0.01	0.58	-0.03	0.28
Ommen	NL	0.25	0.81	0.08	0.49
Ommerkanaal	NL	-0.03	0.65	-0.39	0.22
Archem TOT	NL	0.67	-0.26	0.39	0.15
Dalfsen	NL				

The hydrographs at two stations of the calibrated model are shown in Figure 21. Among all analysed stations, Emlichheim shows the best performance, whereas Archem TOT shows the poorest performance (excluding Osterwald). Overall, the calibration reflects reasonable model accuracy in capturing discharge variation. Both the simulated low and high flows are similar to the observed discharge. At Archem TOT, the model performs poorly on the RVE and NS_w. Archem TOT aggregates data from two discharge stations, making its observed time series less reliable compared to single-station measurements like those at Emlichheim. Following the flood event in August 2010, the model performance at Archem TOT became worse, which could suggest a malfunction or inaccuracy at one of the contributing discharge stations, although this remains uncertain.

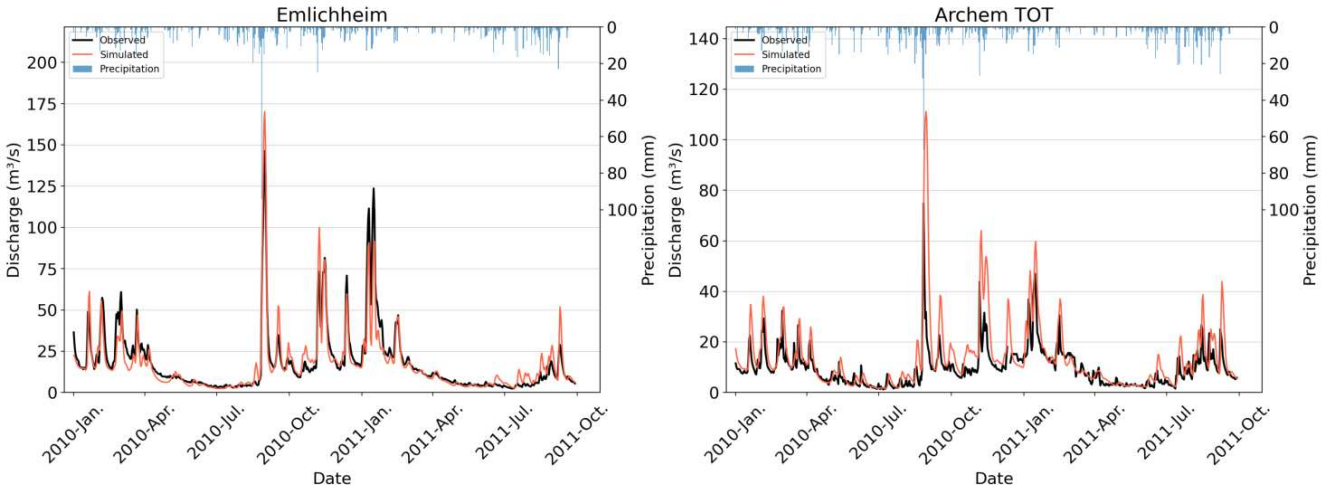

(a) Emlichheim (GE)

(b) Archem TOT (NL)

Figure 21: Hydrographs at two stations during the calibration period

4.1.3 Validation

Table 11 shows the model performance over the four validation periods. When there is no value, there was no observed discharge data during the validation period. The hydrographs of all stations of the four validation periods are shown in Appendix H.

Across all stations, the model performance varies significantly over the different periods, highlighting the difficulty of maintaining consistent accuracy over time. For instance, station Wetteringen in Germany demonstrates a significant decrease in performance from 1998 (0.64) to 2012 (0.26) and 2018 (0.14), but the model's accuracy improves somewhat in 2023 (0.64). A similar trend is observed at Bilk, where the performance declines in 2018 (0.33) and improves in 2023 (0.63). Overall, 2018 shows lower accuracies among stations compared to the other years. Additionally, 2018 also lacks observed discharge data for multiple stations.

German stations show a higher and more stable performance in 1998, 2012, and 2023, particularly when compared to Dutch stations. Neuenhaus and Emlichheim especially have high scores on the multi-objective function. However, Osterwald deviates from this pattern, showing more significant variations in performance. Specifically, the performance at Osterwald in 2023 is poor, primarily due to RVE. As illustrated in Figure H.4, the Wflow sbm model overestimates the discharge throughout the entire period when compared to the measurements.

Ane Gramsbergen performs poorly in both available periods, 2012 and 2023. Especially in 2023, the Wflow sbm model struggles to simulate the observed discharge. The performance of Archem TOT is also poor among all validation periods, but 2023 stands out due to its negative score of -0.65 on the multi-objective function. Figure 22b shows the hydrograph of Archem TOT. The observed time series at Archem TOT in 2023 shows unexpected patterns; moreover, there are small periods where data is missing. The rainfall volume is also not proportional to the amount of observed discharge. Therefore, the observed discharge series is not considered trustworthy.

The decrease in performance at the Dutch discharge stations compared to German stations is expected to be caused by the many canals and weirs in the Dutch part of the Vecht, which are not modelled by Wflow sbm.

The overall trend from Table 11 highlights the difficulty to maintain consistent accuracy in the model results over different periods. This is particularly clear in 2018, where several stations show a marked drop in performance compared to the other years. The reduced accuracy during this period may reflect limitations in the model's ability to capture the low flows of that period.

Table 11: Results of the validation; performance based on the multi-objective function; empty space means no observed discharge data during the period; 2012 means the period 2012 until 2014

		Multi-objective function score			
Station		**1998**	**2012**	**2018**	**2023**
Wettringen	GE	0.64	0.26	0.14	0.64
Bilk	GE	0.64	0.59	0.33	0.63
Gronau	GE	0.44	0.45	0.25	0.69
Ohne	GE	0.67	0.68		0.67
Neuenhaus	GE	0.81	0.67		0.72
Lage Gesamt	GE	0.79	0.63		
Osterwald	GE	0.04	0.22		-0.64
Emlichheim	GE	0.80	0.76	0.69	0.58
De Haandrik	NL			0.15	0.38
Ane Gramsbergen	NL		0.20		-0.88
Ommen	NL		0.47	0.53	0.51
Ommerkanaal	NL		0.24	0.20	0.29
Archem TOT	NL	0.27	0.05		-0.65
Dalfsen	NL	0.53	0.19	0.28	0.07

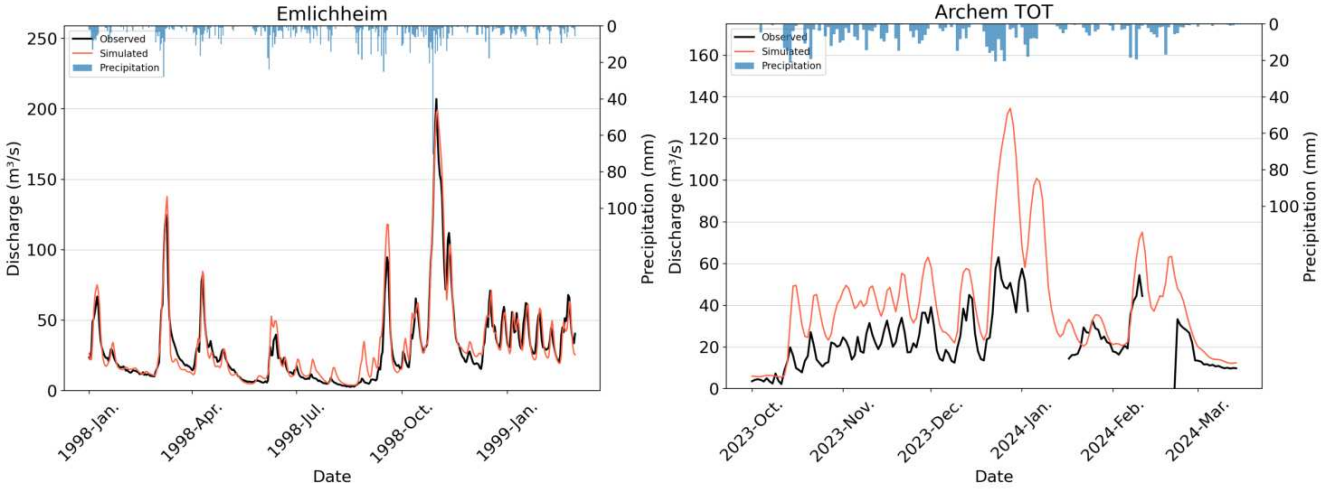

(a) Emlichheim (GE) during 1998 period

(b) Archem TOT (NL) during 2023 period

Figure 22: Hydrographs at Emlichheim and Archem TOT during two different validation periods

4.2 RQ2: Identification and parametrisation of nature-based solutions in the Wflow sbm model

4.2.1 Selection of nature-based solutions

Table 12 shows the nature-based solutions found with their expected effect on the hydrological processes from Table 8.
There are four categories among the nature-based solutions: land use change, changing roughness, enhancing infiltration and water storage.

Land use change
Within the category of land use change, two NBS are considered: afforestation and agroforestry. The predominant current land use in the Vecht is agriculture, as shown in Table 2. Land use change affects hydrological processes such as interception, evaporation, transpiration, infiltration, runoff (through friction), and water retention capacity. It is seen as a dominant factor in the hydrological response of a basin (Babaremu et al., 2024). Afforestation significantly impacts total evaporation and infiltration in a basin, thereby significantly affecting the water balance. Agroforestry, which involves alternating agricultural crops with forest strips, is expected to show similar effects as afforestation but to a lesser extent (Penning et al., 2024).

Changing roughness
Roughness influences both overland and channel flow; increased roughness slows down water flow (Senior et al., 2022). To slow down overland flow, thus altering the land roughness, terracing seems to be a promising measure. Terracing is a soil conservation practice applied to reduce surface runoff, where ridges or 'steps' are constructed along sloped areas (Fashaho et al., 2020). The roughness of the channel can be increased by applying leaky dams and bed vegetation. Leaky dams are structures made of natural materials, such as logs or branches, placed in rivers to slow down water flow. Bed vegetation, increasing the amount of plants and vegetation on the river bed, also affects the roughness of the channel.

Enhancing infiltration
Nature-based solutions that enhance infiltration can raise groundwater tables and alter the ratio between surface and subsurface flow. Changing agricultural practices is a promising approach to increase soil infiltration, particularly in the Vecht basin, where agriculture is predominant. Several agricultural practices can contribute to the improvement of the infiltration. Mulching involves applying organic material to the soil surface, which helps to retain moisture and improve soil structure (Simsek et al., 2017). Planting cover crops during the off-season prevents fields from being fallow, maintaining soil health and reducing erosion (S. Haruna et al., 2018). Stimulating soil fauna, through e.g. earthworms, enhances soil biodiversity and improves infiltration (Amanze et al., 2024). No-till farming eliminates the use of heavy machinery, minimising soil disturbance and leading to improved soil structure and increased infiltration (Maule & Reed, 1993).

Water storage
The construction of natural wetlands is an effective way to store water within a basin. By creating or restoring wetlands, water is retained in specific areas using small dams and dikes. Water is trapped, preventing it from moving laterally and forcing it to infiltrate into the ground. During precipitation events, the wetlands act as natural sponges, absorbing excess water and reducing overland runoff (Ferreira et al., 2022).

Table 12: Selection and expected effects of nature-based solutions on hydrological processes

	NBS	Description	Interception	Evaporation	Transpiration	Infiltration	Runoff	Water retention	Source
Land use change	Afforestation/ reforestation	Planting trees in deforested or non-forested areas	++	+	++	+	–	+	(Ferreira et al., 2022)
	Agroforestry	Agricultural fields with strips of forest	+	+	+	+	–	+	(Penning et al., 2024)
Changing roughness	Leaky dams	Semi-permeable structures to slow water flow	0	0	0	0	–	-	(Bourke et al., 2022)
	Terracing	Creating terraces on slopes	0	+	0	++	–	+	(Penning et al., 2024) (Debele et al., 2023)
	Vegetation of river bed	Planting vegetation within riverbeds	0	0	0	0	-	0	(Penning et al., 2024) (Ourloglou et al., 2020) (Ferreira et al., 2022)
Enhancing infiltration	Mulching	Applying organic materials to the soil surface	0	–	0	+	-	+	(Penning et al., 2024) (Ferreira et al., 2022)
	Cover crops	Growing crops to cover the soil during off-seasons	0	+	+	+	-	+	(Blanco-Canqui, 2024)
	Stimulating soil fauna	Enhancing soil biodiversity and activity (worms etc.)	0	0	0	+	-	+	(Penning et al., 2024)
	Reduced/no-till farming	Limiting soil disturbance to maintain structure	0	0	0	+	-	+	(Penning et al., 2024)
Storage	Wetlands	Creating areas designed to store water	0	++	0	++	–	++	(Penning et al., 2024) (Ferreira et al., 2022)

4.2.2 Implementation of nature-based solutions in Wflow sbm

For each of the nature-based solution types, an implementation strategy is presented below:

- **Land use change**
  In Wflow sbm, several parameters are derived from the land use map, as shown in Table B.5. These parameters only affect the interception, evaporation, transpiration and roughness. The Leaf Area Index (LAI) map, which specifies the monthly LAI values for each grid cell and is relevant for interception, remains static and does not automatically adjust to land use changes. To include LAI variability due to land use change, an average LAI value is determined for each land use type on a monthly basis. When land use changes occur, the LAI values are updated according to the new land use type, see Table I.1.
  In reality, land use also influences infiltration; for example, forests typically have higher infiltration than agricultural land. Therefore, when implementing land use change in the model, infiltration parameters need to be adjusted as well. This can be achieved by modifying *InfiltCapSoil* and *KSatVer*, where *InfiltCapSoil* represents the infiltration capacity and *KSatVer* is the vertical hydraulic conductivity of the soil. Since *InfiltCapSoil* is not likely to affect the infiltration, as its value is already 600 mm/day, the increase in infiltration is modelled by adjusting *KSatVer* using a scaling factor based on the NBS.

- **Changing roughness**
  The roughness in Wflow sbm is split into two components, namely the roughness of the river and the roughness of all other land. The roughness in Wflow sbm is described by Manning's value and can be altered to represent nature-based solutions that influence the surface roughness.

- **Enhancing infiltration**
  The infiltration can be altered with *KSatVer*, similar to the approach in **land use change**.

- **Storage**
  Using the recently added '*re-infiltration*' option, explained in section 2.2.1, wetlands can be represented by setting a h_{thresh} to certain areas where surface water can be stored and re-infiltrated up to a certain threshold. To accurately simulate discharge using the *re-infiltration* approach, the model requires recalibration. However, this step was not taken due to time constraints.

The maps and parameters are summarised in Table 13.

Table 13: Relevant model maps/parameters to implement nature-based solutions

NBS type	**Wflow maps/parameters changed**
Land use change	*land use map* + *LAI map* + *KSatVer*
Changing roughness	Mannings roughness n (channel or land)
Enhancing infiltration	*KSatVer*
Storage	*land use map* + h_{thresh} (new *re-infiltration* option)

4.2.3 Parametrisation of nature-based solutions

The parametrisation of the nature-based solutions of Table 12 is shown in Table 14 and 15. Table 14 shows the values for eight parameters that depend on the land use type. Non-irrigated arable land, which is an agricultural land use, and natural grasslands are added to the table to compare the parameter changes. As can be seen, agroforestry and afforestation lead to longer rooting depths of 400 mm. Next

to that, the roughness increases, as well as the fraction of wood. The LAI map is changed depending on the land use. The averaged LAI values corresponding to land uses are shown in Table I.1 in Appendix I.1.

Table 14: Land use type and their corresponding parameter values; K_{ext} is the extinction coefficient (to calculate canopy gap fraction); N land is the Manning's roughness coefficient of land; PathFrac is the fraction of compacted area per grid cell; RootingDepth is the depth of roots in mm; Sl is the specific leaf storage in mm; Swood is the fraction of wood in the vegetation in mm; WaterFrac is the fraction of water area per grid cell; $alpha_1$ is the root water uptake reduction at soil water pressure head (Deltares, n.d.)

Land use	**Description**	**Kext**	**N land**	**PathFrac**	**RootingDepth**	**Sl**	**Swood**	**WaterFrac**	**alpha$_{h1}$**
211	Non-irrigated arable land	0.6	0.20	0.0	390.4	0.127	0.00	0.0	0
244	Agro-forestry areas	0.8	0.50	0.0	406.0	0.039	0.50	0.0	1
311	Broad-leaved forest	0.8	0.60	0.0	429.8	0.036	0.50	0.0	1
312	Coniferous forest	0.8	0.40	0.0	382.1	0.045	0.50	0.0	1
313	Mixed forest	0.8	0.50	0.0	406.0	0.039	0.50	0.0	1
321	Natural grassland	0.6	0.15	0.0	106.8	0.127	0.01	0.0	1

In Table 15, the parameterization for each nature-based solution is shown. A detailed description of the parameter values found in Table 15 can be found in Appendix I. A detailed description of the found parameter values can be found in Appendix I.1.

Table 15: Nature-based solutions (NBS) clustered by type and their corresponding parameter changes; parameters regarding land use change depicted in Table 14; KsatVer, Manning's land and Manning's channel are multiplication factors; h_{thresh} is in mm; Appendix I.1 gives a detailed description of parametrisation

Type	**NBS**	**Land Use**	**KsatVer** [1]	**Manning's n (channel)** [1]	**Manning's n (land)** [1]	**h$_{thresh}$ (m)**	**Source**
Land use-change	Afforestation (broad-leaved forest)	*Broad-leaved forest* [2]*+ LAI*	1.5				(Horel et al., 2015) (Li et al., 2019) (Yao et al., 2015)
	Afforestation (Coniferous forest)	*Coniferous forest* [2] *+ LAI*	1.5				Same as above
	Afforestation (mixed forest)	*Mixed forest* [2] *+ LAI*	1.5				Same as above
	Agroforestry	*Agroforestry* [2] *+ LAI*	1.25 [4]				
Changing roughness	Leaky dams			1.5			(Senior et al., 2022)
	Terracing		1.3		1.4		(USDA, 2017) (Bisolo et al., 2024) (Fashaho et al., 2020)
	Vegetation of the river bed			1.38			(Ourloglou et al., 2020) (Arcement & Schneider, 1989)
Enhancing infiltration	Mulching		1.2				(Simsek et al., 2017) (Kahlon et al., 2013)
	Cover crops		1.1 to 1.5 [3]				(S. Haruna et al., 2018) (S. I. Haruna et al., 2023) (Peters & Haruna, 2024)
	Stimulating soil fauna		1.2				(Zare et al., 2010) (Amanze et al., 2024)
	Reduced/no till farming		1.05 to 1.4 [3]				(Fér et al., 2020) (Maule & Reed, 1993) (He et al., 2009)
Storage	Wetlands	*Wetland* [5]				0.20	(Cooper et al., 2020)

[1] Values represent multiplication factor.
[2] All non-urban area is changed, while urban area is kept as it is.
[3] Literature is contradictory thus a lower and upper bound is used.
[4] *KsatVer* of agroforestry is assumed to be half of afforestation.
[5] An h_{thresh} (threshold) of 0.20 m is added for water retention.

4.3 RQ3: Evaluation of nature-based solutions on high and low flows

4.3.1 Quick assessment

The implementation of the nature-based solutions, as presented in Table 15, is shown in Appendix I.2.1. The results of the quick assessment are shown in Figures 23 and 24, where the effects of the nature-based solutions are quantified using the daily peak discharge, MAM7 and average discharge.

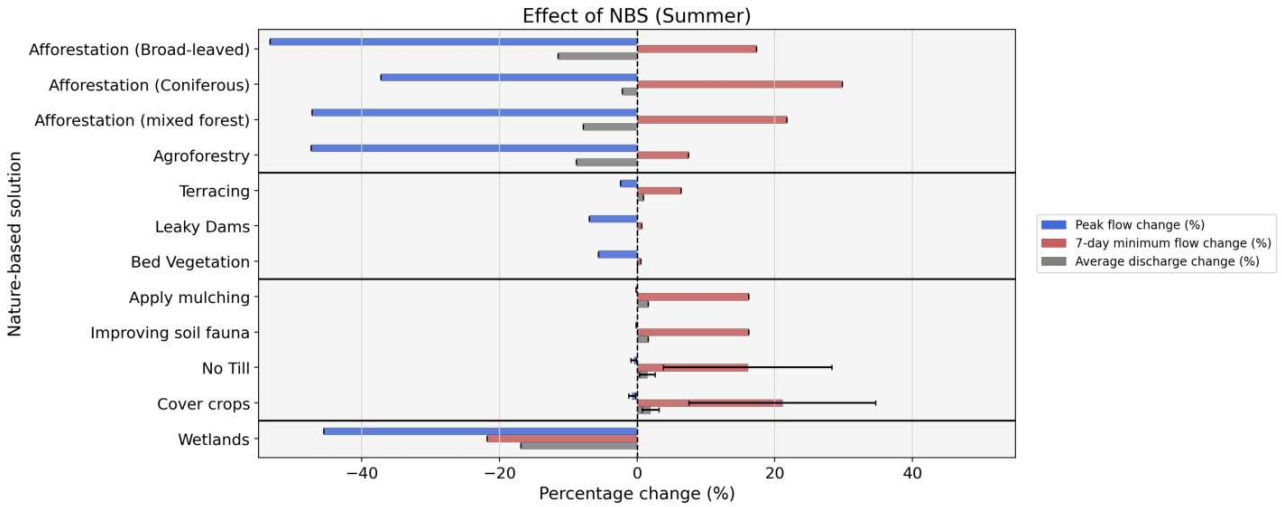

Figure 23: Effects of nature-based solutions, relative to the calibrated model, under extreme rainfall event with summer conditions in the Dinkel sub-catchment; daily peak discharge change is based on the discharge wave caused by the uniform 2-daily rain event at the beginning of July; MAM7 and mean discharge are based on the period of 2017 and 2018

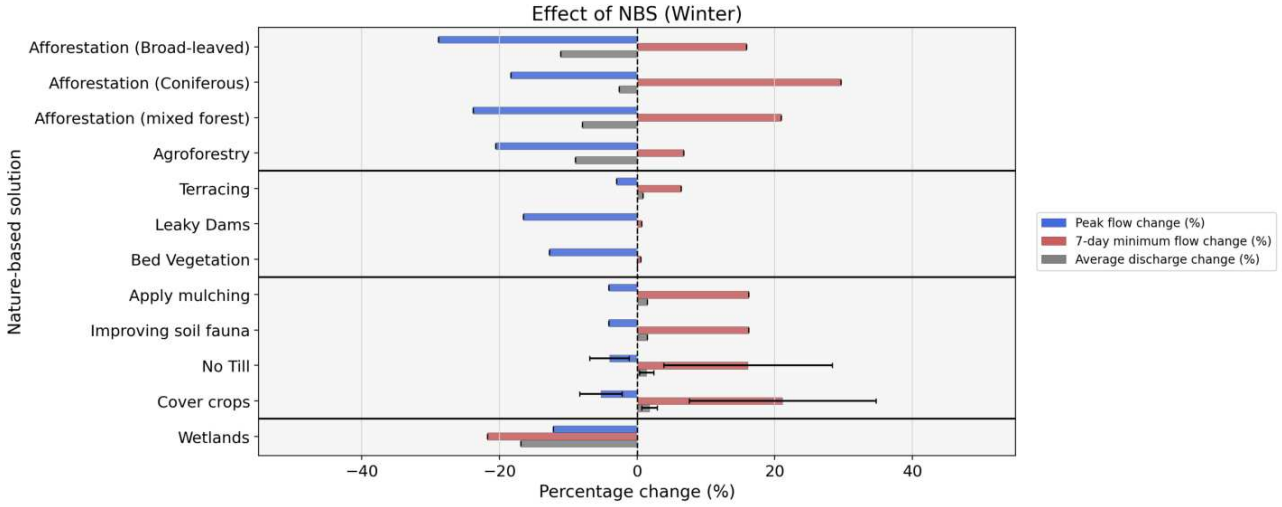

Figure 24: Effects of nature-based solutions, relative to the calibrated model, under extreme rainfall event with winter conditions in the Dinkel sub-catchment; daily peak discharge change is based on the discharge wave caused by the uniform 2-daily rain event at the beginning of March; MAM7 and mean discharge are based on the period of 2017 and 2018

The nature-based solutions within the four categories (land use change, changing roughness, etc.) show a similar trend for the three presented metrics. It is important to consider that the changes are presented in percentages relative to the reference situation. In the case of a 7-day minimum discharge, a change of only a few cubic meters per second can already result in a significant relative change.

In the case of afforestation and agroforestry, the peak flow is reduced significantly, especially under summer conditions. This is less under winter conditions, but still a reduction of 20 to 30 % is observed. Between the forest types, broad-leaved afforestation seems to have the most effect regarding peak flow change (-49 %). On the other hand, coniferous afforestation leads to the highest increase in 7-day minimum discharge (+30 %). The effects of the mixed forest lie between these two types. Agroforestry shows similar effects on the peak flow change but leads to less increase of the 7-day minimum discharge, probably due to the lower increase of *KsatVer* compared to the afforestation scenarios, see Table 15.

In all nature-based solutions under the type 'changing roughness', the peak flow is reduced between 5 and 15 %. Changing roughness has little effect on the 7-day minimum discharge and the average discharge.

The different agricultural practices under 'enhancing infiltration' lead to a very small peak flow reduction of maximum 9 % in case of cover crops under winter conditions. The 7-day minimum discharge is increased between 5 and 35 % among all NBS under 'enhancing infiltration'. This is about the same as the afforestation scenarios.

Constructing wetlands, which falls under the type 'water storage', lead to similar effects as afforestation according to Figures 23 and 24. The peak flow is reduced by m 15 and 45 % for the winter and summer conditions respectively, while the 7-day minimum discharge is increased by around 15 %. The average discharge is decreased due to a change in the water balance, which can be attributed to the increase in infiltration and evaporation.

From the quick assessment, the most promising nature-based solutions are afforestation and wetlands when considering changes in peak flow, 7-day minimum discharge and average discharge. Afforestation shows a decrease in peak flow and an increase in MAM7, while wetlands lead to a decrease in both peak flow and low flows. These effects are smaller in winter conditions than in summer conditions but are still significant. Afforestation and wetlands are further evaluated in the detailed assessment.

4.3.2 Detailed assessment

The representations of the nature-based solutions in Wflow sbm are shown in Figures 25 and 26. For both afforestation and wetlands, there are 5 scenarios each.

Figure 25 shows the afforestation scenarios in the detailed assessment. The top row presents scenarios with afforestation of 75 %, 50 %, and 25 % coverage of the catchment area. In these cases, forest cover is progressively increased and uniformly distributed across the basin to evaluate the impacts of small forest plots, as the grid size is 200 m, which are spread over the entire basin at various scales. The bottom row shows scenarios in which forests are spatially concentrated at both the downstream and the upstream part of the basin. Both cover 50 % of the basin, allowing comparison with the scenario of 50 % scattered afforestation. In all grid cells where afforestation occurs, the parameters are altered according to Table 15.

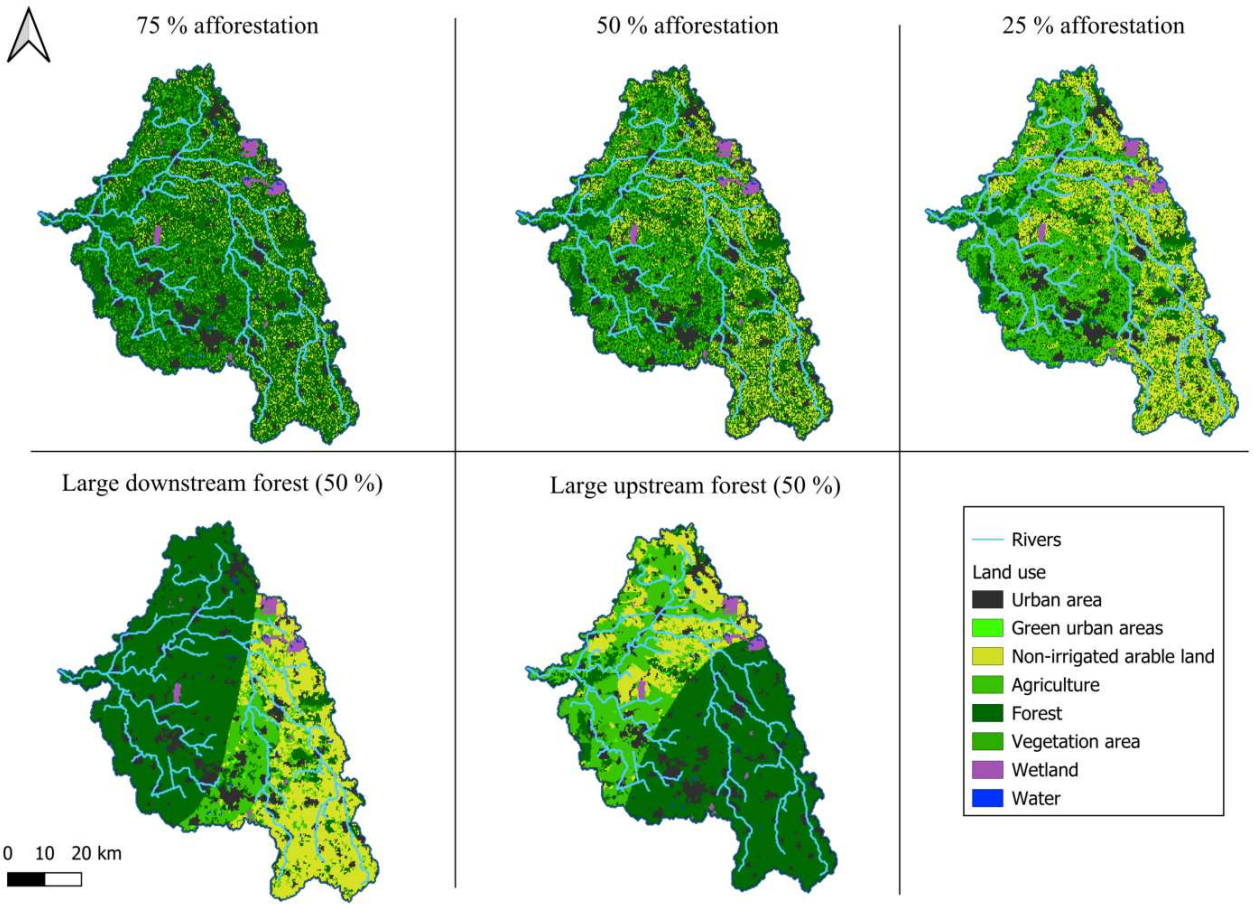

Figure 25: Implementation of afforestation in different scenarios in the detailed assessment; afforestation type is 'mixed forest'

Figure 26 displays scenarios with wetlands. The top row illustrates scattered wetland implementations at two coverage levels, 50 % and 25 %, as well as a clustered wetland scenario with a 25 % coverage. The effects of wetlands over various scales can be evaluated. Next to that, the influence between small, widespread plots of wetlands and more clustered areas of wetlands can be compared. The bottom row shows spatially concentrated wetlands that cover 50 % of the area downstream in one scenario and upstream in the other. Similarly to the afforestation scenarios, this allows for the evaluation of influence by location of the wetlands.

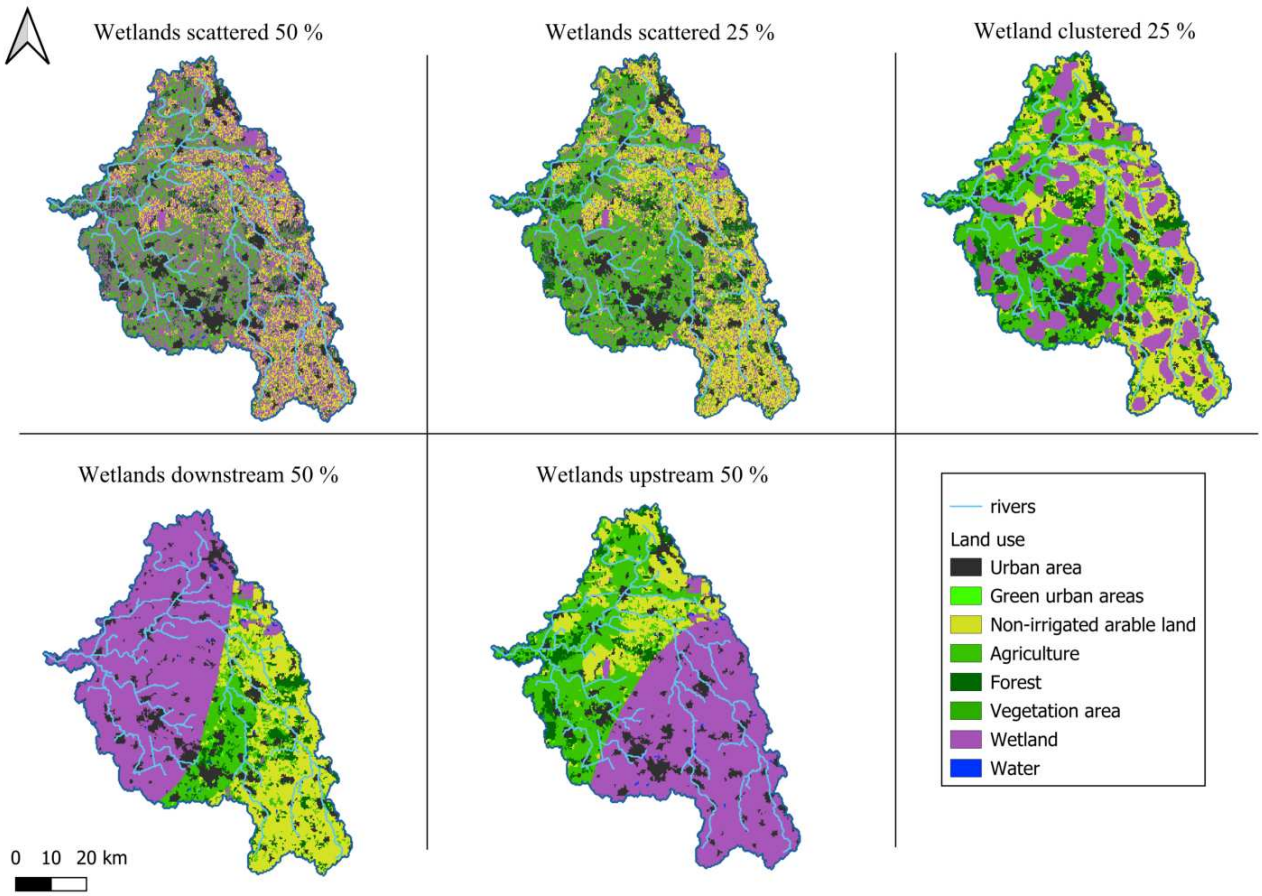

Figure 26: Implementation of wetlands in different scenarios in the detailed assessment

The nature-based solutions are simulated through Wflow sbm and compared with the reference situation under precipitation series according to section 3.3.2. Figure 27 and Figure I.8 show hydrographs with afforestation and wetland scenarios at Dalfsen under summer and winter conditions with a 2-daily sum of rain of 200 mm.

There is a major difference in the discharge due to the rain event under summer and winter conditions. Under winter conditions, there is much more soil moisture, meaning that the soil can take up less water from precipitation, and more water is discharged to the river. This leads to a much higher and wider discharge peak. The discharge wave is about 80 m^3/s higher at its peak and $\sim$ 5 - 7 days longer. Under summer conditions, the peak flow is $\sim$ 430 and under winter conditions $\sim$ 510 m^3/s.

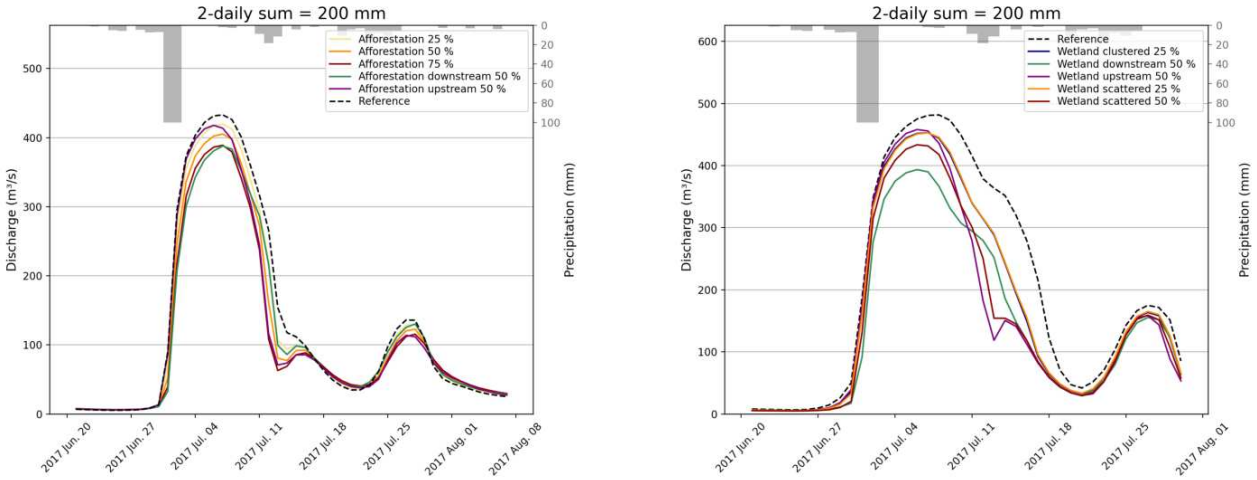

(a) Effects of afforestation at Dalfsen

(b) Effects of wetlands at Dalfsen

Figure 27: Hydrographs at Dalfsen with afforestation and wetland scenarios under summer conditions with a uniform 2-daily rain event with a sum of 200 mm

Since the *'re-infiltration'* option is used only in case of wetlands, the reference models (dashed lines) are not the same between figures 27a and 27b.

Under summer conditions, the scenarios of 75 % afforestation and 50 % afforestation downstream show a similar reduction of the peak discharge, followed by the 50 % afforestation and the 25 % afforestation and 50 % upstream afforestation have the least effect on peak discharge. Increasing the scale of afforestation from 25 % to 75 % has increasingly more effect on the discharge, which is expected. Between the allocation of a 50% forest, downstream afforestation has more effect on the discharge at Dalfsen compared to the upstream afforestation.

In the case of wetlands, the most effective scenario to reduce the peak discharge is the 50 % wetland downstream, followed by the scattered wetlands of 50 %. The scenarios wetland clustered 25 %, wetland scattered 25 % and wetland upstream 50 % show a very similar decrease in peak discharge. The course of the discharge wave is very different between the different wetland scenarios, which is especially clear under summer conditions.

The effects of the nature-based solutions under summer conditions on the peak flow reduction, minimum 7-day average discharge, and average discharge are determined and shown in Figure 28. The effects of nature-based solutions under winter conditions can be seen in Figure I.9 and are similar under summer and winter conditions except for the peak flow reduction, which is, relatively speaking, significantly less under winter conditions. Since the trends are the same, only the effects under summer conditions are shown here.

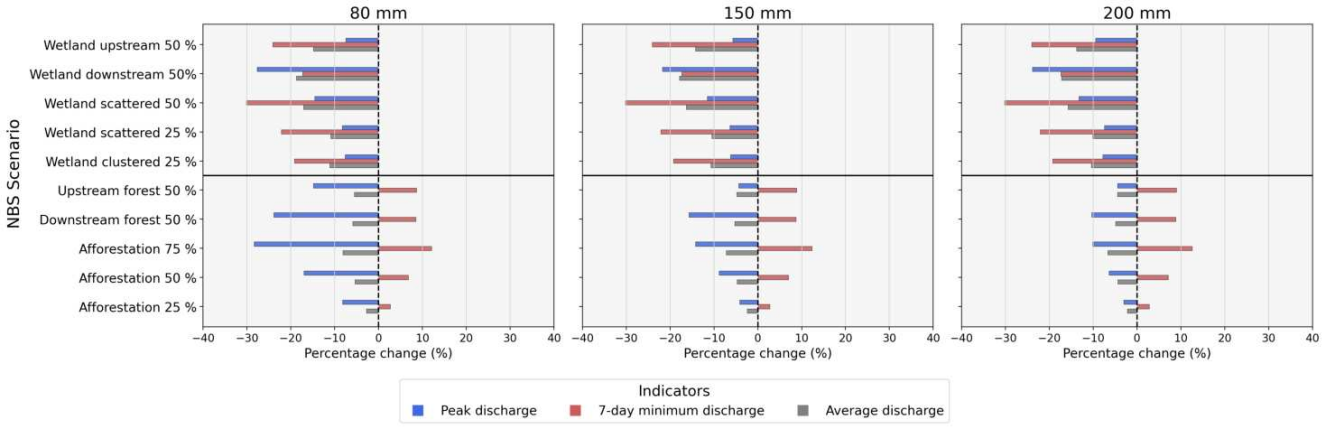

Figure 28: Effects of nature-based solution scenarios at Dalfsen under summer conditions for 3 different rain events; daily peak discharge change is based on the discharge wave caused by the uniform 2-daily rain event at the beginning of July; MAM7 and mean discharge are based on the period of 2017 and 2018

When wetlands are compared with afforestation, quite different effects are observed. Both lead to a decrease in daily peak discharge in quite similar ways when similar scenarios are compared, like scattered 25, scattered 50 %, and the upstream and downstream 50 % wetlands/afforestation scenarios. On the other hand, the effects on the minimum average 7-day discharge (MAM7) and the average discharge between afforestation and wetlands are significantly different. The MAM7 decreases when wetlands are implemented, while afforestation leads to an increase in the MAM7. The large change in evaporation under wetlands is expected to cause the decrease of MAM7, see Figure I.6. The larger the scale of the nature-based solution, the greater the increase or decrease of MAM7. The average discharge of the Vecht basin is more affected by wetlands than afforestation. In the wetlands, this is reduced by 10 to 20 %, while in the case of afforestation, it is reduced by 3 to 8 %.

Figure 29 shows the change in MAM7 in m^3/s. While the relative difference to the reference model can be significant, the differences in daily m^3/s are rather low, between 0 and 1.7 m^3/s. This is due to the low amount of discharge during summer periods in the Vecht.

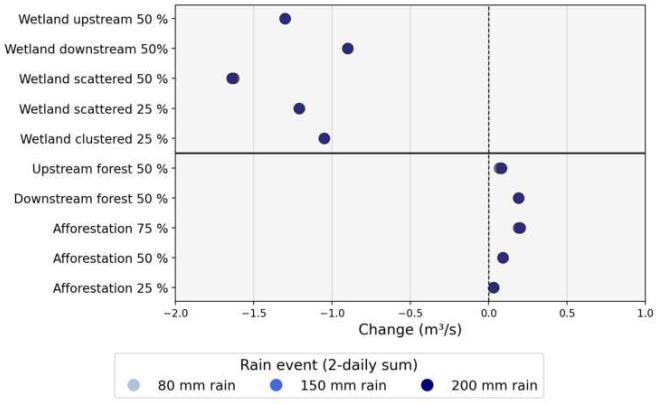

Figure 29: Effect of nature-based solutions on the minimum average 7-day discharge at Dalfsen in m^3/s

The results are expressed in million m^3 and can be seen in Figure 30. As a reference, a large retention area, 'Noord en Zuid Meene', has a capacity of 4.3 million m^3 and covers around 380 ha (de Graaf, 2004).

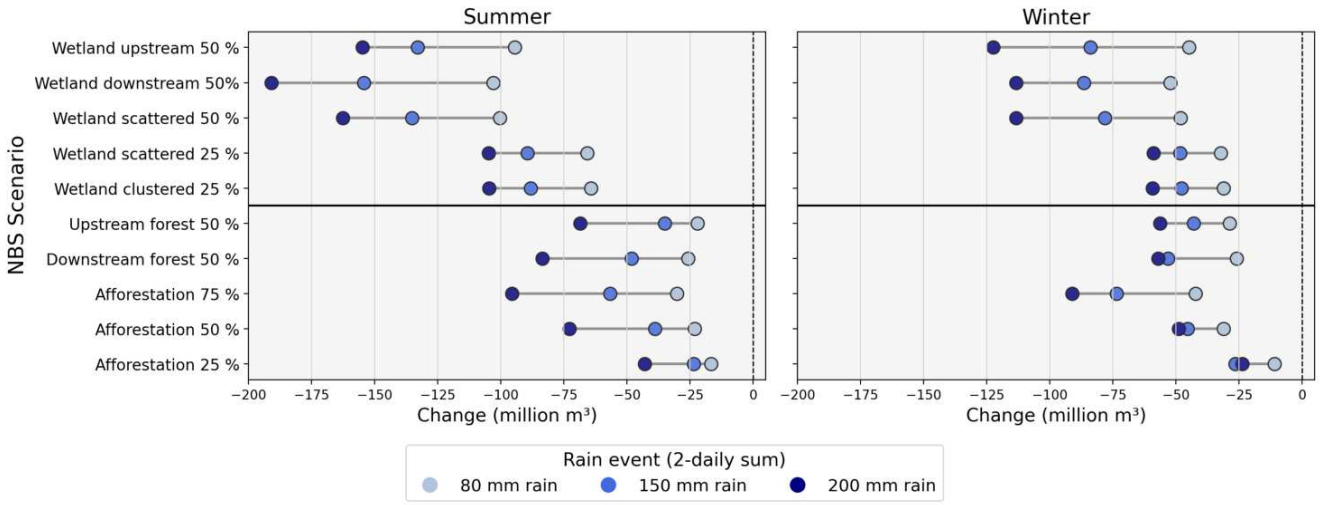

Figure 30: Change in flood volume at Dalfsen under summer and winter conditions for all nature-based solution scenarios in million m^3; flood volume is based on discharge above

There is a greater reduction of flood volumes in the case of the wetland scenarios compared to the afforestation scenarios, although the reductions in peak flows were found to be quite similar. This means more water is stored in the basin or more water is evaporated.

Under summer conditions, the flood volume shows an almost linear reduction over the different rain events. Under winter conditions, especially for the scattered 25 and 50 % afforestation scenarios and the downstream 50 % afforestation, the differences in flood volume between the 150 and 200 mm rain events are small. This means the capacity of extra water storage in the basin has almost reached its maximum. The capacity is not fixed, as it is dependent on the soil moisture of the basin. Since soil moisture is lower in the summer, the capacity for extra water storage is not reached in any scenario.

4.3.3 Evaluation of Limburg '21 rain event

To evaluate a realistic extreme rain event, the rain event of Limburg in 2021 was placed in the Vecht basin at three locations. Figures 31 and 32 show three hydrographs of different stations with different spatial distributions of the '21 rain event.

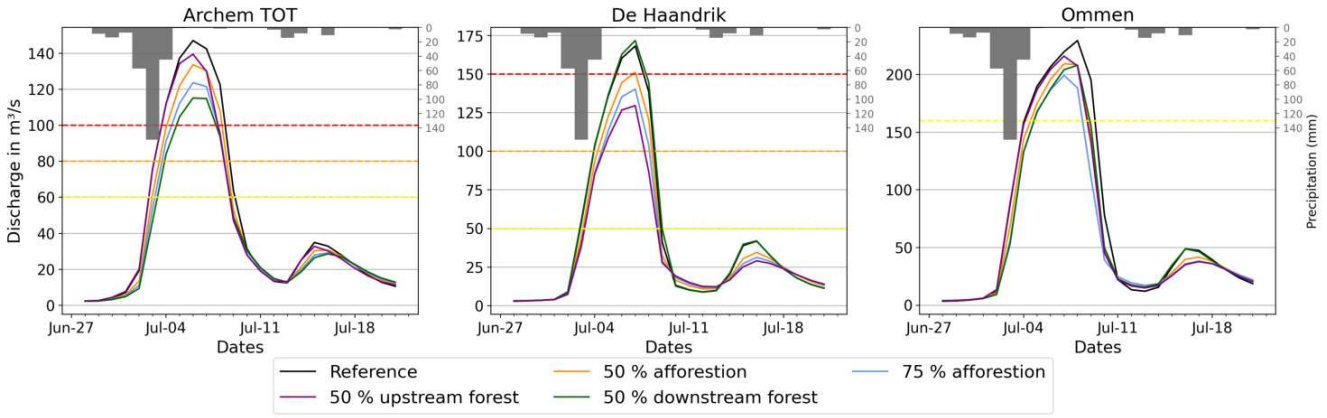

Figure 31: Hydrographs during '21 Limburg rain event of afforestation scenario; left graph at Archem TOT station with rain peak at Archem TOT sub-catchments; middle graph at De Haandrik station with rain peak in the Lage Gesamt sub-catchment; right graph at Ommen station with rain peak in the Lage Gesamt sub-catchment; yellow line is the first warning level; orange line is the second warning level; red line is the third warning level

The warning levels do not mean the same at different discharge stations, as they were obtained through different organizations having their own policies on warning levels. However, they can still give an indication on the severity of the discharge wave in the figures.

Even though the discharge waves of nature-based solutions are often above the warning levels, significant reductions in peak flows are observed. For both afforestation and wetlands, similar results are obtained as in the detailed assessment with regard to the influence of location and scale of the nature-based solutions. The highest effect is observed when the nature-based solution is implemented in the largest spatial scale. The downstream 50 % afforestation has the most effect at stations Archem TOT and Ommen, see left and right graph of Figure 31.

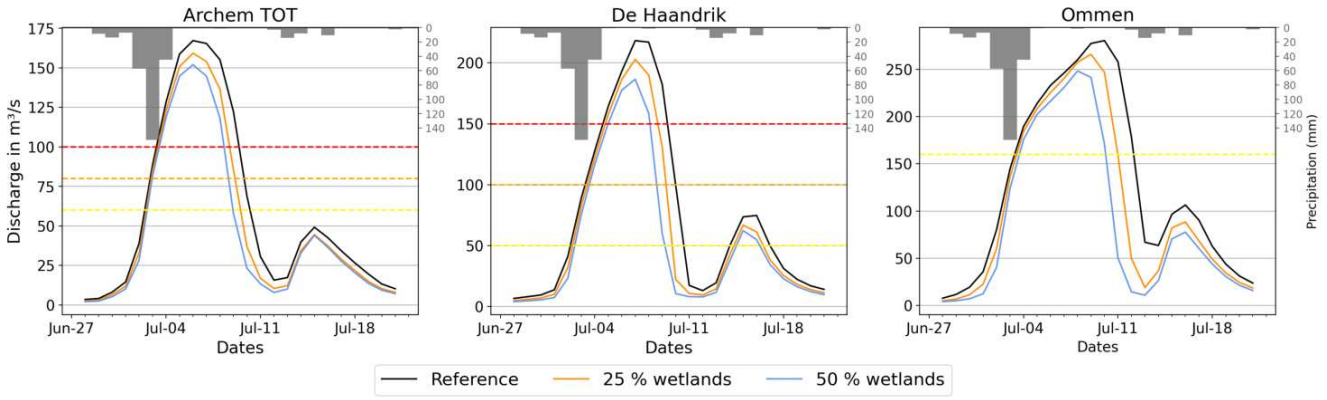

Figure 32: Hydrographs during '21 Limburg rain event of wetland scenario; left graph at Archem TOT station with rain peak at Archem TOT sub-catchments; middle graph at De Haandrik station with rain peak in the Lage Gesamt sub-catchment; right graph at Ommen station with rain peak in the Lage Gesamt sub-catchment; yellow line is the first warning level; orange line is the second warning level; red line is the third warning level

5

Discussion

The discussion describes the limitations of the data, the model, and the methods that may have influenced the outcome. The obtained results are interpreted and are related to existing literature.

5.1 Limitations in data, model and methods

5.1.1 Data

In the first research question, the Wflow sbm model is calibrated and validated using observed discharge series from various measurement stations in the Vecht basin. However, inconsistencies in the observed discharge data were observed across different periods and stations. For instance, the observed discharge at De Haandrik and Emlichheim, which are geographically close, should be similar. However, a significant difference was observed between the discharge series from these two stations, especially during summer periods. This led to different model performances, especially in the NS_{inv}. Furthermore, the discharge stations Archem TOT and Lage Gesamt combine the discharge of multiple stations, increasing the uncertainty of the observed discharge due to potential measurement errors. It is often unknown whether a station is malfunctioning during a certain discharge period. These uncertainties can lead to an inaccurate model performance on the multi-objective function, affecting the calibration of the model.

The precipitation data used in this study was derived from the spatially interpolated raster dataset E-OBS. Surprisingly, there was a difference in precipitation between stations and the E-OBS data, and it is unclear what the reason is for this deviation between E-OBS and measurement data, but it is likely due to data processing. Since E-OBS is derived from station data, rain events may be missed when these occur between measurement stations, which can lead to an inaccurate simulation of the discharge (Bandhauer et al., 2022). However, given the relatively high density of precipitation stations in the Vecht basin, the chance of missing rain events is reduced (Cornes et al., 2018). Moreover, the accuracy of E-OBS is much better than alternative data sources like ERA-5 and RADOLAN. Appendix E provides a comparison of the mean precipitation and a single rain event in 2010 among these three raster datasets and measured data by stations.

5.1.2 Model

The Wflow sbm model only simulates the natural hydrological response of the Vecht basin. The model does not include water from canals or effluent from treatment plants. These contributions are relatively minor during winter periods when river discharges are high. However, during summer periods, when the discharge is low, water from canals and effluent forms a significant portion of the discharge. The exclusion of these inputs in the Wflow sbm model may lead to inaccuracies in the simulated discharge series during dry periods, potentially underestimating the actual discharge.

The Wflow sbm model used in this study uses a daily timestep. During low flow periods, the variability in the discharge series is relatively low, meaning a daily timestep is sufficient. In the case of high flows, however, the daily timestep may not be adequate due to significant sub-daily variations in discharge, which are not covered in a mean daily discharge (Yang et al., 2016). The peak flow is underestimated when the daily mean discharges are simulated compared to hourly discharges. This underestimation is clearer in sub-catchments with a quick response and under short, intense rain events. The difference in hourly and daily discharge is shown in Figure D.1, where the difference in peak discharge is around 15 m^3/s between the hourly and daily discharge.

The infiltration capacity limits how much water can infiltrate the soil. When rainfall intensity exceeds this limit, excess water becomes overland flow. Since the model uses a daily timestep, short rain events are averaged over the day. Consequently, the infiltration capacity, set to 600 mm/day by default for non-paved area, is never exceeded, leading to an underestimation of the overland flow. An hourly model can capture these sub-daily rain events, resulting in a more realistic estimation of overland flow.

The maximum soil depth in the Wflow sbm model is 2 meters, meaning the model is not able to simulate deep groundwater flow (Van Verseveld et al., 2022). In the detailed assessment, the model reaches a near-steady state after simulating two consecutive dry years. As a result, the simulated discharge remained consistent across subsequent dry years, and no further changes were observed in groundwater storage. This makes it challenging to draw definitive conclusions about low flows over multi-year periods.

In simulating wetlands, the Wflow sbm model uses the new *'re-infiltration'* option. Enabling this option leads to a significant change in discharge observed at stations. Peak discharges are larger, and peak waves have a longer duration. The model was not re-calibrated due to time constraints, which may lead to inaccurate simulation of the discharge. This could affect the reliability of the observed effects of wetlands on high and low flows.

In this study, the *KsatHorFrac* parameter plays an important role in the calibration of Wflow sbm, which is also the case in other studies (Imhoff et al., 2020). Sensitivity analysis showed that this parameter significantly influenced the performance of the multi-objective function. The *KsatHorFrac* translates vertical saturated hydraulic conductivity to saturated horizontal conductivity. It isn't easy to measure and, therefore, frequently adjusted during calibration. Calibrating *KsatHorFrac* can compensate for other errors in the simulation of lateral flow processes. This leads to a less realistic representation of hydrological processes, increasing uncertainty in the simulation of nature-based solutions.

5.1.3 Method

The parameterisation of nature-based solutions in the Wflow sbm model is based on often contradictory literature, leading to uncertainty in the estimated effects of nature-based solutions on extremely high and low flows. Specifically, contrary values for the increase of the saturated vertical hydraulic conductivity (*KsatVer*) were found for 'afforestation' measures. The deviation in the reported *KsatVer* increase is described in Appendix I.1, with values ranging from a factor of 1.5 to 4. The literature considers a maximum soil column of 80 cm depth during measurements while adjusting the *KsatVer* in Wflow sbm affects the entire soil column of 2 meters. The uncertainty in the increase of *KsatVer* may have led to an inaccurate representation of afforestation in Wflow sbm.

In both the quick and detailed assessments, a precipitation series was constructed using historical data and uniform rainfall events to simulate low and high flows. The purpose of the uniform rainfall events

was to generate high discharges regardless of the spatial distribution of rain, while data from 2018 were used to generate low discharges, as this was recorded as an extremely dry year. After simulating two consecutive dry years, the modelled discharge and groundwater levels did not change significantly anymore over different years. The groundwater levels were able to recover sufficiently during the winter of 2018 to simulate the same discharge the year after. It could be argued that using a period with zero rainfall would have been more effective for evaluating the impacts of nature-based solutions on droughts in the water system, as this would prevent soil storage from recovering, isolating the effects of nature-based solutions.

This study uses a multi-objective function to calibrate and validate the Wflow sbm model. To determine the model performance, the multi-objective function combines three metrics, NW_w, NS_{inv} and RVE. When simulating nature-based solutions through a hydrological model, the model must be able to simulate a correct water balance by modelling infiltration, evaporation and runoff, as these processes are affected by NBS. The water balance is represented by RVE in the multi-objective function. The calibration results indicate that RVE exceeds 10 % for five discharge stations for the calibration period (Table 10). This means there are potential errors in the observed discharge, or the model is not accurately simulating the water balance in a few sub-catchments, which compromises its ability to simulate nature-based solutions realistically.

The flow indicators used in this study mainly concerned high and low flows, except for the average discharge. By concentrating on the extreme discharges through these indicators, other hydrological processes, like infiltration and transpiration, are less considered. The implications of nature-based solutions on the water system of the Vecht may not be fully addressed. For instance, afforestation leads to a slight increase in the 7-day average minimum discharge, which is beneficial for mitigating droughts. However, it also results in increased evaporation and reduced mean discharge, affecting the water balance of the Vecht. While this impact is partially reflected in the average discharge indicator, a more detailed analysis of the effects of NBS on individual hydrological processes, like infiltration and evaporation, would have been relevant.

5.2 Interpretation of results

5.2.1 Model performance

The performance of Wflow sbm is determined using the multi-objective function. The overall performance is considered satisfactory. The performance on the NS_w is significantly better than the performance on the NS_{inv}. Most stations show a NS_w value above 0.8, while the maximum observed NS_{inv} is 0.7 (Table 10). This indicates the difficulty in accurately simulating high and low flows simultaneously. Most studies that implement Wflow sbm use a performance metric different from the multi-objective function used in this study, making direct comparison difficult. Based on the evaluation of hydrographs, the Wflow sbm model in this study seems to show similar performance to the models used by Aerts et al. (2022) and Van Verseveld et al. (2022) where the Rhine, Meuse, Moselle and American catchments were evaluated. Overall, the German part of the basin performs better than the Dutch part, possibly due to the influence of canals in the Dutch part and errors in observed discharge; see sections 5.1.1 and 5.1.2. A reduction in performance is observed in all three metrics of the multi-objective function in the Dutch part.

5.2.2 Effects of nature-based solutions on high and low flows

From the quick assessment, afforestation and wetlands show the most significant effects on the high and low flows at Lage Gesamt, leading to a further evaluation of these two nature-based solutions. The detailed assessment indicates that peak flow reduction is similar between afforestation and wetlands. However, larger differences are observed when examining the Mean Annual 7-day Minimum Flow (MAM7) and average discharge. Afforestation results in an increase in MAM7, whereas wetlands show a decrease. The change in MAM7 concerns a maximum of 1.5 m^3/s, which is not much. When examining low flows, afforestation is a more effective measure to increase low flows. Both nature-based solutions lead to a reduction in average discharge, with wetlands causing a notably larger decrease compared to afforestation. This means the water balance is more affected in the case of wetlands than afforestation, see Figure I.6.

Location and scale of NBS

The results of this study indicate the importance of the spatial scale at which nature-based solutions are implemented. For both afforestation and wetlands, the minimum implemented spatial scale is 25 % of all non-urban areas in the Vecht basin, which corresponds to 1000 km^2. The observed effects on the peak flow were relatively small, lower than 10 %. The reduction in flood wave volume, on the other hand, was large, between 25 and 100 million m^3. This is a large reduction compared to existing retention areas like 'Noord en Zuid Meene', which has a capacity of 4.3 million m^3 (de Graaf, 2004).

The location of NBS has a significant effect when comparing the downstream and upstream 50 % scenarios. When evaluating the discharge at Dalfsen, the downstream 50 % scenarios reduced the peak flow to a greater extent than the upstream 50 % scenarios. This is contradictory to results found by Ferreira et al. (2022, p. 227).

For average and low flows, spatial scale plays a significantly larger role than location. Between the scattered upstream and downstream 50 % scenarios, the difference in average discharge and MAM7 change are small.

Afforestation

The observed effects of afforestation on high and average flows in this study align with findings from similar research. This study shows that afforestation reduces peak flow, which is also found in other studies. For instance, Mourad et al. (2022) reports a reduction in runoff due to afforestation of 19 and 26 %. In this study, peak flow reductions of 8 % to 30 % were observed under summer conditions with a 2-day rainfall total of 80 mm. However, these reductions require a large-scale implementation of afforestation, as stated by Badjana et al. (2023). Still, Badjana et al. (2023) states that afforestation reduces the peak flow. A similar land use change study by Deltares, which implemented a 100 % afforestation scenario in Wflow sbm, found significant reductions in peak flows for various rain events (Penning et al., 2024). In this study by Penning et al. (2024), the Geul catchment was considered which has an area of 340 km^2.

Afforestation also led to a decrease in average discharge, which is a consistent finding with similar studies. Haas et al. (2024) finds a decrease of 3 % in annual streamflow in case of maximum 30 % afforestation. Buechel et al. (2022) found a decrease of 3 % in case of 10 % afforestation. The 25 % afforestation scenario in this study reduces the average discharge of 3 %, mostly because of increased transpiration and interception.

This study finds an increase in MAM7 in the case of afforestation, which contradicts the existing literature. Buechel et al. (2022) finds a decrease of 4 % in low flows, defined by the Q90 discharge, due to afforestation. Similarly, a data analysis study by Farley et al. (2005) also shows that low flows are reduced because of afforestation, showing contrary results to this study. All discharge waves under afforestation scenarios

decrease at a lower rate than the reference situation, also at low discharges, see Figure I.10. The baseflow is not affected significantly, possibly due to the lack of detailed groundwater simulation.

Wetlands
The impacts of wetland restoration have been researched in various modelling approaches. For instance, Grapes et al. (2006) used a groundwater model, MODFLOW, to evaluate groundwater regimes in floodplain wetlands in the UK. Similarly, Hattermann et al. (2006) used the SWIM model to include wetlands in modelling a river basin in Germany. Fleischmann et al. (2018) coupled a hydrological and hydrodynamic model to simulate hydrological processes and states the importance of such a coupled model for accurate simulation of flood wave attenuation and evapotranspiration in a basin. These three studies use various approaches for modelling wetlands. This study uses a relatively simple approach without coupling to a groundwater model or hydrodynamic model. Due to these different modelling approaches, it is difficult to make a direct and exact comparison between this study and existing literature. Moreover, wetlands come in various forms, and their implications on the hydrological cycle are not always the same, as noted by Bullock and Acreman (2003).

However, the trends in observed effects of NBS align with existing literature. For instance, wetlands are considered a promising measure for flood mitigation (Cruz & Miranda, 2018). This aligns with this study, where a peak flow decrease was found when implementing wetlands. Next to that, a significant decrease in average discharge is observed, which corresponds to the study done by Hattermann et al. (2006). The decrease in average discharge occurs due to a significant increase in total evaporation, which wetlands are known for.
Ameli and Creed (2019) states that wetlands supply baseflow due to their contribution to groundwater recharge, but this effect is not observed in this study, as the average discharge and average 7-day minimum discharge both decreased. The increase in saturated water depth due to wetlands in this study was quite minimal, see Figure I.6, meaning the contribution of extra groundwater to the baseflow was also minimal.

5.2.3 Generalizations

The findings of this study, while valuable for understanding the impacts of nature-based solutions (NBS) on the Vecht basin, require careful consideration before being generalized to other basins. The effectiveness of afforestation and wetlands in mitigating extreme flows is inherently linked to the specific characteristics of the Vecht basin, like elevation, land use, soil properties, climatic conditions and human interventions in river systems. For instance, the significant influence of canals and effluents during summers in the Vecht basin may not be relevant in other, more natural river systems. Furthermore, the urban area in the Vecht basin covers 10 % of the entire area. The proposed nature-based solutions may have much less effect in other river basins, where urban areas cover a larger fraction of the entire basin.

The implementation of nature-based solutions in this study is partly dependent on the parameters defined in Wflow sbm. Since other hydrological models have their own model structure, the approach to incorporate nature-based solutions can vary considerably leading to different effects of NBS. Therefore, the implementation of NBS should be considered carefully before comparing results with those of other modelling studies.

6

Conclusion & recommendations

6.1 Conclusion

After calibration, Wflow sbm showed satisfactory performance on the proposed multi-objective function, with scores between 0.15 and 0.76 during the calibration. The accuracy of discharge simulation is higher in the German part of the Vecht compared to the Dutch part. Wflow sbm performs better in simulating high flows (NS_w) than low flows (NS_{inv}), while the performance of RVE varies much over different stations. In the relatively large sub-catchment with Archem TOT as the outflow point, the model's performance was less reliable. While performance varies significantly over different validation periods, a similar trend was observed. The accuracy of the simulated discharge is less in dry validation periods, 2012 and 2018.

After defining selection boundaries and criteria, 12 nature-based solutions were identified. Their effects on different hydrological processes were estimated to help parameterisation. The nature-based solutions concerned land use change, changing roughness, enhancing infiltration and water storage. These NBS groups were parametrised that concerned parameters related to soil properties, land use, surface roughness and threshold to hold water on plots (the results of this are shown in Table 15).

To evaluate the nature-based solutions, the indicators 'Daily peak discharge', 'flood volume', '7-day minimum daily discharge' and 'average discharge' are used. During the quick assessment, the effects of the nature-based solutions on high and low flows were simulated for the Dinkel sub-catchment. Afforestation and wetlands turned out to be the most significant nature-based solutions and were further evaluated in the detailed assessment. These two measures were simulated through various spatial scale/location scenarios and precipitation series. Among these scenarios, a similar trend was observed. Afforestation and wetlands showed similar effects of decreasing peak flow and average discharge. For low flows, afforestation led to a slight increase, while wetlands led to a decrease in average 7-day minimum discharge. Increasing the spatial scale of nature-based solutions led to more observed effects. Next to that, downstream implementation showed more effect when considering the discharge at Dalfsen. In the case of the extreme rain event in Limburg '21, both nature-based solutions could have reduced the peak flow significantly, leading to a lower risk of floods.

The goal of this study was to **quantify the effects of nature-based solutions on high and low flows in the river Vecht basin under extreme hydroclimatic conditions, using the distributed hydrological model 'Wflow sbm'**.

Overall, large-scale implementation of nature-based solutions, such as afforestation and wetland, significantly influences high flow conditions in the Vecht River basin. In contrast, low flows are less affected by these nature-based solutions. Furthermore, the average discharge is reduced, primarily due to changed evaporation rates resulting from these NBS. The spatial scale is crucial when implementing nature-based

solutions in order to significantly affect the high and low flows of the river Vecht.

6.2 Recommendations

Suggestions for future modelling of nature-based solutions using hydrological models and for further research are made.

6.2.1 Implementing nature-based solutions in hydrological models

From the discussion, several suggestions can be considered for future simulation of nature-based solutions to minimise uncertainties and improve the reliability of model outcomes.

- This study uses global, European and national data for simulation. Since a model is only as good as its data, the model performance could be increased when more detailed, local data is used.
- The Wflow sbm model uses a daily timestep. As described in the discussion, this may lead to an underestimation of peak discharges, especially for short, intense peak waves due to extreme rainfall events. An hourly timestep would result in a more accurate simulation, as sub-daily variation will be visible in the results. This would also lead to a more realistic approach of the infiltration capacity, which is never exceeded in the daily model. When hourly infiltration capacity is used, exceedance may occur, leading to overland flow.
- In case of afforestation, the saturated vertical hydraulic conductivity is increased over the entire soil column of 2 meters. It is not yet possible to assign different values for different soil depths manually, however, this is advised to incorporate in the Wflow sbm model.
- This model uses a single hydrological model without coupling to a groundwater model or hydrodynamic model. For modelling large wetland areas, coupling to a groundwater model is advised. Adding a hydrodynamic model to the evaluation would also allow the simulation of more nature-based solutions, such as re-meandering the river or floodplain restoration.
- In this study, no unnatural contributions are implemented to the river flow of the Vecht, like canal inflow and effluent. To increase the accuracy of the simulation, it is advised to gather information about these contributions and implement them in the Wflow sbm model.

6.2.2 Further research

This study focuses on the effect of nature-based solutions on extremely high and low flows. These high and low flows are generated using 2-daily, uniform rain events and a historically dry year in the Vecht basin. The 2-daily, uniform rain events are not realistic rain events that might occur in the future, but they are just for evaluating nature-based solutions. Future research could focus on a more realistic approach with regard to climate change. It is interesting to investigate whether the implementation of nature-based solutions can mitigate the consequences of climate change in terms of extremely heavy rainfall or prolonged periods of very little rain. The effectiveness of these nature-based solutions can be simulated under various climate change scenarios, including shifts in seasonal rainfall patterns and changes in the frequency and intensity of rainfall events. The KNMI'23 scenarios present different climate change scenarios, which could be used to design precipitation and potential evaporation scenarios.

While this study focused on high and low flows, which are closely related to floods and droughts, future studies could look more into groundwater dynamics due to nature-based solutions, which relate particularly to prolonged dry periods. Research into how wetlands and afforestation affect soil infiltration, recharge, and water table depths would be valuable in getting a comprehensive understanding of how these nature-based solutions affect the hydrology of the basin.

The nature-based solutions proposed in this study were implemented on a large scale, with over 25 % of all non-urban areas to forest/wetlands. While it is evident that a large scale is necessary to obtain significant effects, the scale at which nature-based solutions, such as afforestation or wetlands, can be realistically implemented in the Vecht remains uncertain. Further research is needed to determine appropriate implementation scales and their effects on high and low flows.

References

Aerts, J. P. M., Hut, R. W., van de Giesen, N. C., Drost, N., van Verseveld, W. J., Weerts, A. H., & Hazenberg, P. (2022, 8). Large-sample assessment of varying spatial resolution on the streamflow estimates of the wflow_sbm hydrological model. *Hydrology and Earth System Sciences*, *26*(16), 4407–4430. doi: 10.5194/hess-26-4407-2022

Agus, F., Farida, & van Noordwijk, M. (2004). Hydrological Impacts of Forest, Agroforestry and Upland Cropping as a Basis for Rewarding Environmental Service Providers in Indonesia. . In *Proceedings of a workshop in padang/singkarak.* Bogor: ICRAF-SEA.

Akhtar, M., Ahmad, N., & Booij, M. J. (2009, 7). Use of regional climate model simulations as input for hydrological models for the Hindukush-Karakorum-Himalaya region. *Hydrology and Earth System Sciences*, *13*(7), 1075–1089. doi: 10.5194/hess-13-1075-2009

Amanze, C., Eluagu, K., Nwosu, O., Ukabiala, N., Okoror, P., & Okoroafor, C. (2024, 2). Organic Carbon Storage and Structural-Hydraulic Properties of Ultisol under Agricultural Land Use Systems at Umuahia. *African Journal of Agriculture and Food Science*, *7*(1), 21–35. doi: 10.52589/ajafs-hcekb6wi

Ameli, A. A., & Creed, I. F. (2019, 6). Does Wetland Location Matter When Managing Wetlands for Watershed-Scale Flood and Drought Resilience? *JAWRA Journal of the American Water Resources Association*, *55*(3), 529–542. doi: 10.1111/1752-1688.12737

Arcement, G. J., & Schneider, V. R. (1989). *Guide for Selecting Manning's Roughness Coefficients for Natural Channels and Flood Plains* (Tech. Rep.).

Asselman, N., van Heeringen, K. J., de Jong, J., & Geertsema, T. (2022). *Juli 2021 overstroming en wateroverlast in zuid limburg* (Tech. Rep.). Delft: Deltares.

Babaremu, K., Taiwo, O., & Ajayi, D. (2024, 1). Impacts of Land Use and Land Cover Changes on Hydrological Response: A Review of Current Understanding and Implications for Watershed and Water Resources Management. *TWIST*, *19*(1), 256–267.

Badjana, H. M., Cloke, H. L., Verhoef, A., Julich, S., Camargos, C., Collins, S., ... Clark, J. (2023, 9). Can hydrological models assess the impact of natural flood management in groundwater-dominated catchments? *Journal of Flood Risk Management*, *16*(3). doi: 10.1111/jfr3.12912

Bandhauer, M., Isotta, F., Lakatos, M., Lussana, C., Båserud, L., Izsák, B., ... Frei, C. (2022, 2). Evaluation of daily precipitation analyses in E-OBS (v19.0e) and ERA5 by comparison to regional high-resolution datasets in European regions. *International Journal of Climatology*, *42*(2), 727–747. doi: 10.1002/joc.7269

Bates, P. D., Horritt, M. S., & Fewtrell, T. J. (2010, 6). A simple inertial formulation of the shallow water equations for efficient two-dimensional flood inundation modelling. *Journal of Hydrology*, *387*(1-2), 33–45. doi: 10.1016/j.jhydrol.2010.03.027

Beersma, J., Hakvoort, H., Jilderda, R., Overeem, A., & Versteeg, R. (2019). *Neerslagstatistiek en -reeksen voor het waterbeheer 2019* (Tech. Rep.). Amersfoort: STOWA.

Bessembinder, J., Bintanja, R., van Dorland, R., Homan, C., Overbeek, B., Selten, F., & Siegmund, P. (2023). *KNMI'23 climate scenarios for the Netherlands* (Tech. Rep.). de Bilt: Koninklijk Nederlands Meteorologisch Instituut. Retrieved from `https://cdn.knmi.nl/system/ckeditor/attachment_files/data/000/000/358/original/KNMI23_climate_scenarios_user_report.pdf`

Bisolo, A., Rodrigues, M. F., da Conceição, F. G., & Pellegrini, A. (2024). Spatial Variability and Correlation between Soil Physical Properties under No-Tillage with and without Agricultural Terraces. *Brazilian Archives of Biology and Technology*, *67*(SPE1). doi: 10.1590/1678-4324-PSSM-2024230802

Blanco-Canqui, H. (2024, 4). Assessing the potential of nature-based solutions for restoring soil ecosystem services in croplands. *Science of The Total Environment*, *921*, 170854. doi: 10.1016/j.scitotenv.2024.170854

Booij, M. J., & Krol, M. S. (2010, 8). Balance between calibration objectives in a conceptual hydrological model. *Hydrological Sciences Journal*, *55*(6), 1017–1032. doi: 10.1080/02626667.2010.505892

Bourke, M., Wilkinson, M., & Srdjevic, Z. (2022). *Nature-based solutions for flow reduction in catchment headwaters.* Edward Elgar Publishing Limited.

Brooks, R. H., & Corey, A. T. (1964). *HYDRAULIC PROPERTIES OF POROUS MEDIA* (Tech. Rep.).

Bruijn, K. d., & Maas, B. (2023). *Methode voor bovenregionale stresstesten voor grootschalige neerslag, ten behoeve van een landelijk uniform beeld* (Tech. Rep.). Delft: Deltares.

Bruijn, K. d., & Slager, K. (2022). *Wat als 'de waterbom' elders in Nederland was gevallen?* (Tech. Rep.). Delft: Deltares.

Buechel, M., Slater, L., & Dadson, S. (2022, 1). Hydrological impact of widespread afforestation in Great Britain using a large ensemble of modelled scenarios. *Communications Earth & Environment*, *3*(1), 6. doi: 10.1038/s43247-021-00334-0

Bullock, A., & Acreman, M. (2003, 6). The role of wetlands in the hydrological cycle. *Hydrology and Earth System Sciences*, *7*(3), 358–389. doi: 10.5194/hess-7-358-2003

Büttner, G., & Kosztra, B. (2011). *Manual of CORINE Land Cover changes EEA subvention 2011 Project Manager* (Tech. Rep.).

Chow, V., Maidment, D., & Mays, L. (1988). *Applied Hydrology*. New York: McGraw-Hill Book Company.

Cohen-Shacham, E., Walters, G., Janzen, C., & Maginnis, S. (2016). *Nature-based solutions to address global societal challenges*. IUCN International Union for Conservation of Nature. doi: 10.2305/iucn.ch.2016.13.en

Cooper, R. J., Hawkins, E., Locke, J., Thomas, T., & Tosney, J. (2020, 11). Assessing the environmental and economic efficacy of two integrated constructed wetlands at mitigating eutrophication risk from sewage effluent. *Water and Environment Journal*, *34*(4), 669–678. doi: 10.1111/wej.12605

Cornes, R. C., van der Schrier, G., van den Besselaar, E. J. M., & Jones, P. D. (2018, 9). An Ensemble Version of the E-OBS Temperature and Precipitation Data Sets. *Journal of Geophysical Research: Atmospheres*, *123*(17), 9391–9409. doi: 10.1029/2017JD028200

Cruz, R. d., & Miranda, O. L. (2018, 6). Incorporating wetlands in hydrologic and hydraulic models for flood zone delineation: An application to Durán, Ecuador. *International Journal of Disaster Risk Reduction*, *28*, 375–383. doi: 10.1016/j.ijdrr.2018.03.023

Debele, S. E., Leo, L. S., Kumar, P., Sahani, J., Ommer, J., Bucchignani, E., ... Di Sabatino, S. (2023, 12). Nature-based solutions can help reduce the impact of natural hazards: A global analysis of NBS case studies. *Science of the Total Environment*, *902*. doi: 10.1016/j.scitotenv.2023.165824

de Graaf, J. (2004). *Inzet retentiegebieden Noord Meene en Zuid Meene* (Unpublished doctoral dissertation). University of Twente, Enschede.

Deltares. (n.d.). *CORINE mapping.* Retrieved from `https://github.com/Deltares/hydromt_wflow/blob/5bc0f54ad961dd3ebe639eba88e414e1b8325919/hydromt_wflow/data/lulc/corine_mapping.csv`

Devia, G. K., Ganasri, B., & Dwarakish, G. (2015). A Review on Hydrological Models. *Aquatic Procedia*, *4*, 1001–1007. doi: 10.1016/j.aqpro.2015.02.126

Dwarakish, G., & Ganasri, B. (2015, 12). Impact of land use change on hydrological systems: A review of current modeling approaches. *Cogent Geoscience*, *1*(1), 1115691. doi: 10.1080/23312041.2015.1115691

Eilander, D., Boisgontier, H., Bouaziz, L. J. E., Buitink, J., Couasnon, A., Dalmijn, B., ... van Verseveld, W. (2023, 3). HydroMT: Automated and reproducible model building and analysis. *Journal of Open Source Software*, *8*(83), 4897. doi: 10.21105/joss.04897

Farley, K. A., Jobbágy, E. G., & Jackson, R. B. (2005, 10). Effects of afforestation on water yield: a global synthesis with implications for policy. *Global Change Biology*, *11*(10), 1565–1576. doi: 10.1111/j.1365-2486.2005.01011.x

Fashaho, A., Ndegwa, G. M., Lelei, J. J., Musandu, A. O., & Mwonga, S. M. (2020, 3). Effect of land terracing on soil physical properties across slope positions and profile depths in medium and high altitude regions of Rwanda. *South African Journal of Plant and Soil*, *37*(2), 91–100. doi: 10.1080/02571862.2019.1665722

Feddes, R. (1982). *Simulation of plant growth and crop production* (Tech. Rep.). Wageningen: Wageningen University & Research.

Fér, M., Kodešová, R., Hroníková, S., & Nikodem, A. (2020, 6). The effect of 12-year ecological farming on the soil hydraulic properties and repellency index. *Biologia*, *75*(6), 799–807. doi: 10.2478/s11756-019-00373-1

Ferreira, C., Kalantari, Z., Hartmann, T., & Pereira, P. (2022). Nature-based Solutions for Flood Mitigation. Cham: Springer. Retrieved from `https://link.springer.com/bookseries/698`.

Ferreira, C., Kašanin-Grubin, M., Solomun, M., Sushkova, S., Minkina, T., Zhao, W., & Kalantari, Z. (2023, 6). Wetlands as nature-based solutions for water management in different environments. *Current Opinion in Environmental Science & Health*, *33*, 100476. doi: 10.1016/j.coesh.2023.100476

Fleischmann, A., Siqueira, V., Paris, A., Collischonn, W., Paiva, R., Pontes, P., ... Tanimoun, B. (2018, 6). Modelling hydrologic and hydrodynamic processes in basins with large semi-arid wetlands. *Journal of Hydrology*, *561*, 943–959. doi: 10.1016/j.jhydrol.2018.04.041

Gash, J. H. C. (1979, 1). An analytical model of rainfall interception by forests. *Quarterly Journal of the Royal Meteorological Society*, *105*(443), 43–55. doi: 10.1002/qj.49710544304

Grapes, T., Bradley, C., & Petts, G. (2006, 4). Hydrodynamics of floodplain wetlands in a chalk catchment: The River Lambourn, UK. *Journal of Hydrology*, *320*(3-4), 324–341. doi: 10.1016/j.jhydrol.2005.07.028

Haas, H., Kalin, L., Sun, G., & Kumar, S. (2024, 8). Understanding the effects of afforestation on water quantity and quality at watershed scale by considering the influences of tree species and local moisture recycling. *Journal of Hydrology*, *640*, 131739. doi: 10.1016/j.jhydrol.2024.131739

Hartgring, S. (2023). *On forecasting the Rur river* (Unpublished doctoral dissertation). TU Delft, Delft.

Haruna, S., Anderson, S., Nkongolo, N., & Zaibon, S. (2018, 6). Soil Hydraulic Properties: Influence of Tillage and Cover Crops. *Pedosphere*, *28*(3), 430–442. doi: 10.1016/s1002-0160(17)60387-4

Haruna, S. I., Ritchey, E., Mosley, C., & Ku, S. (2023, 1). Effects of cover crops on soil hydraulic properties during commodity crop growing season. *Soil Use and Management*, *39*(1), 218–231. doi: 10.1111/sum.12803

Hattermann, F., Krysanova, V., Habeck, A., & Bronstert, A. (2006, 12). Integrating wetlands and riparian zones in river basin modelling. *Ecological Modelling*, *199*(4), 379–392. doi: 10.1016/j.ecolmodel.2005.06.012

He, J., Wang, Q., Li, H., Tullberg, J. N., McHugh, A. D., Bai, Y., ... Gao, H. (2009, 9). Soil physical properties and infiltration after long-term no-tillage and ploughing on the Chinese Loess Plateau. *New Zealand Journal of Crop and Horticultural Science*, *37*(3), 157–166. doi: 10.1080/01140670909510261

Hendriks, D., & Mens, M. (2024). *De droogte van 2022: een brede analyse van de ernst en maatschappelijke gevolgen* (Tech. Rep.). Delft: Deltares.

Herman, J. D., Kollat, J. B., Reed, P. M., & Wagener, T. (2013, 7). Technical Note: Method of Morris effectively reduces the computational demands of global sensitivity analysis for distributed watershed models. *Hydrology and Earth System Sciences*, *17*(7), 2893–2903. doi: 10.5194/hess-17-2893-2013

Horel, A., Tóth, E., Gelybo, G., Kasa, I., Bakacsi, Z., & Farkas, C. (2015). *Effects of Land Use and Management on Soil Hydraulic Properties* (Vol. 7; Tech. Rep. No. 1). doi: 10.1515/geo-2015-0053

Huffman, R., Fangmeier, D., Elliot, W., & Workman, S. (2013, 9). Chapter 5: Infiltration and Runoff. In *Soil and water conservation engineering* (Seventh Edition ed., pp. 81–113). American Society of Agricultural and Biological Engineers. doi: 10.13031/swce.2013.5

Hundecha, Y., & Bárdossy, A. (2004, 6). Modeling of the effect of land use changes on the runoff generation of a river basin through parameter regionalization of a watershed model. *Journal of Hydrology*, *292*(1-4), 281–295. doi: 10.1016/j.jhydrol.2004.01.002

Imhoff, R. O., van Verseveld, W. J., van Osnabrugge, B., & Weerts, A. H. (2020, 4). Scaling Point-Scale (Pedo)transfer Functions to Seamless Large-Domain Parameter Estimates for High-Resolution

Distributed Hydrologic Modeling: An Example for the Rhine River. *Water Resources Research*, *56*(4). doi: 10.1029/2019WR026807

Jeuken, A., Ray, P., Penning, E., Bouaziz, L., Tracy, J., Wi, S., ... Hegnauer, M. (2023, 9). Challenges for upscaling hydrological effectiveness of nature-based solution for adaptation to climate change in watersheds. *Aquatic Ecosystem Health and Management*, *26*(2), 19–32. doi: 10.14321/aehm.026.02.019

Journée, M., Goudenhoofdt, E., Vannitsem, S., & Delobbe, L. (2023, 9). Quantitative rainfall analysis of the 2021 mid-July flood event in Belgium. *Hydrology and Earth System Sciences*, *27*(17), 3169–3189. doi: 10.5194/hess-27-3169-2023

Kahlon, M. S., Lal, R., & Ann-Varughese, M. (2013, 1). Twenty two years of tillage and mulching impacts on soil physical characteristics and carbon sequestration in Central Ohio. *Soil and Tillage Research*, *126*, 151–158. doi: 10.1016/j.still.2012.08.001

Klaassen, W., Bosveld, F., & De Water, E. (1998, 12). Water storage and evaporation as constituents of rainfall interception. *Journal of Hydrology*, *212-213*(1-4), 36–50. doi: 10.1016/S0022-1694(98)00200-5

Klein, A. (2022). *Hydrological Response of the Geul Catchment to the Rainfall in July 2021* (Doctoral dissertation, University of Delft, Delft). Retrieved from `http://repository.tudelft.nl/`.

Klein, A., & van der Vat, M. (2024). *Scoping Study of the Vecht, Berkel and Oude IJssel river basins* (Tech. Rep.). JCAR ATRACE.

Leegwater, I. (2024). *Investigating the effects of nature-based solutions in the Vecht river basin* (Unpublished doctoral dissertation). University of Enschede, Enschede.

Le Moine, N. (2008). *Le bassin versant de surface vu par le souterrain : une voie d'amélioration des performances et du réalisme des modèles pluie-débit ?* (Unpublished doctoral dissertation). Université Pierre et Marie Curie, Paris.

Li, H., Liao, X., Zhu, H., Wei, X., & Shao, M. (2019). Soil physical and hydraulic properties under different land uses in the black soil region of northeast China. *Canadian Journal of Soil Science*, *99*(4), 406–419. doi: 10.1139/cjss-2019-0039

Marhaento, H., Booij, M. J., Rientjes, T. H. M., & Hoekstra, A. Y. (2019, 12). Sensitivity of Streamflow Characteristics to Different Spatial Land-Use Configurations in Tropical Catchment. *Journal of Water Resources Planning and Management*, *145*(12). doi: 10.1061/(asce)wr.1943-5452.0001122

Maule, C. P., & Reed, W. B. (1993). Infiltration under no-till and conventional tillage systems in Saskatchewan. *Canadian Agricultural Engineering*.

McVittie, A., Cole, L., Wreford, A., Sgobbi, A., & Yordi, B. (2018, 12). Ecosystem-based solutions for disaster risk reduction: Lessons from European applications of ecosystem-based adaptation measures. *International Journal of Disaster Risk Reduction*, *32*, 42–54. doi: 10.1016/j.ijdrr.2017.12.014

Ministerie van Infrastructuur en Waterstaat. (2019). *Nederland beter weerbaar tegen droogte. Eindrapportage Beleidstafel Droogte* (Tech. Rep.).

Ministerie van Infrastructuur en Waterstaat. (2022). *Eindadvies Beleidstafel wateroverlast en hoogwater - Voorkomen kan niet, voorbereiden wel* (Tech. Rep.). Ministerie van Infrastructuur en Waterstaat.

Mourad, K. A., Nordin, L., & Andersson-Sköld, Y. (2022). Assessing flooding and possible adaptation measures using remote sensing data and hydrological modeling in Sweden. *Climate Risk Management*, *38*, 100464. doi: 10.1016/j.crm.2022.100464

Nasta, P., Szabó, B., & Romano, N. (2021, 10). Evaluation of pedotransfer functions for predicting soil hydraulic properties: A voyage from regional to field scales across Europe. *Journal of Hydrology: Regional Studies*, *37*, 100903. doi: 10.1016/j.ejrh.2021.100903

Neal, J., Schumann, G., & Bates, P. (2012). A subgrid channel model for simulating river hydraulics and floodplain inundation over large and data sparse areas. *Water Resources Research*, *48*(11). doi: 10.1029/2012WR012514

Ourloglou, O., Stefanidis, K., & Dimitriou, E. (2020). Assessing nature-based and classical engineering

solutions for flood-risk reduction in urban streams. *Journal of Ecological Engineering*, *21*(2), 46–56. doi: 10.12911/22998993/116349

Paul, M. (2016). *Impacts of Land Use and Climate Changes on Hydrological Processes in South Dakota Watersheds* (Unpublished doctoral dissertation). South Dakota State University, South Dakota.

Penning, E., Klein, A., Asselman, N., de Louw, P., Kaandorp, V., van Geest, G., ... Schoonderwoerd, E. (2024, 1). *Sponswerking van Landschappen in Nederland* (Tech. Rep.). Delft: Deltares.

Peters, O., & Haruna, S. I. (2024, 9). Does no-till cover crop influence in situ measured soil water potential and saturated hydraulic conductivity? *Soil and Water Research*. doi: 10.17221/27/2024-swr

Poggio, L., de Sousa, L. M., Batjes, N. H., Heuvelink, G. B. M., Kempen, B., Ribeiro, E., & Rossiter, D. (2021, 6). SoilGrids 2.0: producing soil information for the globe with quantified spatial uncertainty. *SOIL*, *7*(1), 217–240. doi: 10.5194/soil-7-217-2021

Pushpalatha, R., Perrin, C., Moine, N. L., & Andréassian, V. (2012, 2). A review of efficiency criteria suitable for evaluating low-flow simulations. *Journal of Hydrology*, *420-421*, 171–182. doi: 10.1016/j.jhydrol.2011.11.055

Raška, P., Bezak, N., Ferreira, C. S., Kalantari, Z., Banasik, K., Bertola, M., ... Hartmann, T. (2022, 5). Identifying barriers for nature-based solutions in flood risk management: An interdisciplinary overview using expert community approach. *Journal of Environmental Management*, *310*. doi: 10.1016/j.jenvman.2022.114725

Rawls, W., & Brakensiek, D. (1985). Prediction of soil water properties for hydrologic modeling. *Watershed Management in the Eighties*, 293–299.

Richards, L. A. (1931, 11). Capillary conduction of liquids through porous mediums. *Physics*, *1*(5), 318–333. doi: 10.1063/1.1745010

Ruangpan, L., Vojinovic, Z., Di Sabatino, S., Leo, L. S., Capobianco, V., Oen, A. M., ... Lopez-Gunn, E. (2020, 1). Nature-based solutions for hydro-meteorological risk reduction: a state-of-the-art review of the research area. *Natural Hazards and Earth System Sciences*, *20*(1), 243–270. doi: 10.5194/nhess-20-243-2020

Sarigil, G., Cavus, Y., Aksoy, H., & Eris, E. (2024, 8). Frequency curves of high and low flows in intermittent river basins for hydrological analysis and hydraulic design. *Stochastic Environmental Research and Risk Assessment*, *38*(8), 3079–3092. doi: 10.1007/s00477-024-02732-0

Senior, J. G., Trigg, M. A., & Willis, T. (2022, 9). *Physical representation of hillslope leaky barriers in 2D hydraulic models: A case study from the Calder Valley* (Vol. 15) (No. 3). John Wiley and Sons Inc. doi: 10.1111/jfr3.12821

Simsek, U., Erdel, E., & Barik, K. (2017). Effect of mulching on soil moisture and some soil characteristics.

Singh, A. (2018). A Concise Review on Introduction to Hydrological Models. *GRD Journal for Engineering*, *3*(10). Retrieved from `www.grdjournals.com`

Skaalsveen, K., Ingram, J., & Clarke, L. E. (2019, 6). *The effect of no-till farming on the soil functions of water purification and retention in north-western Europe: A literature review* (Vol. 189). Elsevier B.V. doi: 10.1016/j.still.2019.01.004

Smakhtin, V. U. (2001). Low flow hydrology: a review. *Journal of Hydrology*, *240*, 147–186. Retrieved from `www.elsevier.com/locate/jhydrol`

Sorooshian, S., & Moradkhani, H. (2009). General Review of Rainfall-Runoff Modeling: Model Calibration, Data Assimilation, and Uncertainty Analysis. *Hydrological Modelling and the Water Cycle*. doi: 10.1007/978-3-540-77843-1{_}1

Spruyt, A., & Fujisaki, A. (2021). *Ontwikkeling zesde-generatie model Overijsselse Vechtdelta Modelbouw, kalibratie en validatie* (Tech. Rep.).

ten Berge, A. (2024). *Robustness of hydrological models for simulating impact of climate change on high and low streamflow in the Lesse* (Unpublished doctoral dissertation). University of Twente, Enschede.

Tradowsky, J. S., Philip, S. Y., Kreienkamp, F., Kew, S. F., Lorenz, P., Arrighi, J., ... Wanders, N.

(2023, 7). Attribution of the heavy rainfall events leading to severe flooding in Western Europe during July 2021. *Climatic Change*, *176*(7), 90. doi: 10.1007/s10584-023-03502-7

USDA. (2017). *Terrace design: Technical Note* (Tech. Rep.). Texas: United States Department of Agriculture.

Van Verseveld, W. J., Weerts, A. H., Visser, M., Buitink, J., Imhoff, R. O., Boisgontier, H., ... Russell, B. (2022, 8). *Wflow_sbm v0.6.1, a spatially distributed hydrologic model: from global data to local applications.* Retrieved from `https://gmd.copernicus.org/preprints/gmd-2022-182/gmd-2022-182.pdf` doi: 10.5194/gmd-2022-182

Verdonschot, P. F., & Verdonschot, R. C. (2017). *Meetprogramma Overijsselse Vecht : nulsituatie 2017 en effecten maatregelen* (Tech. Rep.). Retrieved from `https://research.wur.nl/en/publications/ffad09b5-8d86-49ed-8f93-ef81ee08a236` doi: 10.18174/440223

Vertessy, R. A., & Elsenbeer, H. (1999). *Distributed modeling of storm flow generation in an Amazonian rain forest catchment: Effects of model parameterization* (Tech. Rep.).

Waterschap Vechtstromen. (2021). *Waterbeheerprogramma 2020-2027* (Tech. Rep.). Retrieved from `https://www.vechtstromen.nl/bestuur/waterbeheerprogramma-2022-2027/`

World Meteorological Organization. (2008). *Guide to Hydrological Practices* (6th ed., Vol. 1). Geneva: WMO. Retrieved from `www.wmo.int`

WWAP. (2018). *Nature-based solutions for water.* United Nations Educational, Scientific and Cultural Organization.

Yamazaki, D., Ikeshima, D., Sosa, J., Bates, P. D., Allen, G. H., & Pavelsky, T. M. (2019, 6). MERIT Hydro: A High-Resolution Global Hydrography Map Based on Latest Topography Dataset. *Water Resources Research*, *55*(6), 5053–5073. doi: 10.1029/2019WR024873

Yang, X., Liu, Q., He, Y., Luo, X., & Zhang, X. (2016, 3). Comparison of daily and sub-daily SWAT models for daily streamflow simulation in the Upper Huai River Basin of China. *Stochastic Environmental Research and Risk Assessment*, *30*(3), 959–972. doi: 10.1007/s00477-015-1099-0

Yao, S., Zhao, C., Zhao, X., Wang, S., Li, Y., & Tian, L. (2015). *Effects of land use on soil saturated hydraulic conductivity of Horqin Sand Land* (Tech. Rep.).

Zare, M., Majid, A., Mikayilov, F., Zare, M., Afyuni, M., & Abbaspour, K. C. (2010). *Effects of Biosolids Application on Temporal Variations in Soil Physical and Unsaturated Hydraulic Properties* (Tech. Rep.). Retrieved from `https://www.researchgate.net/publication/233729673`

Appendix

A Vecht pictures

Figures A.1b and A.1a show the current situation at De Haandrik, located closely to the border between the Netherlands and Germany. The left figure shows the crossing itself, where water can be let the Vecht river from the canal (from bottom right to top left). The right figure shows the Vecht in the downstream direction from De Haandrik.

(a) Vecht towards Dalfsen from De Haandrik **(b)** Crossing at De Haandrik

Figure A.1: Pictures of De Haandrik

B Parameters in Wflow

Table B.1: Model Parameters related to vertical processes

Parameter	Description	Unit	Default
`cfmax`	degree-day factor	mm °C^{-1} day^{-1}	3.75653
`tt`	threshold temperature for snowfall	°C	0.0
`tti`	threshold temperature interval length	°C	1.0
`ttm`	threshold temperature for snowmelt	°C	0.0
`whc`	water holding capacity as fraction of current snow pack	-	0.1
`w_soil`	soil temperature smooth factor	-	0.1125
`cf_soil`	controls soil infiltration reduction factor when soil is frozen	-	0.038
`g_tt`	threshold temperature for snowfall above glacier	°C	0.0
`g_cfmax`	Degree-day factor for glacier	mm °C^{-1} day^{-1}	3.0
`g_sifrac`	fraction of the snowpack on top of the glacier converted into ice	day^{-1}	0.001
`glacierfrac`	fraction covered by a glacier	-	0.0

glacierstore	water within the glacier	mm	5500.0
theta_s	saturated water content (porosity)	-	0.6
theta_r	residual water content	-	0.01
kv_0	Vertical hydraulic conductivity at soil surface	mm day^{-1}	3000.0
f	scaling parameter (controls exponential decline of kv_0)	mm^{-1}	0.001
hb	air entry pressure of soil (Brooks-Corey)	cm	10.0
soilthickness	soil thickness	mm	2000.0
infiltcappath	infiltration capacity of the compacted areas	mm day^{-1}	10.0
infiltcapsoil	soil infiltration capacity	mm day^{-1}	100.0
maxleakage	maximum leakage from saturated zone	mm day^{-1}	0.0
c	Brooks-Corey power coefficient for each soil layer	-	10.0
kvfrac	multiplication factor applied to kv_z (vertical flow)	-	1.0
waterfrac	fraction of open water (excluding rivers)	-	0.0
pathfrac	fraction of compacted area	-	0.01
rootingdepth	rooting depth	mm	750.0
rootdistpar	controls how roots are linked to water table	-	-500.0
cap_hmax	water depth beyond which capillary flux ceases	mm	2000.0
cap_n	coefficient controlling capillary rise	-	2.0
et_reftopot	multiplication factor to correct reference evaporation	-	1.0
sl	specific leaf storage	mm	-
swood	storage woody part of vegetation	mm	-
kext	extinction coefficient (to calculate canopy gap fraction)	-	-
cmax	maximum canopy storage	mm	1.0
e_r	Gash interception model parameter	-	0.1
canopygapfraction	canopy gap fraction	-	0.1
Delta_t	model time step	s	-
maxlayers	maximum number of soil layers	-	-
n	number of grid cells	-	-
nlayers	number of soil layers	-	-
n_unsatlayers	number of unsaturated soil layers	-	-
riverfrac	fraction of river	-	-
act_thickl	thickness of soil layers	mm	-
sumlayers	cumulative sum of soil layers thickness, starting at soil surface	mm	-
stemflow	stemflow	mm Δt^{-1}	-
throughfall	throughfall	mm Δt^{-1}	-
ustorelayerdepth	amount of water in the unsaturated store, per layer	mm	-
satwaterdepth	saturated store	mm	-
zi	pseudo-water table depth (top of the saturated zone)	mm	-

`soilwatercapacity`	soilwater capacity	mm	-
`canopystorage`	canopy storage	mm	-
`precipitation`	precipitation	mm Δt^{-1}	-
`temperature`	temperature	°C	-
`potential evaporation`	potential evaporation	mm Δt^{-1}	-
`pottrans_soil`	interception subtracted from potential evaporation	mm Δt^{-1}	-
`transpiration`	transpiration	mm Δt^{-1}	-
`ae_ustore`	actual evaporation from unsaturated store	mm Δt^{-1}	-
`interception`	interception loss by evaporation	mm Δt^{-1}	-
`soilevap`	total soil evaporation from unsaturated and saturated store	mm Δt^{-1}	-
`soilevapsat`	soil evaporation from saturated store	mm Δt^{-1}	-
`actcapflux`	actual capillary rise	mm Δt^{-1}	-
`actevapsat`	actual transpiration from saturated store	mm Δt^{-1}	-
`actevap`	total actual evapotranspiration	mm Δt^{-1}	-
`runoff_river`	runoff from river based on `riverfrac`	mm Δt^{-1}	-
`runoff_land`	runoff from land based on `waterfrac`	mm Δt^{-1}	-
`ae_openw_l`	actual evaporation from open water (land)	mm Δt^{-1}	-
`ae_openw_r`	actual evaporation from river	mm Δt^{-1}	-
`net_runoff_river`	net runoff from river (`runoff_river` - `ae_openw_r`)	mm Δt^{-1}	-
`avail_forinfilt`	water available for infiltration	mm Δt^{-1}	-
`actinfilt`	actual infiltration into the unsaturated zone	mm Δt^{-1}	-
`actinfiltsoil`	actual infiltration into non-compacted fraction	mm Δt^{-1}	-
`actinfiltpath`	actual infiltration into compacted fraction	mm Δt^{-1}	-
`infiltsoilpath`	infiltration into the unsaturated zone	mm Δt^{-1}	-
`infiltexcess`	infiltration excess water	mm Δt^{-1}	-
`excesswater`	water that cannot infiltrate due to saturated soil (saturation excess)	mm Δt^{-1}	-
`exfiltsatwater`	water exfiltrating during saturation excess conditions	mm Δt^{-1}	-
`exfiltustore`	water exfiltrating from unsaturated store because of change in water table	mm Δt^{-1}	-
`excesswatersoil`	excess water for non-compacted fraction	mm Δt^{-1}	-
`excesswaterpath`	excess water for compacted fraction	mm Δt^{-1}	-
`runoff`	total surface runoff from infiltration and saturation excess	mm Δt^{-1}	-
`vwc`	volumetric water content per soil layer (including `theta_r` and saturated zone)	-	-
`vwc_perc`	volumetric water content per soil layer (including `theta_r` and saturated zone)	%	-
`rootstore`	root water storage in unsaturated and saturated zone (excluding `theta_r`)	mm	-
`vwc_root`	volumetric water content in root zone (including `theta_r` and saturated zone)	-	-

`vwc_percroot`	volumetric water content in root zone (including `theta_r` and saturated zone)	%	-
`ustoredepth`	total amount of available water in the unsaturated zone	mm	-
`transfer`	downward flux from unsaturated to saturated zone	mm Δt^{-1}	-
`recharge`	net recharge to saturated zone	mm Δt^{-1}	-
`actleakage`	actual leakage from saturated store	mm Δt^{-1}	-
`snow`	snow storage	mm	-
`snowwater`	liquid water content in the snow pack	mm	-
`rainfallplusmelt`	snowmelt + precipitation as rainfall	mm Δt^{-1}	-
`glacierstore`	water within the glacier	mm	-
`tsoil`	top soil temperature	°C	-
`leaf_area_index`	leaf area index	m^2 m^{-2}	-
`waterlevel_land`	water level land	mm	-
`waterlevel_river`	water level river	mm	-

Table B.2: Model Parameters related to lateral processes

Parameter	**Description**	**Unit**	**Default**
`mannings_n (n)`	Manning's roughness	s $m^{-\frac{1}{3}}$	0.036
`width`	river width	m	-
`zb`	river bed elevation	m	-
`length`	river length	m	-
`n`	number of cells	-	-
`ne`	number of edges/links	-	-
`active_n`	active nodes	-	-
`active_e`	active edges	-	-
`g`	acceleration due to gravity	m s^{-2}	-
`alpha`	stability coefficient (Bates et al., 2010)	-	0.7
`h_thresh`	depth threshold for calculating flow	m	0.001
`Delta_t`	model time step	s	-
`q`	river discharge (subgrid channel)	m^3 s^{-1}	-
`q_av`	average river channel (+ floodplain) discharge	m^3 s^{-1}	-
`q_channel_av`	average river channel discharge	m^3 s^{-1}	-
`zb_max`	maximum channel bed elevation	m	-
`mannings_n_sq`	Manning's roughness squared at edge/link	(s $m^{-\frac{1}{3}}$)^2	-
`h`	water depth	m	-
`eta_max`	maximum water elevation	m	-
`eta_src`	water elevation of source node of edge	m	-
`eta_dst`	water elevation of downstream node of edge	m	-
`hf`	water depth at edge/link	m	-
`h_av`	average water depth	m	-
`dl`	river length	m	-
`dl_at_link`	river length at edge/link	m	-

`width_at_link`	river width at edge/link	m	-
`a`	flow area at edge/link	m^2	-
`r`	hydraulic radius at edge/link	m	-
`volume`	river volume	m^3	-
`error`	error volume	m^3	-
`inwater`	lateral inflow	$m^3\ s^{-1}$	-
`inflow`	external inflow (abstraction/supply/demand)	$m^3\ s^{-1}$	0.0
`inflow_wb`	inflow waterbody (lake or reservoir model) from land part	$m^3\ s^{-1}$	0.0
`bankfull_volume`	bankfull volume	m^3	-
`bankfull_depth`	bankfull depth	m	-
`froude_limit`	if true a check is performed if froude number > 1.0 (algorithm is modified)	-	-
`reservoir_index`	river cell index with a reservoir	-	-
`lake_index`	river cell index with a lake	-	-
`waterbody`	water body cells (reservoir or lake)	-	-
`reservoir`	an array of reservoir models `SimpleReservoir`	-	-
`lake`	an array of lake models `Lake`	-	-
`floodplain`	optional 1D floodplain routing `FloodPlain`	-	-

Table B.3: Parameters regarding the 1D Floodplain option

Parameter	**Description**	**Unit**	**Default**
`depth (flood_depth)`	flood depths	m	-
`volume`	cumulative flood volume (per flood depth)	m^3	-
`width`	cumulative floodplain width (per flood depth)	m	-
`a`	cumulative floodplain flow area (per flood depth)	m^2	-
`p`	cumulative floodplain wetted perimeter (per flood depth)	m	-
`mannings_n (n)`	Manning's roughness for the floodplain	$s\ m^{-\frac{1}{3}}$	0.072
`mannings_n_sq`	Manning's roughness squared at edge/link	$(s\ m^{-\frac{1}{3}})^2$	-
`volume`	flood volume	m^3	-
`h`	flood depth	m	-
`h_av`	average flood depth	m	-
`error`	error volume	m^3	-
`a`	flow area at edge/link	m^2	-
`r`	hydraulic radius at edge/link	m	-
`hf`	flood depth at edge/link	m	-
`zb_max`	maximum bankfull elevation at edge	m	-
`q0`	discharge at previous time step	$m^3\ s^{-1}$	-
`q`	discharge	$m^3\ s^{-1}$	-
`q_av`	average discharge	$m^3\ s^{-1}$	-
`hf_index`	index with hf above depth threshold	-	-

Table B.4: Parameters derived from soil maps (Imhoff et al., 2020)

Parameter	Description	PTF
thetaS	Average saturated soil water content [m3/m3]	✓
thetaR	Average residual water content [m3/m3]	✓
KsatVer	Vertical saturated hydraulic conductivity at soil surface [mm/day]	✓
SoilThickness	Soil thickness [mm]	✓
SoilMinThickness	Minimum soil thickness [mm] (equal to SoilThickness)	✓
M	Model parameter [mm] that controls exponential decline of KsatVer with soil depth (fitted with curve_fit, bounds checked)	✓
M_	Model parameter [mm] that controls exponential decline of KsatVer with soil depth (fitted with numpy linalg regression, bounds checked)	✓
M_original	M without checking bounds	✓
M_original_	M_ without checking bounds	✓
f	Scaling parameter controlling the decline of KsatVer [mm-1] (fitted with curve_fit, bounds checked)	✓
f_	Scaling parameter controlling the decline of KsatVer [mm-1] (fitted with numpy linalg regression, bounds checked)	✓
c_n	Brooks Corey coefficients [-] based on pore size distribution, a map for each of the wflow_sbm soil layers	✓
KsatVer_[z]	KsatVer [mm/day] at soil depths [z] of SoilGrids data [0.0, 5.0, 15.0, 30.0, 60.0, 100.0, 200.0]	✓
wflow_soil	Soil texture based on USDA soil texture triangle	✓
KsatHorFrac	Horizontal saturated hydraulic conductivity [mm/day]	

Table B.5: Parameters derived from land use maps

Parameter map	Description
landuse	Landuse class [-]
Kext	Extinction coefficient in the canopy gap fraction equation [-]
Sl	Specific leaf storage [mm]
Swood	Fraction of wood in the vegetation/plant [-]
RootingDepth	Length of vegetation roots [mm]
PathFrac	The fraction of compacted or urban area per grid cell [-]
WaterFrac	The fraction of open water per grid cell [-]
N	Manning Roughness [-]
alpha_h1	Root water uptake reduction at soil water pressure head h1 (0 or 1) [-]

Table B.6: Parameter with default values

Parameter	Description	Value	Unit
Cf_max	Degree-day factor	3.75653	mm/°C/day
cf_soil	controls soil infiltration reduction factor in frozen soil	0.038	-
EoverR	Gash interception model parameter	0.11	-
InfilCapPath	Infiltration capacity paved area	5	mm
InfilCapSoil	Infiltration capacity unpaved area	600	mm
MaxLeakage	Maximum leakage from saturated zone	0	mm/day
rootdistpar	controls how roots are linked to water table	-500	-
TT	threshold temperature for snowfall	0	°C
TTI	threshold temperature interval length	2	°C
TTM	threshold temperature for snowmelt	0	°C
WHC	Water holding capacity as fraction of snowpack	0.1	-
G_Cfmax	Degree-day factor for glacier	5.3	mm/°C/day
G_SIfrac	fraction of snowpack on top of glacier converted to ice	0.002	-
G_TT	fraction of snowpack on top of glacier converted to ice	1.3	°C
KsatHorFrac	Horizontal conductivity fraction	100	-

C Data gathering

Table C.1: Data description of discharge stations; Deltares means data from Deltares server where some data sources are unknown; NRW stands for Landesamt für Nature, Umwelt und Verbraucherschutz Nordrhein-Westfalen; NLWKN is the Niedersächsischer Landesbetrieb für Wasserwirtschaft, Küsten- und Naturschutz; FEWS is the operational forecasting system

Station name	Country	From	Until	Source(s)
Bilk	GE	1975-01-11	2024-05-31	Deltares (1975-2017), NRW (1996-2024)
Wettringen	GE	1975-01-11	2024-05-31	Deltares (1975-2017), NRW (1996-2024)
Ohne	GE	1968-01-02	2024-04-30	Deltares (1968-2017), FEWS (2019-2024)
Gronau	GE	1996-01-11	2024-05-31	NRW (1996-2024)
Lage I	GE	1963-01-03	2017-12-31	NLWKN
Lage II	GE	1963-01-05	2017-12-31	NLWKN
Lage III	GE	1972-01-04	2017-12-31	NLWKN
Lage Gesamt	GE	1963-01-05	2017-12-31	NLWKN
Dinkel	GE	2020-01-05	2023-11-06	FEWS (2020-2023)
Neuenhaus	GE	1950-01-01	2024-05-31	NLWKN, FEWS (2020-2024)
Osterwald	GE	1963-01-11	2024-05-31	NLWKN, FEWS (2020-2024)
Emlichheim	GE	1950-01-01	2024-05-31	NLWKN, FEWS (2017-2024) Waterschap Vechtstromen (Christmas 23/24)
De Haandrik	NL	2007-01-01	2024-05-28	Waterschap Vechtstromen
Ane Gramsbergen	NL	2005-07-15	2024-05-31	Deltares (2005-2016), FEWS (2020-2024), Waterschap Vechtstromen (Christmas 23/24)
ST Hardenberg	NL	1997-07-01		Deltares
ST Marienberg	NL	1998-07-01		Deltares
ST Junne	NL	1989-01-01		Deltares
Ommen	NL	2001-10-14	2024-05-31	Deltares (2001-2015), RWS (2015-2024), Waterschap Vechtstromen (Christmas 23/24)
Ommerkanaal	NL	2001-10-14	2024-05-31	Deltares (2001-2015), RWS (2015-2024), Waterschap Vechtstromen (Christmas 23/24)
Archem TOT	NL	1996-01-01	2017-12-04	Deltares (1996-2017), FEWS (2022-2024)
DM Dalfsen	NL	2012-12-06	2024-05-13	Waterschap Drentse Overijsselse Delta

D Daily vs hourly discharge

Figure D.1 shows the observed hourly and daily discharges at Bilk and the rain at Steinfurt Burgsteinfurt, which is the closest precipitation station to the sub-catchment upstream from Bilk.

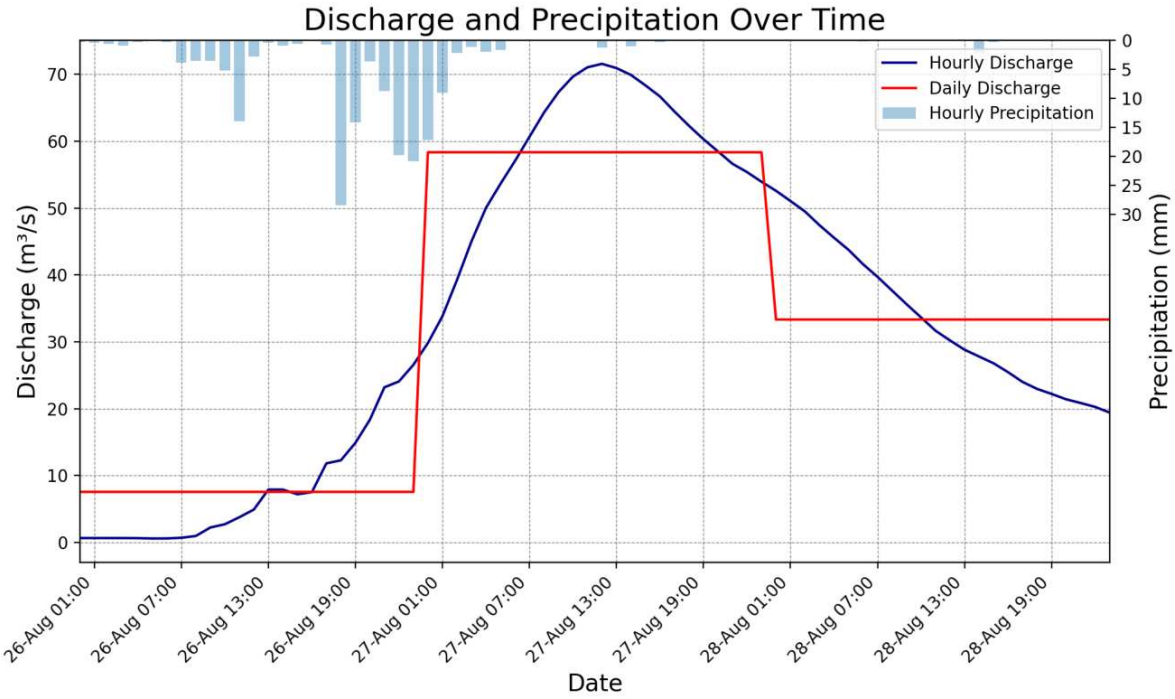

Figure D.1: Hourly vs daily discharge at station Bilk; rain from Steinfurt Burgsteinfurt

E Rain data

E-OBS, ERA5 and RADOLAN contain long periods and cover the whole basin. The resolutions of E-OBS are quite low, especially of ERA5. Their accuracy compared to the measurement stations are shown in Figure E.1, where the mean precipitation from stations and E-OBS/ERA5/RADOLAN are shown. From these scatterplots, it becomes clear that RADOLAN shows low relation between the simulated and observed time series and will therefore not be used further. E-OBS and ERA5 perform significantly better than RADOLAN and from these two data sources, E-OBS shows much more relation between the precipitation by E-OBS and precipitation measured by the stations. E-OBS is considered to be the most accurate data source when the mean precipitation over the basin is considered.

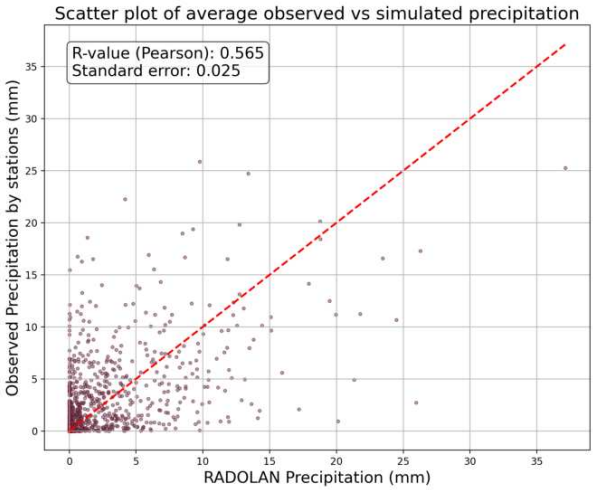

(a) Mean precipitation of all observed stations and RADOLAN (period of 3 years)

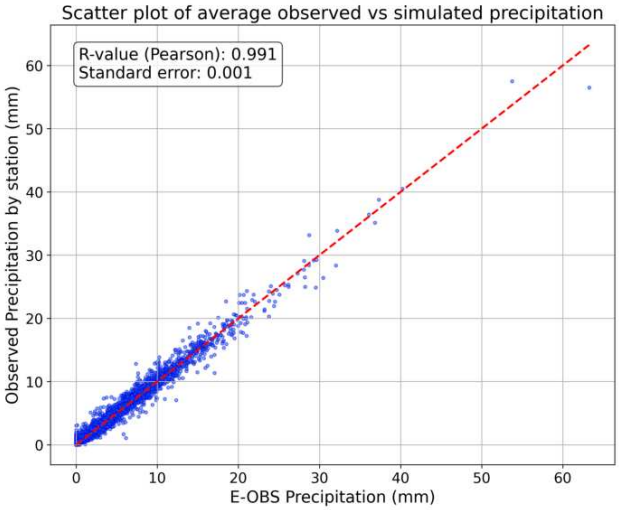

(b) Mean precipitation of all observed stations and E-OBS (period over 20 years)

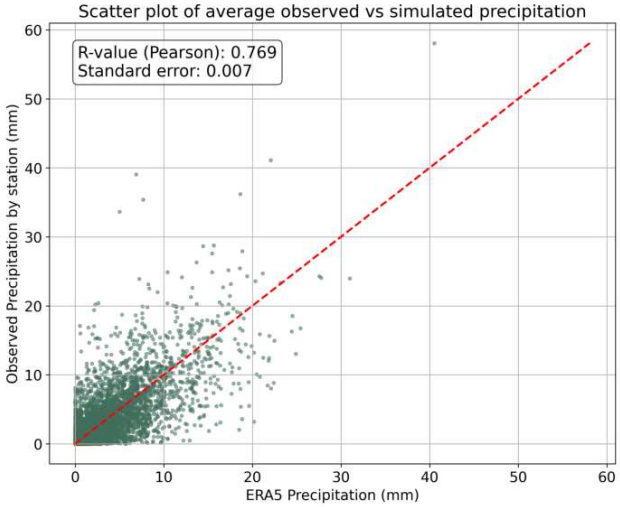

(c) Mean precipitation of all observed stations and ERA5 (period over 20 years)

Figure E.1: Scatterplots of the mean precipitation over all stations (observed) and the whole Vecht basin area (E-OBS, ERA5 and RADOLAN)

Since RADOLAN showed low accuracy in Figure E.1a, it is not included in the following results. As the scatterplots show the mean precipitation, it describes the accuracy of the precipitation on a basin scale. On a local scale, E-OBS has a higher accuracy. Figure E.2 shows the precipitation during a flood event in August 2010, where the precipitation peak of E-OBS is much closer to the observed precipitation of 135 mm. It is concluded that E-OBS is more suitable than ERA5 and therefore will be used to run Wflow sbm.

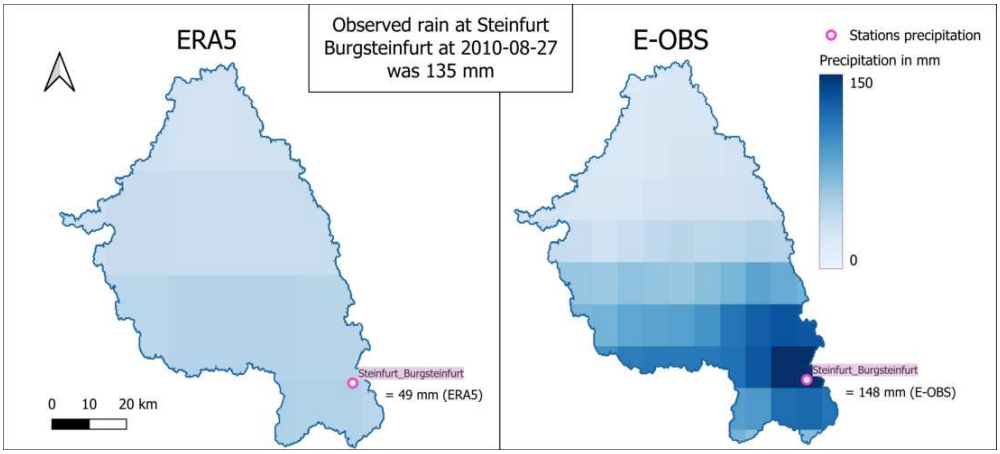

Figure E.2: Comparison ERA5 vs E-OBS on 2010-08-27 at Steinfurt-Burgsteinfurt (flood event in Germany)

F Sensitivity analysis

InfiltCapPath

InfiltCapPath shows very low impact on the model results. The parameter only influences the characteristics of areas with compacted surface which is mainly urban area. This area is not very large in the Vecht basin which explains its low influence

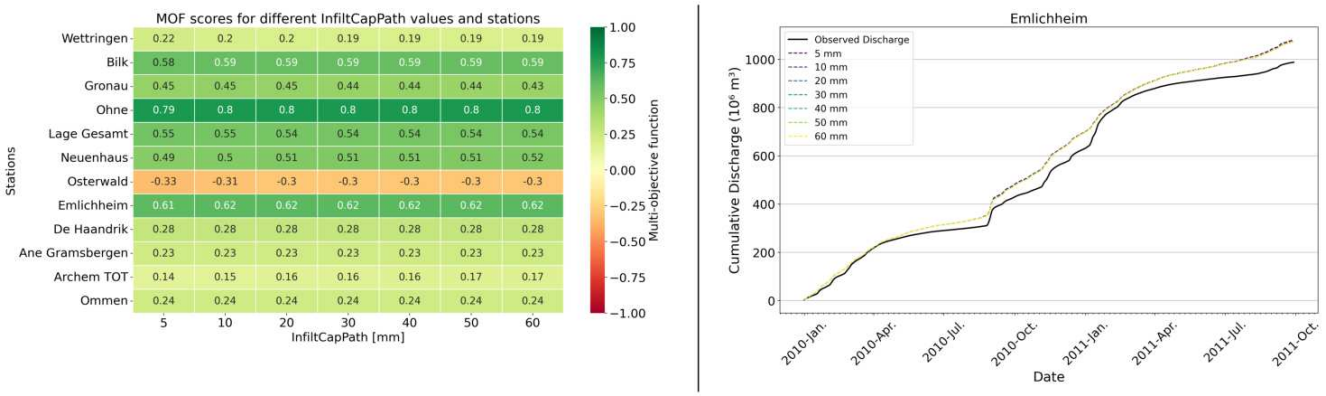

Figure F.1: esults sensitivity analysis InfiltCapPath; scores on multi-objective function (MOF) for different stations in heatmap on the left; right figure shows cumulative discharge at Emlichheim

InfiltCapSoil

InfiltCapSoil has low influence on the results. It only has effect when its value is lower than 150 mm. During the simulation period, there has not been more than 150 mm of precipitation in the Vecht basin. Therefore, changing *InfiltCapSoil* only impacts the results when its value is lower than 150 mm.

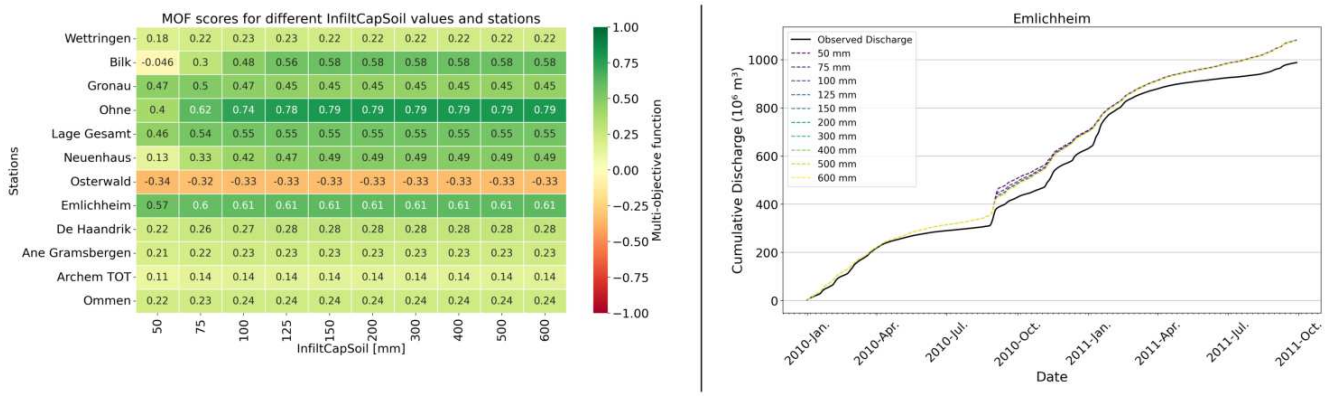

Figure F.2: esults sensitivity analysis InfiltCapSoil; scores on multi-objective function (MOF) for different stations in heatmap on the left; right figure shows cumulative discharge at Emlichheim

rootdistpar

rootdistpar has no impact on the results.

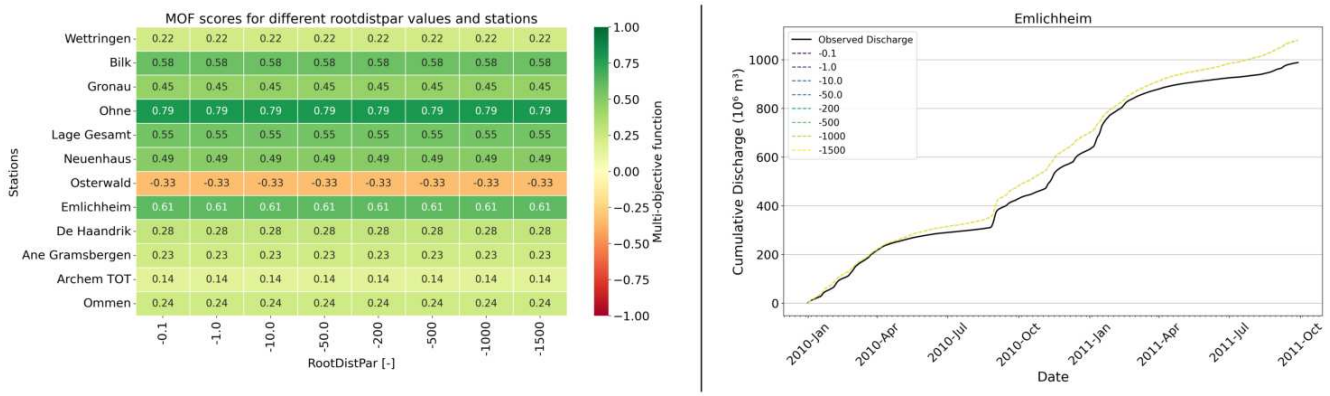

Figure F.3: esults sensitivity analysis RootDistPar; scores on multi-objective function (MOF) for different stations in heatmap on the left; right figure shows cumulative discharge at Emlichheim

G Calibration

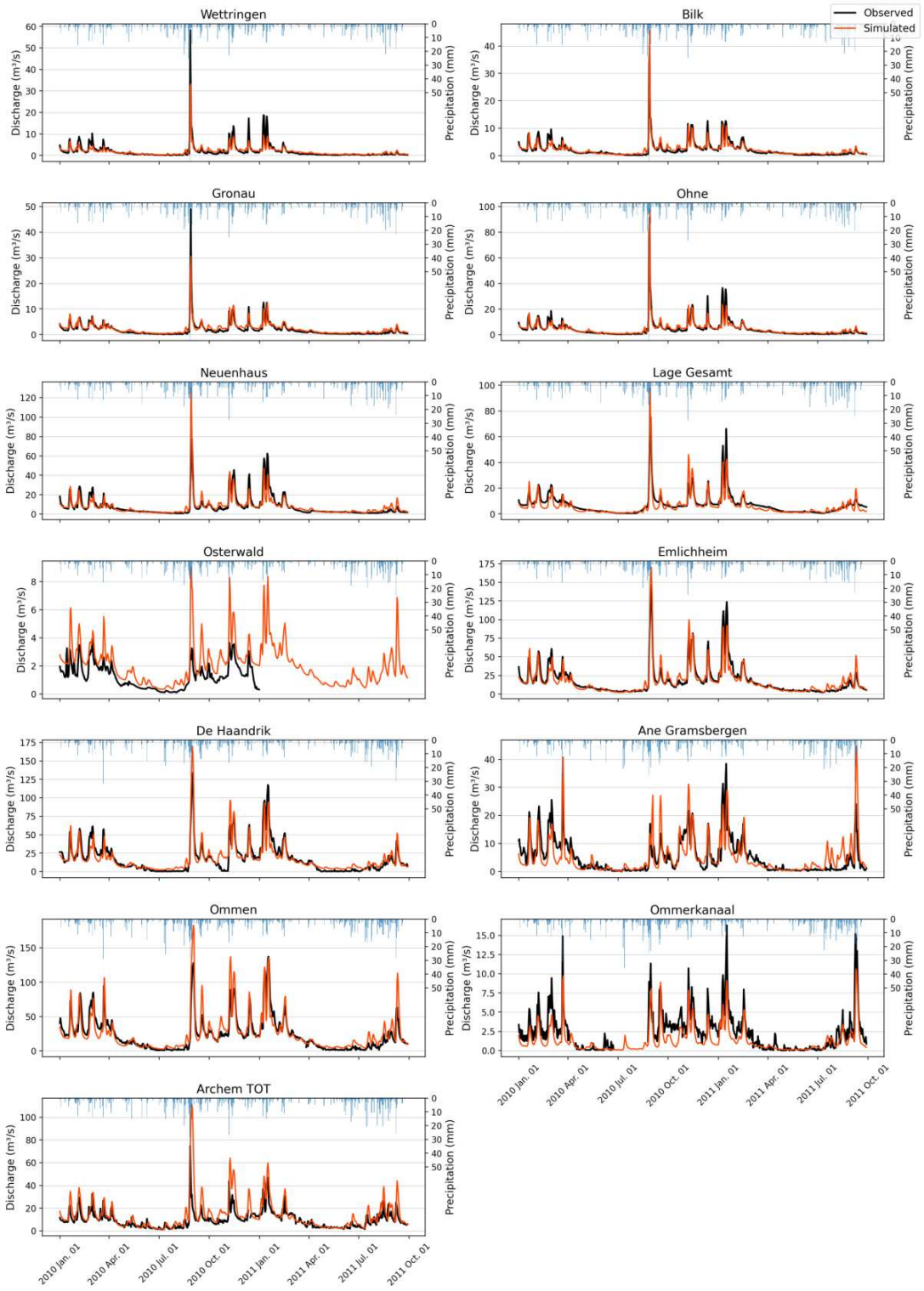

Figure G.1: Hydrographs of the calibrated model during calibration period of 2010

H Validation

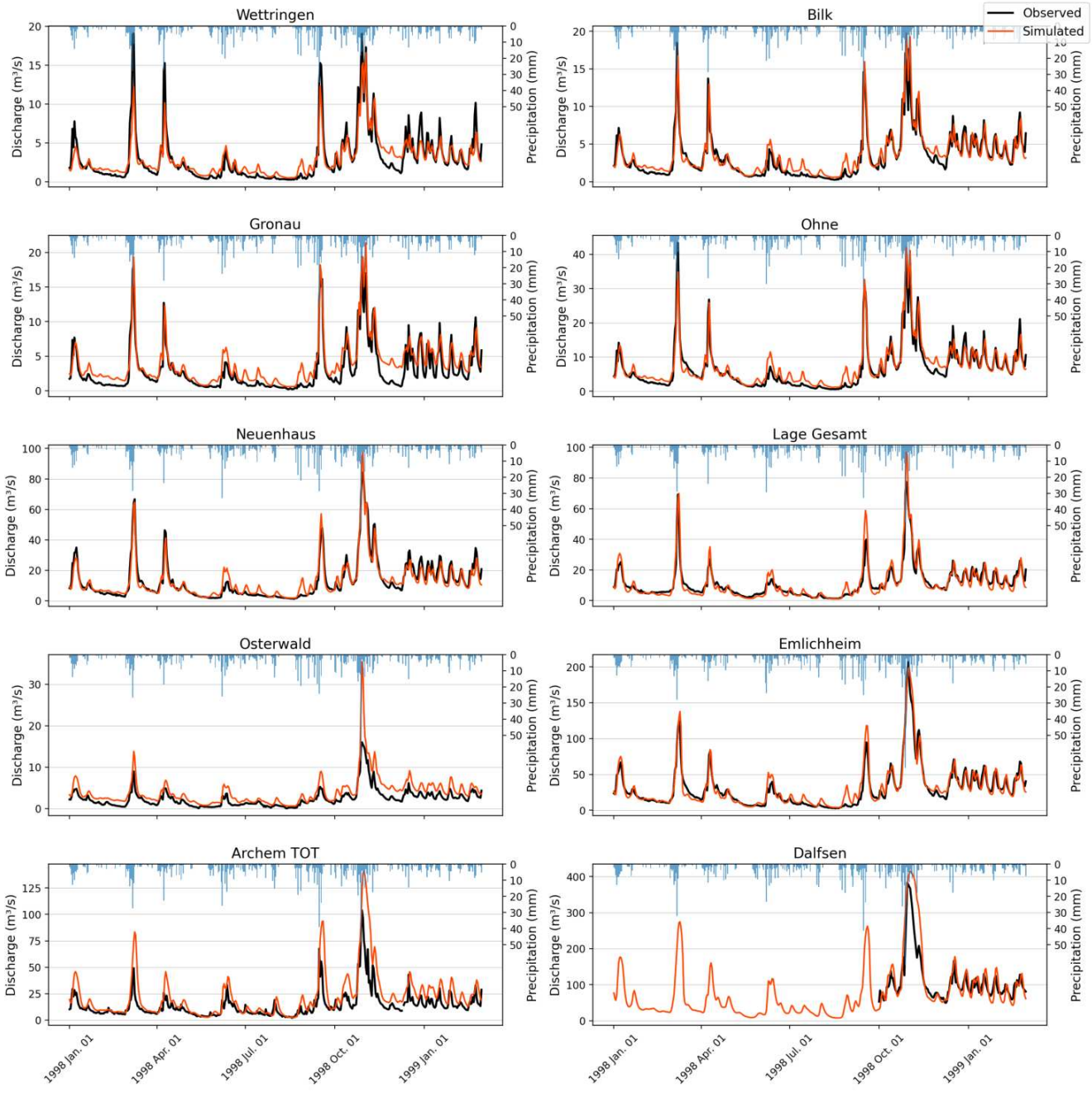

Figure H.1: Hydrographs of validation period 1998; Dalfsen is not considered in analysis from March 1999 since there is an error in observed discharge

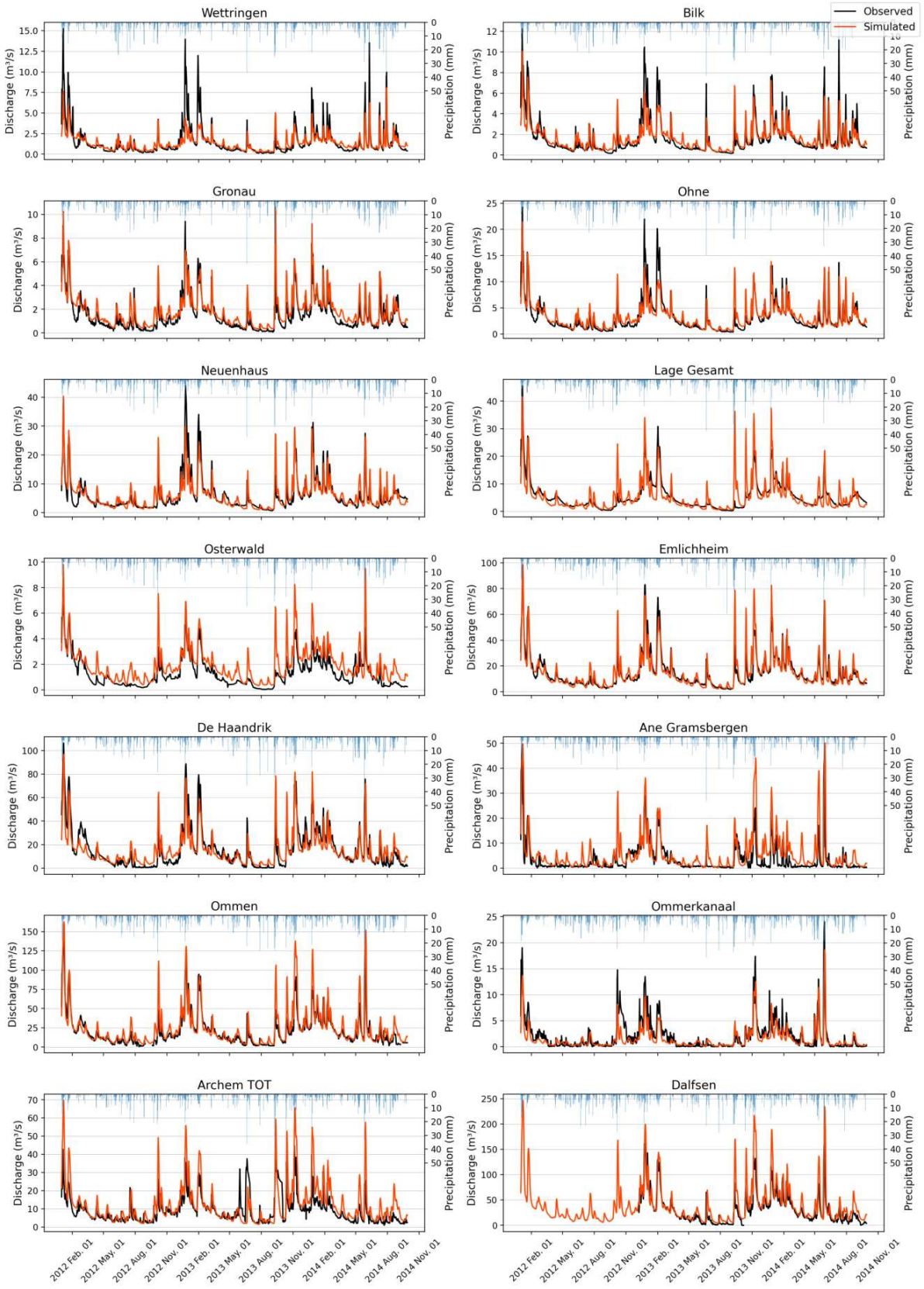

Figure H.2: Hydrographs of validation period 2014

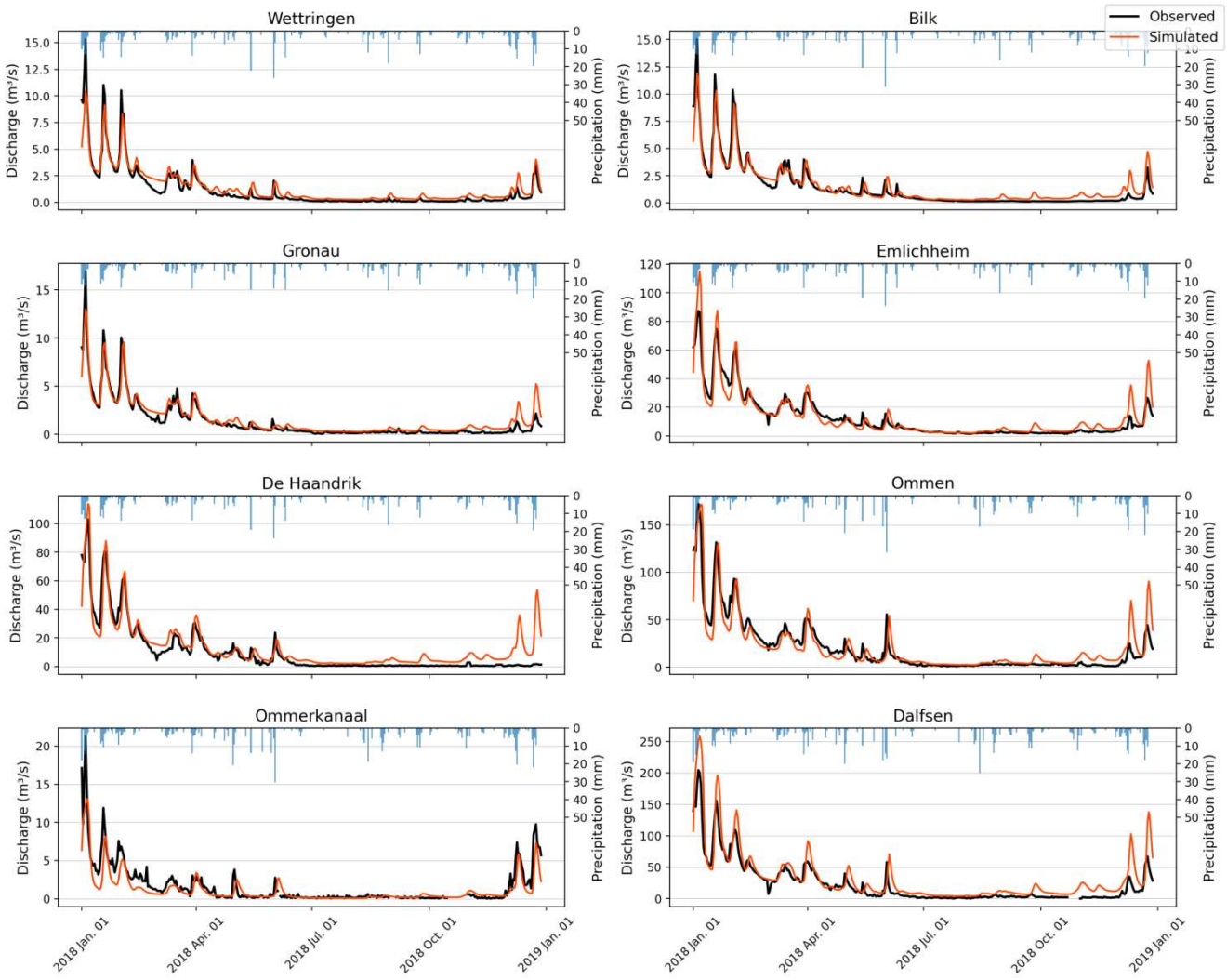

Figure H.3: Hydrographs of validation period 2018

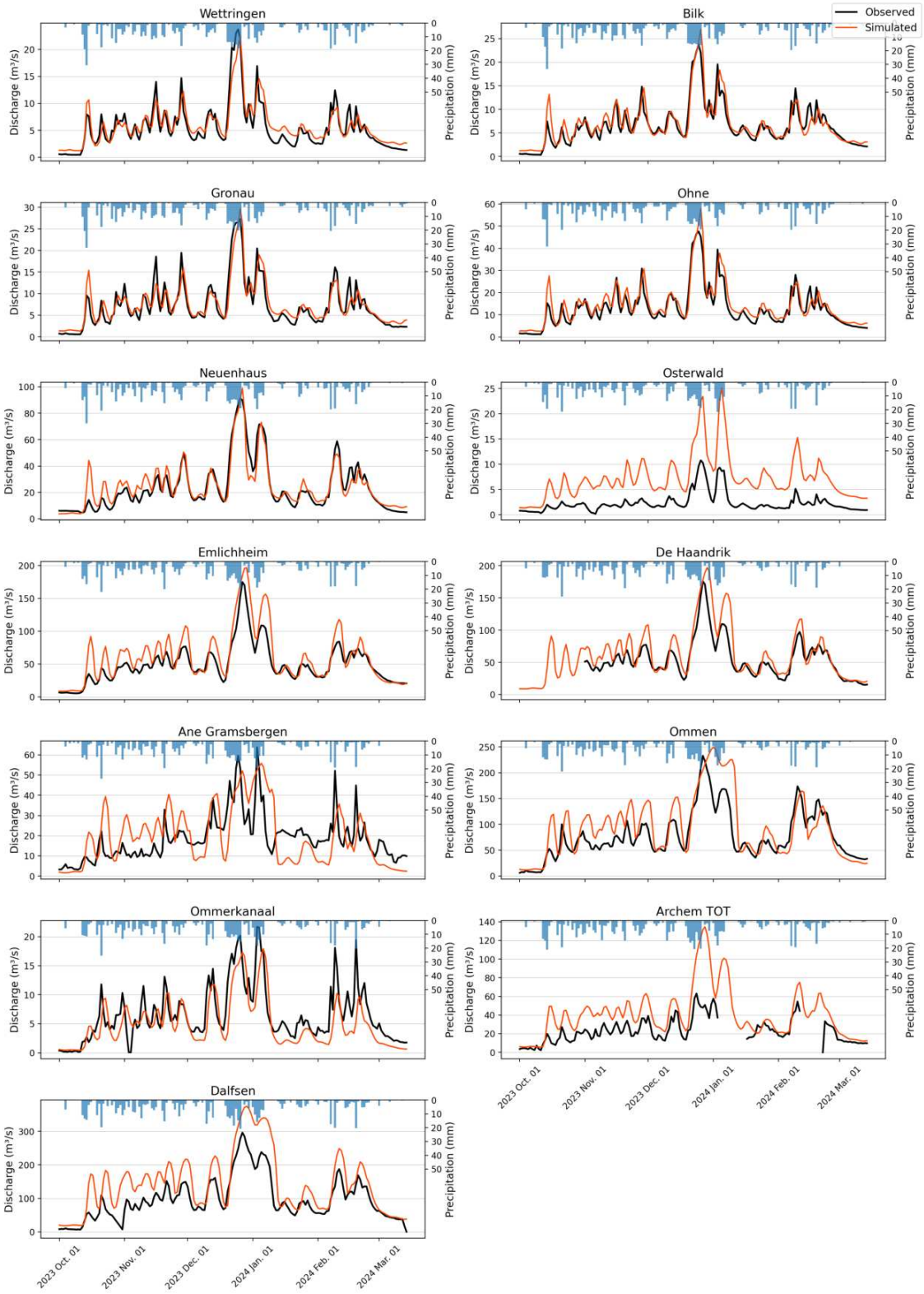

Figure H.4: Hydrographs of validation period 2023

I Nature-based solutions

I.1 Parametrization of nature-based solutions

The parametrization of nature-based solutions presented in Table 15 is further explained below for each nature-based solution type

Land use change
Changing the land use, affects parameters shown in Table 14, which influence evaporation. The LAI values are changed accordingly to Table I.1
However, afforestation also affects infiltration of water into the soil. This change in infiltration is implemented in the Wflow sbm model through the *KsatVer* parameter. Horel et al. (2015) shows that the saturated hydraulic conductivity of forest, under different soil types, is significantly higher, ranging from 1.5 to 2 times higher than arable land and grasslands. Altough, only the topsoils is considered. Li et al. (2019) shows how the saturated hydraulic conductivity changes over depth between forest and agricultural land, where the Ksat is significantly large for forest up to a depth of 80 cm. The same is found by Yao et al. (2015), where the saturated hydraulic conductivity is factor 2.5 to 4 larger in forest compared to farmland. Since Wflow sbm has a soil depth of 2 m, an approximation is made based on the aforementioned literature sources and a linear relation between Ksat increase due to afforestion and depth is assumed. This lead to an increase factor of 1.5 for Ksat when afforestation is considered.

It is assumed that trees in agroforestry cover around 50 % of the agricultural land, leading to an increase factor of 1.25 for the saturated hydraulic conductivity.

Increasing roughness
The nature-based solutions 'leaky dams', 'terracing' and 'vegetation of the river bed' are implemented using the Manning's value, for either the land or the channel. Terracing also increase the hydraulic conductivity, according to literature. For terracing, the hydraulic conductivity is also increased by a factor of 1.3, based on Bisolo et al. (2024) and Fashaho et al. (2020). An approximation is made for Wflow sbm where a soil thickness of 2 m is used, while literature researches the soil to a depth of 1 m. USDA (2017) describes guidelines for the implementation of terracing. A guideline is provided for land slopes ranging from 0 to 1 degree, and a minimum slope of 1 degree selected as the threshold for implementing terraces in the Vecht. The area in the Vecht where the slope is larger than 1 degree, can be seen in Figure I.3

Senior et al. (2022) investigates hillslope leaky barriers and their representation in 2D hydraulic models. The Manning's value is changed increased by a factor of 2.5. However, this was more focuses on a small area, which is not representable for an area like the Dinkel that is much larger. Therefore, the Manning's value increase factor is set to 1.5.

For the implementation of river bed vegetation, the Manning's roughness value of the whole channel in the Dinkel is increased by a factor of 1.38, approximated using Table 2, going from 'medium' to 'large' in the amount of vegetation from Arcement and Schneider (1989).

Improving infiltration
Mulching is expected to improve soil infiltration by increasing saturated hydraulic conductivity. Based

on a review of multiple literature sources, an increase factor of 1.2 is used in the Wflow model (Kahlon et al., 2013) (Simsek et al., 2017). While these studies typically focus on the hydraulic conductivity of the topsoil, the Wflow model considers a 2-meter soil column. The average increase factor reported in the literature is 1.8, but this is set to 1.2 in Wflow due to the deeper soil column compared to literature.

There is considerable uncertainty regarding the improvement of hydraulic conductivity when cover crops are involved. S. I. Haruna et al. (2023) states that the saturated hydraulic conductivity is twice as high under cover crops during July. An increase in saturated hydraulic conductivity in the topsoil is also found by S. Haruna et al. (2018). Peters and Haruna (2024) finds a large increase in the topsoil under cover crops, with an increase factor of 20. This is considered unrealistic and shows that it is difficult to measure. To account for this variability, a range of increase factors from 1.1 to 1.5 will be applied.

Soil fauna improvements can be quantified through increased organic carbon storage, which is indicative of active soil fauna. A larger organic carbon storage would imply more soil fauna (Amanze et al., 2024). Zare et al. (2010) shows that by applying biosolids, which increase organic carbon storage, can enhance saturated hydraulic conductivity by a factor of 1.5.

No-till farming also has the potential to enhance hydraulic conductivity, although with significant uncertainty. Fér et al. (2020) shows that no till farming can increase hydraulic conductivity in the topsoil by a factor of 5, while other studies report a more modest, of e.g. a increase factor of 2.5, effect (He et al., 2009). On the other hand, Skaalsveen et al. (2019) describes that no till farming sometimes leads to a reduction in saturated hydraulic conductivity. Due to this high uncertainty, lower and upper increase factors are approximated based on literature, with increase factors of 1.05 and 1.4 respectively. The literature primarily focuses on soil depths of up to 0.8 meters, whereas the Wflow model considers a 2-meter soil column. Therefore, values from the literature have been adjusted for the Wflow model's deeper soil column.

Water retention

Water retention is implemented using the *'re-infiltration'* option with a h_{thresh} value of 0.2 m, which is a realistic water depth in wetland areas according to Cooper et al. (2020). The wetlands have this h_{thresh} value.

Table I.1: Averaged LAI map for different land use types; LU means 'land use'; urban and water land use types have a LAI of 0

		Month											
LU	**Description**	**1**	**2**	**3**	**4**	**5**	**6**	**7**	**8**	**9**	**10**	**11**	**12**
111	Continuous urban fabric	0.0	0.0	0.0	0.0	0.0	0.0	0.0	0.0	0.0	0.0	0.0	0.0
112	Discontinuous urban fabric	0.0	0.0	0.0	0.0	0.0	0.0	0.0	0.0	0.0	0.0	0.0	0.0
121	Industrial or commercial units	0.0	0.0	0.0	0.0	0.0	0.0	0.0	0.0	0.0	0.0	0.0	0.0
122	Road and rail networks	0.0	0.0	0.0	0.0	0.0	0.0	0.0	0.0	0.0	0.0	0.0	0.0
124	Airports	0.0	0.0	0.0	0.0	0.0	0.0	0.0	0.0	0.0	0.0	0.0	0.0
131	Mineral extraction sites	0.0	0.0	0.0	0.0	0.0	0.0	0.0	0.0	0.0	0.0	0.0	0.0
132	Dump sites	0.0	0.0	0.0	0.0	0.0	0.0	0.0	0.0	0.0	0.0	0.0	0.0
133	Construction sites	0.0	0.0	0.0	0.0	0.0	0.0	0.0	0.0	0.0	0.0	0.0	0.0
141	Green urban areas	0.6	0.3	0.4	0.7	0.9	1.1	1.2	1.1	0.9	0.6	0.7	0.6
142	Sport and leisure	1.1	0.7	0.8	1.3	1.8	2.2	2.4	2.3	1.9	1.3	1.3	0.9
211	Non-irrigated arable land	1.1	0.5	0.7	1.2	1.7	2.2	2.4	2.1	1.8	1.0	1.3	1.0
231	Pastures	1.4	0.9	1.1	1.9	2.1	2.4	2.9	2.8	2.4	1.5	1.8	1.3
242	Cultivation patterns	1.4	0.8	1.0	1.7	2.0	2.4	3.0	2.8	2.3	1.5	1.7	1.3
243	Agricultural with vegetation	1.4	0.9	1.1	2.0	2.4	2.7	3.1	3.1	2.7	1.7	1.7	1.2
311	Broad-leaved forest	1.1	0.6	0.8	1.5	2.4	2.8	2.9	2.7	2.3	1.4	1.3	1.0
312	Coniferous forest	1.3	0.9	1.1	1.7	2.5	3.1	3.4	3.2	2.8	1.7	1.7	1.1
313	Mixed forest	1.3	0.9	1.1	1.8	2.8	3.3	3.6	3.4	3.0	1.9	1.6	1.1
321	Natural grasslands	1.2	0.7	0.8	1.4	2.0	2.4	2.6	2.4	2.0	1.3	1.5	1.0
322	Moors and heathland	1.2	0.9	1.0	1.5	2.1	2.7	3.1	2.9	2.4	1.6	1.6	1.0
324	Transitional woodland-shrub	1.0	0.6	0.7	1.2	2.1	2.7	2.9	2.7	2.2	1.3	1.3	0.9
411	Inland marshes	1.2	0.7	0.9	1.5	2.0	2.5	2.9	2.7	2.1	1.4	1.6	1.1
412	Peat bogs	0.9	0.5	0.6	0.9	1.4	2.1	2.5	2.2	1.7	0.9	1.1	0.8
511	Water courses	0.0	0.0	0.0	0.0	0.0	0.0	0.0	0.0	0.0	0.0	0.0	0.0
512	Water bodies	0.0	0.0	0.0	0.0	0.0	0.0	0.0	0.0	0.0	0.0	0.0	0.0

I.2 Quick assessment of nature-based solutions

The location of the Dinkel sub-catchment is shown in Figure I.1. The outflow point of the Dinkel is at station Lage Gesamt.

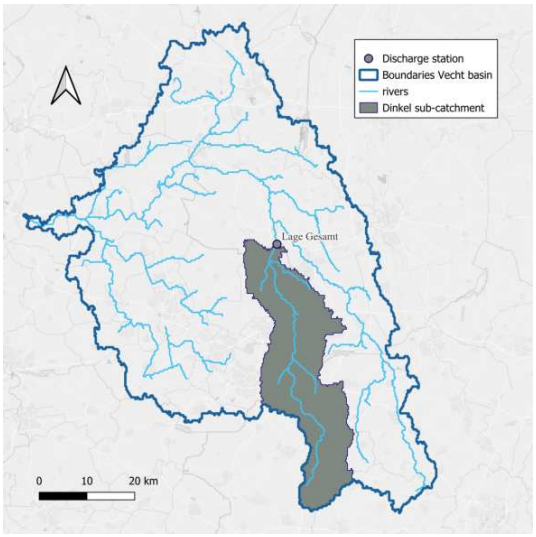

Figure I.1: Dinkel sub-catchment

I.2.1 Implementation of nature-based solutions in the quick assessment

The four different nature-based solution types (see Figure 15) are implemented in Wflow sbm in different ways. In the quick assessment, these are only applied in the Dinkel area and in an extreme spatial manner.

The land use change interventions can be seen in Figure I.2, where the land use changes are applied to all land uses that are originally not 'urban' or 'water'.

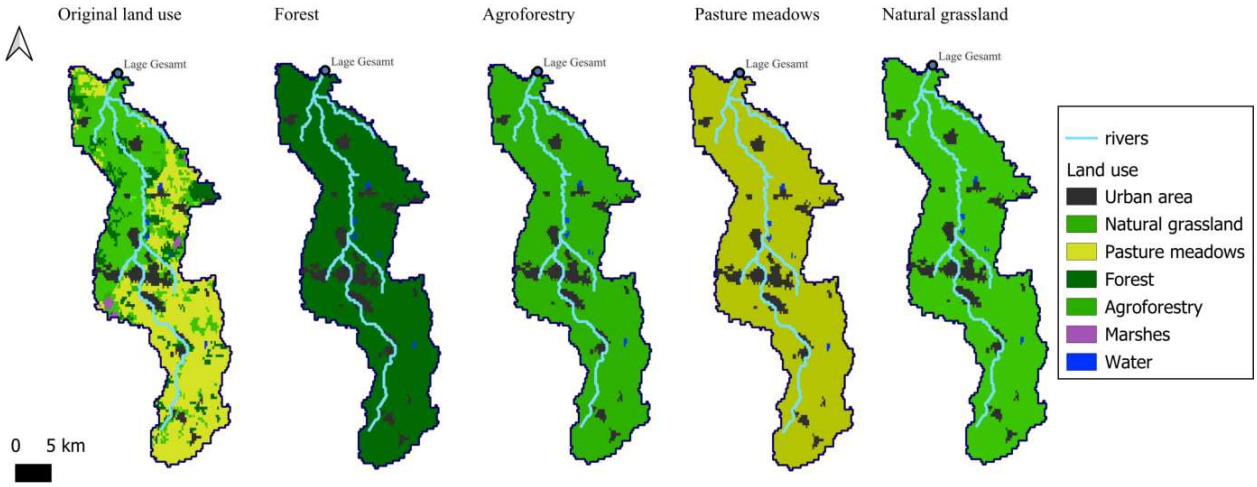

Figure I.2: Implementation of land use change in Wflow sbm in the Dinkel in the quick assessment

In implementing roughness nature-based solutions, either the land roughness coefficient or the channel roughness coefficient is changed, depending on the type of nature-based solution. The roughness coefficient is represented by the Manning's number.
In 'terracing', the land roughness coefficient is increased by a factor of 1.4, together with an increase factor for the KsatVer of 1.3 (see Table 15). This is only applied to the areas where the slope is larger than 1 degree, since terracing can only be applied to land with a slope. The area with a slope larger than 1 degree is shown in green on the top right of Figure I.3.
The nature-based solutions 'bed vegetation' and 'leaky dams' are applied to the channel, meaning only the channel roughness coefficient is altered. These can be seen at the bottom of Figure I.3. In 'bed vegetation', the channel roughness is increased by a factor of 1.38, while in 'leaky dams', it is increased by a factor of 1.5.

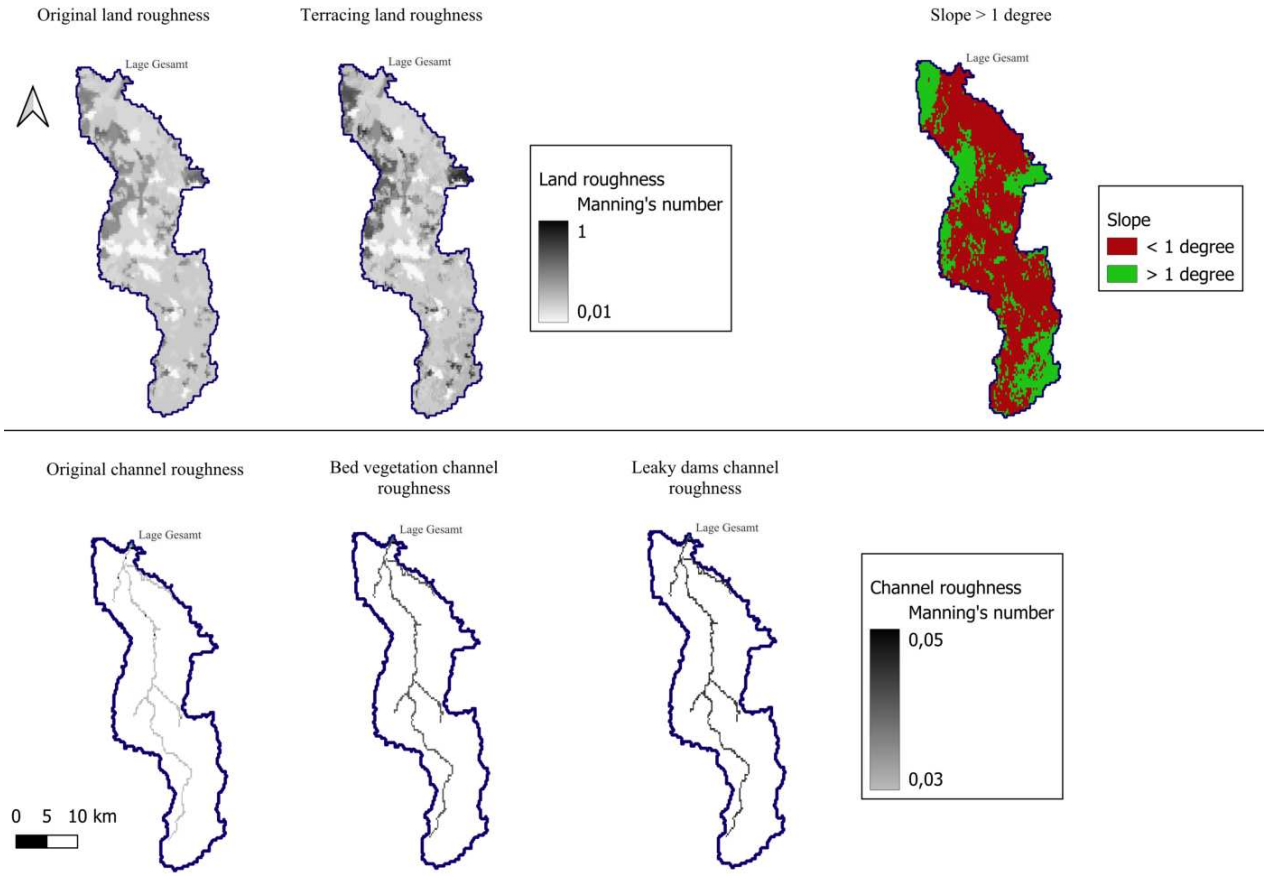

Figure I.3: Implementation of roughness NBS interventions in Wflow sbm in the Dinkel in the quick assessment

The nature-based solutions that improve infiltration in the area are shown in Figure I.4, where the saturated vertical hydraulic conductivity can be seen. 'No till farming' and 'cover crops' only apply to agricultural area, thus the increase of the vertical saturated hydraulic conductivity is only applied to these agricultural areas.
In the case of 'no till farming', the KsatVer is changed with a factor of 1.05 to 1.4 (see Table 15). In 'improve soil fauna', KsatVer is increased with a factor of 1.2 and in 'cover crops', it is increased with a factor of 1.1 to 1.5. 'Mulching' increases the KsatVer by a factor of 1.2. The values of KsatVer in Figure I.4 are at the topsoil.

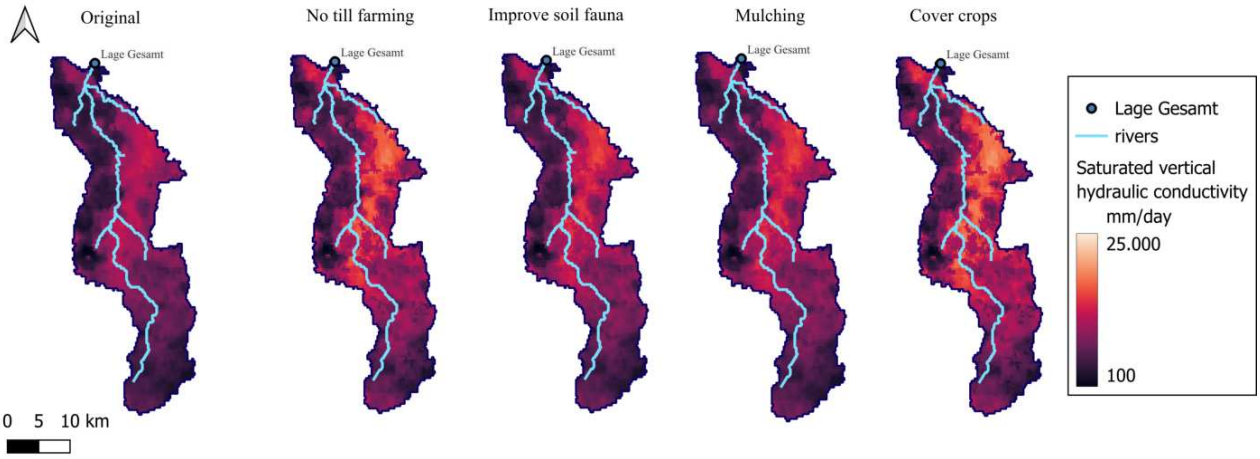

Figure I.4: Implementation of infiltration NBS interventions in Wflow sbm in the Dinkel in the quick assessment

The water retention areas are implemented in the 'wetlands' areas in Figure I.5, where the area is wetted. The areas with wetlands have an h_{thresh} value of 0.2 m.

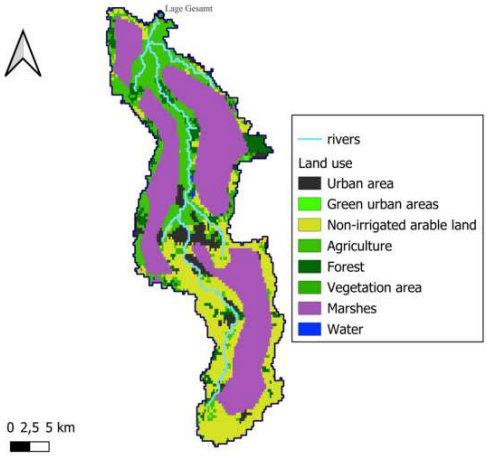

Figure I.5: Implementation of water retention in Wflow sbm in the Dinkel in the quick assessment

I.3 Detailed assessment

The effects of afforestation and wetlands on the cumulative evaporation and discharge during a dry year (2018d, see section 3.3.3) are shown in Figure I.6. As can be seen, wetlands have have more effect on the cumulative evaporation and discharge.

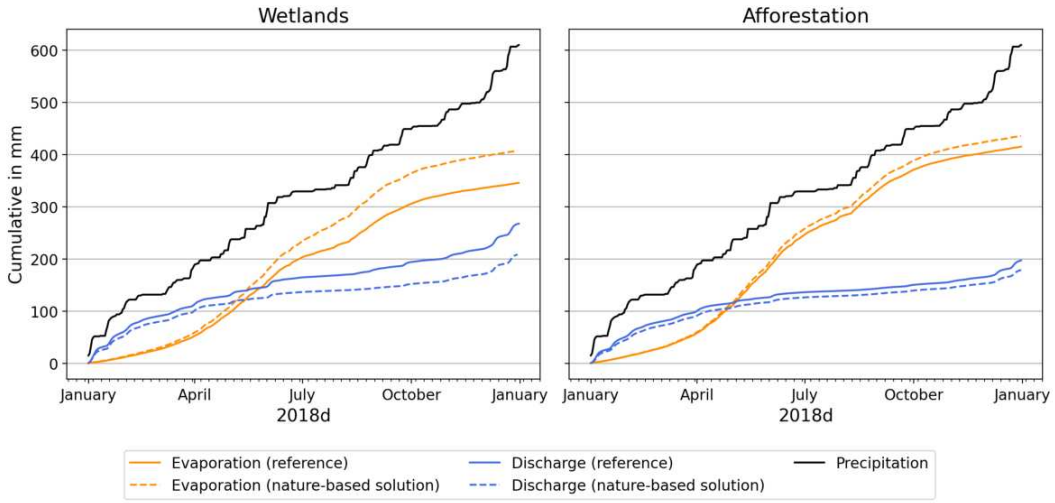

Figure I.6: Spatially averaged cumulative precipitation, discharge (at Dalfsen) and total evaporation in mm for afforestation and wetlands; under summer conditions with a 2-daily rainfall sum of 80 mm

Figure I.7 shows the average saturated water depth in the Vecht basin over the entire period of the detailed assessment for both wetlands and afforestation. Only the scattered 50 % NBS scenarios are shown. Afforestation have a larger effect on the saturated water depth compared to wetlands.

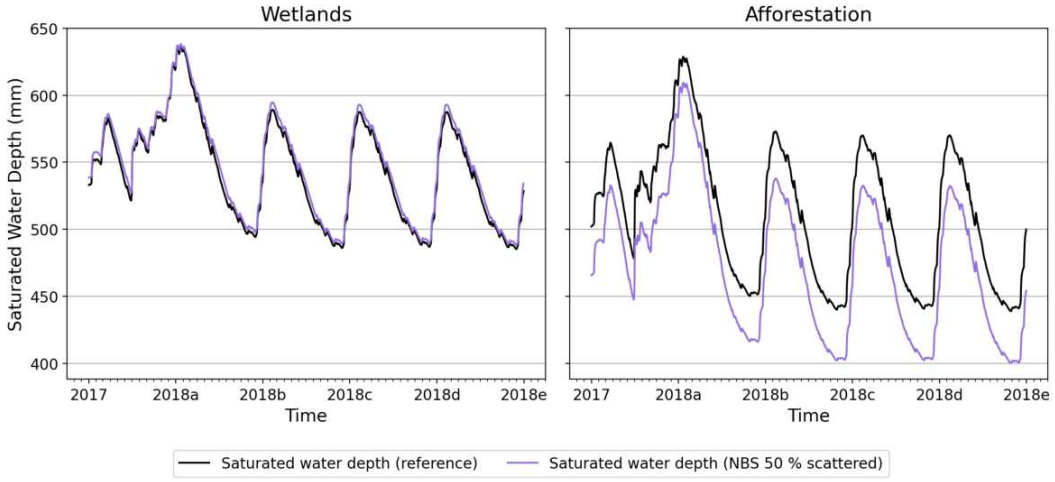

Figure I.7: Average saturated water depth during the detailed assessment for afforestation and wetlands for 5 years; under summer conditions with a 2-daily rainfall sum of 80 mm

Figure I.8 shows the effects of the NBS scenarios on the peak discharge at Dalfsen under winter conditions with a two-daily rainfall sum of 200 mm.

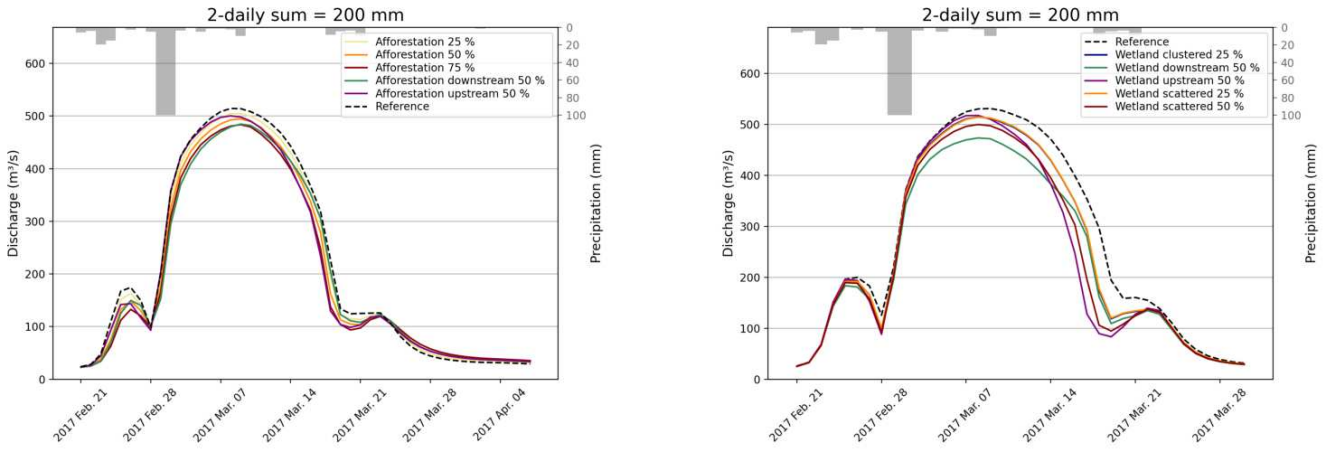

(a) Effects of afforestation at Dalfsen

(b) Effects of wetlands at Dalfsen

Figure I.8: fig: Hydrographs at Dalfsen with afforestation and wetland scenarios under winter conditions with a uniform 2-daily rain event with a sum of 200 mm

Figure I.9 shows the effects of NBS under winter conditions for all nature-based solutions under the three different 2-daily rainfall sums.

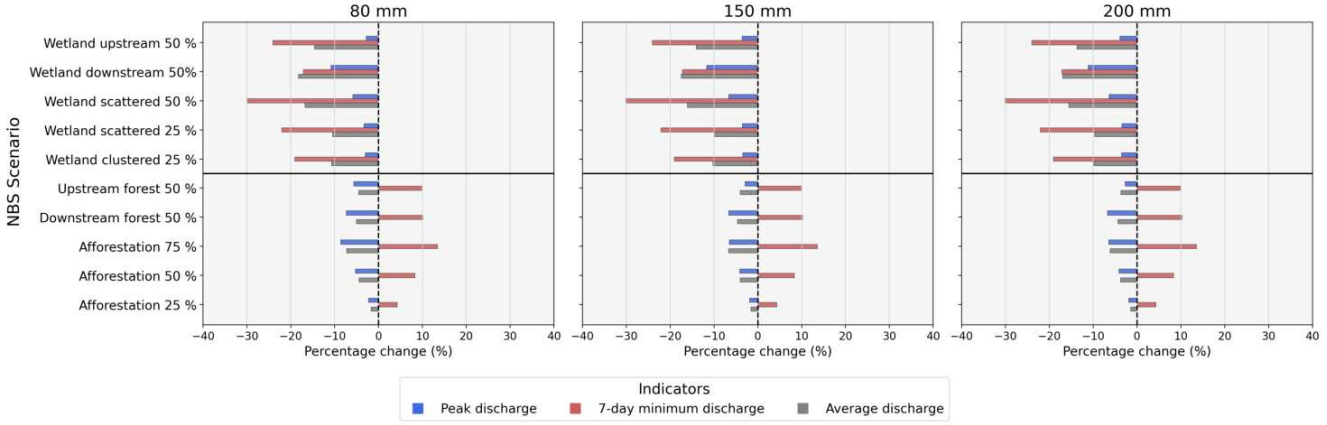

Figure I.9: Effects of nature-based solution scenarios at Dalfsen in the winter scenario for 3 different rain events; peak daily discharge change is based on the discharge wave caused by the uniform 2-daily rain event in the beginning of March; MAM7 and mean discharge are based on the period of 2017 and 2018

The lowest simulated discharges during the detailed assessment among various affectation scenarios are shown in Figure I.10.

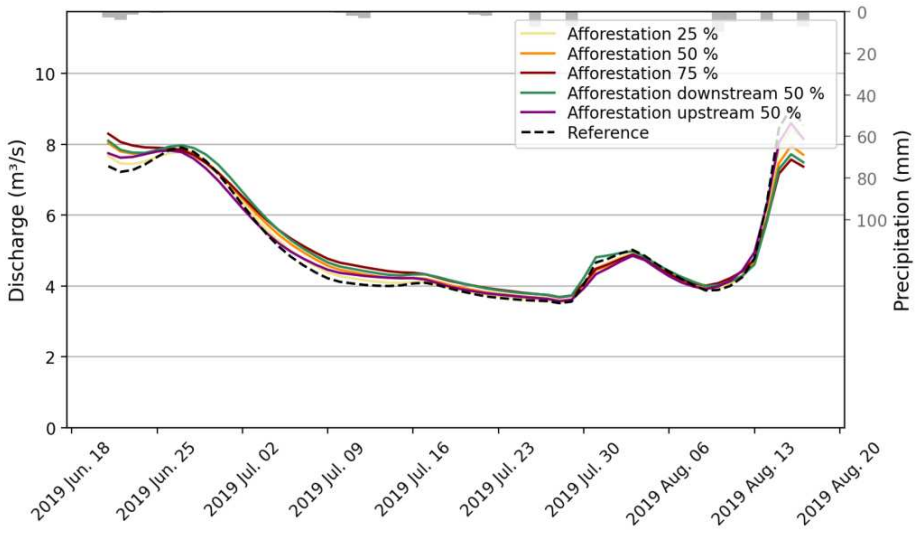

Figure I.10: Lowest flows during detailed assessment at Dalfsen station for afforestation scenarios

I.4 Evaluation '21 rain

In order to derive warning levels in m^3/s, a Q-h relationship is determined using water level and discharge data. The warning levels were obtained by NLWKN in water levels and are transformed to warning levels in discharge.

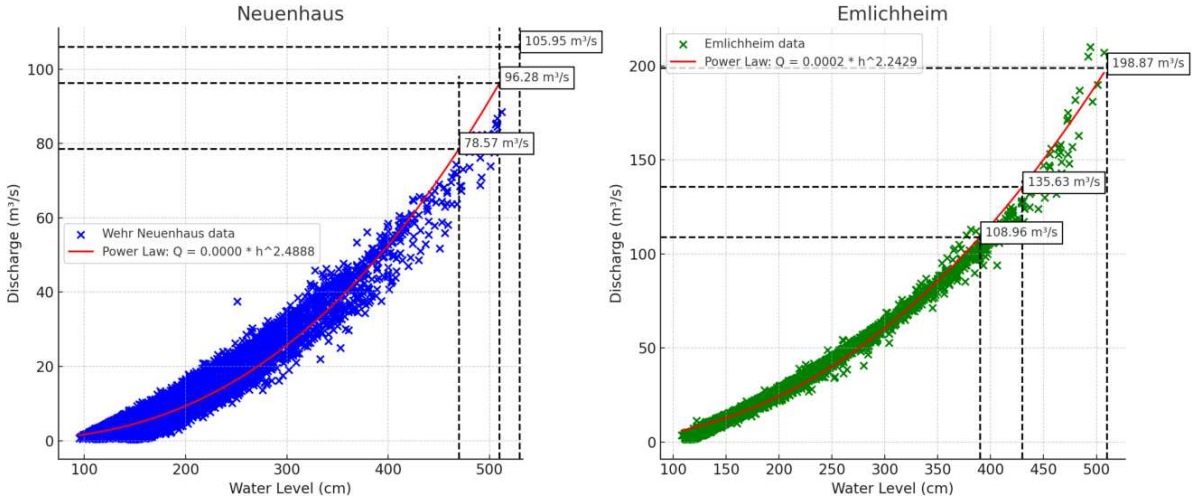

Figure I.11: Q-h relationship at Emlichheim and Neuenhaus

JCAR
ATRACE

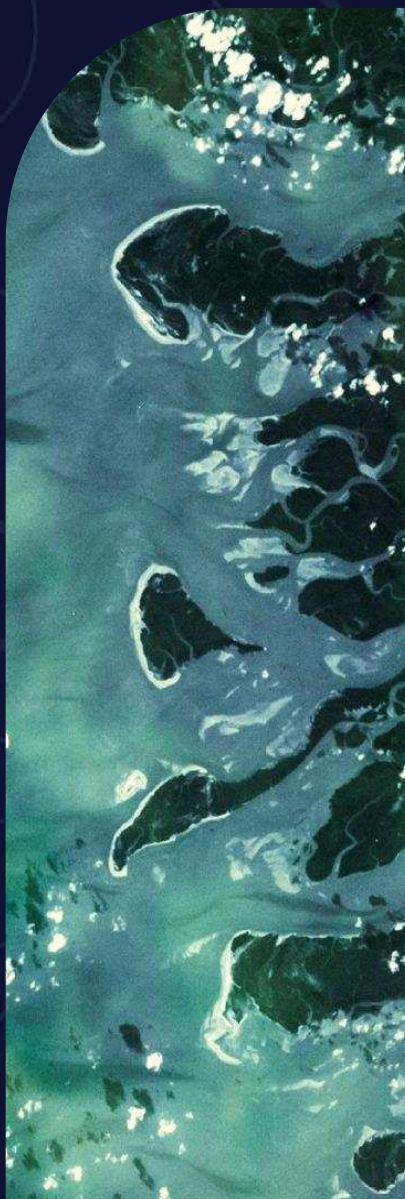

UNIVERSITY
OF TWENTE.

Deltares